

Master of science in mechanical engineering  
June 2018



# Impact of Sidewall Pressure on High Voltage Cables

Robin Berglind

This thesis is submitted to the Faculty of Mechanics at Blekinge Institute of Technology in partial fulfilment of the requirements for the degree of Master of Science in Mechanical Engineering. The thesis is equivalent to 20 weeks of full time studies.

The authors declare that they are the sole authors of this thesis and that they have not used any sources other than those listed in the bibliography and identified as references. They further declare that they have not submitted this thesis at any other institution to obtain a degree.

**Contact Information:**

Author:

Robin Berglind

E-mail: [robe13@student.bth.se](mailto:robe13@student.bth.se)

University advisor:

Ansel Berghuvud

Department of mechanical engineering

Faculty of Mechanics

Blekinge Institute of Technology

SE-371 79 Karlskrona, Sweden

Internet: [www.bth.se](http://www.bth.se)

Phone: +46 455 38 50 00

Fax: +46 455 38 50 57

## Abstract

When a high voltage cable is transported throughout factory it is affected by sidewall pressure in cable bends between the roller supports and the cable. The problem is when the sidewall pressure is too high it will deform the cable which can have a negative impact on the conductivity of the cable. The roller supports can also get damaged because of fatigue. These negative consequences are the subject to exploration by implementing known analytical solution of contact mechanics developed by Hertz together with finite element analysis and experimental testing.

Two possible methods of measuring the radial force is studied to be able adjust the roller supports positions to reduce the sidewall pressure on the cable. The first one is to use the pressure film to determine the radial force. The second one is to by measuring the compression in cable to thereafter translate it to radial force by having the relation between compression and radial force for the specific cable.

Two different types of high voltage cables, a direct current (DC) cable and an alternating current (AC) cable is studied by using finite element method and experimental tests to see the relation between the compression and radial force in the cable. Also in these experimental tests the pressure films are used and evaluated to see if this measuring technique combined with Hertzian's theory make it possible determining the radial force.

For the method of using the pressure films to determine the radial force the result shows it is difficult to translate the pressure from the films to radial force for a high voltage because of the cable's armouring wires. The conclusion about these the pressure films is that they are good to use to describe the compression and can be used as relative measurement between the rollers but not for determine the radial force.

The result shows it is a possible to describe relation between compression and radial force for a high voltage cable and use this information to determine the radial force by measuring the compression. But the conclusion is that it is ineffective and less accurate way of measuring the radial force.

These results from this thesis are important for further research within the area and they help creating a greater understanding of sidewall pressure related problems in cables.

**Keywords:** High voltage cable, Contact mechanics, Finite element analysis and Pressure film.

# Sammanfattning

När en högspänningskabel transporteras genom fabriken så utsätts den för sidotryck i kabelböjar mellan kabel och rullstöd. Problemet är när sidotrycket blir allt för stort så kommer det att deformera kabeln vilket kan ha en negativ påverkan på kabelns ledningsförmåga. Rullstöden kan också ta skada på grund av utmattning. Dessa negativa konsekvenser är det området som ska studeras genom att implementera känd analytisk lösning av kontaktmekanik framtagen av Hertz tillsammans med finita element analys och experimentella tester.

Två möjliga metoder av att mäta den radiella kraften studeras för att göra det möjligt att justera rullstödens positioner för att minska sidotrycket på kabeln. Den första är att använda tryckfilmer för att bestämma den radiella kraften. Den andra är att mäta intryckning i kabeln för att sedan översätta detta till radiell kraft genom att ha förhållandet mellan intryckning och radiell kraft för den specifika kabeln.

Två olika högspänningskablar, en likströms kabel (DC) och en växelström (AC) kabel studeras genom att använda finita elementmetoden, tryckfilmer och experimentella tester för att beskriva förhållandet mellan intryckning och kraft mellan kabel och rullstöd. Under tiden dessa experimentella testerna genomförs används tryckfilmer kombinerat med Hertz teori till att utvärdera denna mätmetod för att kunna se om det går att översätta trycket till radiell kraft.

Resultatet av att använda tryckfilmerna visar att det är svårt att översätta trycket från filmerna till en radiell kraft på grund av kabelns armeringstrådar. Slutsatsen kring dessa tryckfilmer är att de lämpar sig för att beskriva intryckningen och kan användas för relativa mätningar mellan rullarna. Tryckfilmerna lämpar det sig mindre till använda trycket från filmerna för att beskriva den radiella kraften för en högspänningskabel.

Resultaten visar att det går beskriva förhållandet mellan intryckning och kraft för en högspänningskabel för att kunna använda den uppmätta intryckningen för att bestämma den radiella kraften. Men slutsatsen är att den är en ineffektiv och ett mindre noggrant sätt att mäta den radiella kraften.

Dessa resultat från examensarbetet är viktiga för framtida studier inom området och de hjälper till att skapa en bättre förståelse kring sidotrycksrelaterade problem i kablar.

**Nyckelord:** Högspänningskabel, Kontaktmekanik, Finita element analys, Tryckfilm.

# Preface

This thesis states the end of my education in master of science in mechanical engineering with emphasis on structural mechanics. The thesis work was conducted at Blekinges Institute of Technology and performed at NKT in Karlskrona and would not have been feasible without the invaluable supervision and guidance from Ansel Berghuvud, BTH, Joacim Malm, NKT and Peter Hoff, NKT. I would like to take the opportunity to express my gratitude towards those that guided me through this fantastic experience.

I thank you all.

*Robin R. Berglind*  
**Karlskrona, June 10<sup>th</sup>, 2018**

# Nomenclature

---

<b>Symbol</b>	<b>Description</b>	<b>Unit</b>
$\alpha$	Total elastic compression	(mm)
$\alpha_1$	Compression in unequal diameter crossed cylinders	(mm)
$\alpha_2$	Compression in two cylinders in contact with axes parallel	(mm)
$D$	Diameter of body	(mm)
$D_1$	Diameter small	(mm)
$D_2$	Diameter large	(mm)
$r_c/D_c$	Radius or Diameter of cable	(mm)
$r_r/D_r$	Radius or Diameter of roller	(mm)
$d_y$	Compression in y direction	(mm)
$a$	Large ellipse radius	(mm)
$b$	Large ellipse radius 2	(mm)
$l$	Contact length	(mm)
$\Delta u$	Displacement of a spring	(m)
$u$	Length of spring	(m)
$A$	Inverse of $D_1$	(mm <sup>-1</sup> )
$B$	Inverse of $D_2$	(mm <sup>-1</sup> )
$A_A$	Area	(mm <sup>2</sup> )
$C_A$	Contact area	(mm <sup>2</sup> )
$g$	Gravitational acceleration constant 9.81m/s <sup>2</sup>	(m/s <sup>2</sup> )
$\beta$	Angle	(°)
$\theta$	Angle for ellipse integral	(rad)

$P$	Force	(N)
$P_p$	Point load	(N)
$P_r$	Load between cable and roller	(N)
$\bar{P}$	Uniform load	(N/m)
$k$	Stiffness spring	(N/m)
$m_l$	Mass per length of the cable	(kg/mm)
$E$	Elastic modulus	(Pa)
$G$	Shear modulus	(Pa)
$p$	Pressure	(MPa)
$\sigma$	Normal stress	(MPa)
$V$	Material parameter	(mm <sup>2</sup> /N)
$S_{mp}$	Stiffness modifying parameter	(mm <sup>2</sup> /N)
$Q$	Combined material parameter	(mm <sup>2</sup> /N)
$e$	Eccentricity of ellipse contact	
$K$	Complete elliptic integrals of the first class respectively with modulus e	
$E$	Complete elliptic integrals of the second class respectively with modulus e	
$\nu$	Poisson's ratio	
$[K_{stiff}]$	Stiffness matrix	
$i$	Step variable for a for loop	
$[ \ ]$	Matrix	
$\{ \}$	Vector	
$\epsilon$	Strain	

<b><i>Acronym</i></b>	<b><i>Description</i></b>
<i>ABB</i>	ASEA Brown Boveri Ltd
<i>AC</i>	Alternating Current
<i>CAD</i>	Computer Aided Design
<i>DC</i>	Direct Current
<i>FEM/FEA</i>	Finite Element Method/ Finite Element Analysis
<i>HVC</i>	High Voltage Cables
<i>INP</i>	Input file generated by ABAQUS
<i>MI</i>	Paper Lapped
<i>NKT</i>	Nordiske Kabel og Traadfabriker
<i>ODB</i>	Output file generated by ABAQUS
<i>XPPE</i>	Cross-Linked Polyethylene

# Table of Contents

<b>1</b>	<b>INTRODUCTION.....</b>	<b>1</b>
1.1	Background.....	1
1.1.1	Organization of NKT .....	1
1.1.2	Cable compositions .....	1
1.1.3	Background to the problem .....	2
1.2	Problem statement .....	4
1.3	NKT's Interests.....	4
1.4	General Interests .....	4
1.5	Sustainability aspects .....	4
1.6	Ethical aspects.....	4
1.7	Aim, objectives .....	5
1.8	Delimitations .....	6
1.9	Thesis Questions.....	7
<b>2</b>	<b>THEORETICAL FRAMEWORK.....</b>	<b>8</b>
2.1	Hertzian's theory .....	8
2.1.1	Hertzian's theory for crossed cylinders.....	9
2.1.2	Hertzian's theory for two cylinders in contact with axes parallel.....	13
2.2	Finite element method (FEM) .....	14
2.3	Pressure films .....	16
2.3.1	How the pressure films work and their pressure ranges.....	17
<b>3</b>	<b>METHOD .....</b>	<b>18</b>
3.1	General methods .....	18
3.1.1	Risk analyse.....	18
3.1.2	Planning schedule.....	18
3.1.3	Five Whys .....	18
3.2	Complex system describing.....	19
3.2.1	Critical thinking.....	20
3.2.1.1	Logical reasoning .....	20
3.2.1.2	Check the produced result .....	20
3.2.1.3	Start with a simple model and improve it step by step.....	21
3.2.1.4	Discretization of a complex system.....	21
3.2.2	Conversation.....	21

3.2.3	Idea generation .....	22
3.3	Working process of answering first thesis question .....	23
3.3.1	Usage the pressure film to determine the radial force in static case .....	23
3.3.2	Usage of the pressurefilm to determine the radial force in dynamic case.....	26
3.3.1	Verify the method of determine the radial force by experimental test .....	29
3.4	Working process of answering second thesis question .....	30
3.4.1	FEM to determine the relation between compression and radial force.....	30
3.4.1.1	Finding material properties for the FEM model.....	31
3.4.1.2	Simulation automation process.....	33
3.4.1.3	Cable model and FEM setup for double armoured DC cable.....	34
3.4.1.4	Cable model and FEM setup for bundled AC cable.....	36
3.4.2	By using experiment tests .....	38
3.4.3	Describing the stiffness of a nonhomogeneous cable .....	39
3.4.4	Theoretically divide the total compression into local compressions.....	41
3.4.5	Using the ellipse diameters, Hertzian’s theory and applied force.....	43
3.5	Experimental test .....	45
3.5.1	Pointload test .....	45
3.5.1.1	Theoretical model of the pointload test .....	46
3.5.1.2	FEM model of the pointload test in ORCAFLEX .....	47
3.5.2	Squeeze rig test.....	48
3.5.2.1	The experiment for the double armoured DC cable .....	51
3.5.2.2	The experiment for the bundled AC cable.....	52
<b>4</b>	<b>RESULT .....</b>	<b>53</b>
4.1	The result of using the pressure film to determine the radial force.....	53
4.1.1	Small single armoured DC cable used in Pointload test .....	53
4.1.2	Double armoured DC cable and bundled AC cable in Squeeze test .....	54
4.2	Relation between compression and radial force for a double armoured DC cable. ..	55
4.2.1	FEM result for double armoured DC cable.....	55
4.2.2	Result from force and displacement sensor for a double armoured DC cable...	56
4.2.3	Pressure film result for a double armoured DC cable .....	60
4.3	Relation between compression and radial force for a bundled AC cable.....	63
4.3.1	FEM result for bundled AC cable. ....	63
4.4	Ellipse diameter result for bundled AC cable.....	65

4.5	Result from force and displacement sensor for a bundled AC cable.....	67
<b>5</b>	<b>DISCUSSION .....</b>	<b>69</b>
5.1	Using the pressure film to determine the radial force.....	69
5.2	Comparison between the results of using FEM, sensor and ellipse diameter result for describing the relation between compression and force for a double armored DC cable. ...	70
5.3	Comparison between the results of using FEM, sensor and ellipse diameter result for describing the relation between compression and force for the bundled AC cable.....	72
5.4	The hydraulic cylinder.....	75
<b>6</b>	<b>CONCLUSION .....</b>	<b>76</b>
6.1	Using the pressure film determine the force.....	76
6.2	Use the compression to determine the radial force.....	76
<b>7</b>	<b>FUTURE WORKS.....</b>	<b>77</b>
7.1	Measuring the force between the roller and the cable.....	77
7.1.1	Force sensor film.....	77
7.1.2	Radial force sensor.....	78
7.2	Improve the FEM model.....	79
7.2.1	Make a representation of the armouring wires.....	79
7.2.1	Plasticity.....	79
7.3	The cable is temperature dependent .....	79
<b>1</b>	<b>REFERENCES .....</b>	<b>80</b>
<b>APPENDIX A:.....</b>		<b>82</b>
A.1	Solving the eccentricity .....	82
A.2	Risk analyse for the project .....	83
A.3	Geometrical theory – Before study known theories .....	85
A.4	Study the behavior of the two crossed steel cylinders.....	89
A.5	Finite element method for two steel cylinders.....	93
	Comparison between Hertzian’s theory and FEM for two crossed steel cylinders.....	96
A.6	Compression in a nonarmoured cable.....	98
A.7	Relation between total compression for a nonarmoured .....	99
A.8	The MATLAB code for solving the eccentricity.....	101
A.9	MATLAB script for two steel cylinders.....	103
A.10	MATLAB script for dividing the total compression into local compression between roller and cable and between holder and cable.....	106

A.11	MATLAB script for solving the eccentricity by using the ellipse diameters .....	109
A.12	MATLAB script for translating pressure from the pressure films to force .....	111
A.13	Automatic simulation process.....	112
<b>APPENDIX B</b>	.....	<b>114</b>
B.1	About software .....	114
B.2	Diagram structure .....	114

## Table of Figures

Figure 1.1 - Cable compositions and cable types.	1
Figure 1.2 - Cable and roller supports.	2
Figure 1.3 - Caterpillar makes it possible to transport the cables through the roller support track in the factory.	2
Figure 1.4 - Sidewall pressure accruing in the radius of the roller support track.	3
Figure 1.5 - Elastic deformation of a cable.	6
Figure 1.6 - Plastic deformation of a cable.	6
Figure 2.1 - Unequal diameter cylinders crossed with their axes at right angle.	9
Figure 2.2 - Two cylinders in contact with axes parallel.	13
Figure 2.3 - Bowl formed contact.	13
Figure 2.4 - The theory of FEM.	14
Figure 2.5 - Two springs in series.	15
Figure 2.6 - Example of used pressure film and pressure chart. Inspired by (FUJIFILM, 2018)	16
Figure 2.7 - The pressure film's different layers. Inspired by (FUJIFILM, 2018)	17
Figure 2.8 - Pressure ranges for different types of pressure films. Inspired by (FUJIFILM, 2018)	17
Figure 3.1 - Analyze a complex system. Inspired by (Broman, 2003)	19
Figure 3.2 - Determine force by using the maximum pressure and ellipse diameter from the pressure film LLW.	23
Figure 3.3 - Pressure distribution for ellipse contact.	24
Figure 3.4 - Determine the maximum pressure by pressure film LLW and LW.	25
Figure 3.5 - Single part cable rolling over pressure films.	27
Figure 3.6 - Bundled cable rolling over pressure films.	28
Figure 3.7 - Stress-strain curve for different materials.	31
Figure 3.8 - Using MATLAB as a server and ABAQUS as a client.	33
Figure 3.9 - Double armoured DC cable.	34
Figure 3.10 - Boundary condition and mesh for a double armoured DC cable.	35
Figure 3.11 - Bundled AC cable.	36
Figure 2.12 - Boundary condition and mesh for a bundled AC cable.	37
Figure 3.13 - Different load angles for the bundled cable.	38
Figure 3.14 - Nonhomogeneous cable translated to homogenous cable for every specific load case.	39
Figure 3.15 - Local compression of a cable in the upcoming experiment.	41
Figure 3.16 - Theoretical divide the total compression.	42
Figure 3.17 - Theoretical model of the Pointload test.	45
Figure 3.18 - Pointload test in reality.	45
Figure 3.19 - Theoretical model of point load test.	46
Figure 3.20 - Simulation of pointload test in ORCAFEX.	47
Figure 3.21 - The squeeze rig.	48
Figure 3.22 - Equipment for the squeeze rig.	49
Figure 3.23 - Equipment mounted in Squeeze rig.	50
Figure 3.24 - Roller support mounted in the middle of the Squeeze rig's clamp.	50
Figure 3.25 - A double armored cable in the squeeze rig.	51
Figure 3.26 - The experiment for a bundled cable.	52

Figure 3.27 - Different load angles.	52
Figure 4.1 - The result from the pressure films at point load test.	53
Figure 4.2 - Pressure distribution on the armouring wires	54
Figure 4.3 - Relation between compression and force for a double armored cable by using FEM.	55
Figure 4.4 - Force sensor registered data for load case 6000N for double armored cable.	56
Figure 4.5 - Displacement sensor registered data for load case 6000N for the double armored cable.	57
Figure 4.6 - Total compression in a double armored cable by using the sensor result.	58
Figure 4.7 - Division of the total compression for double armored cable.	59
Figure 4.8 - The relation between the compression and force for a double armored cable by using the sensor result.	59
Figure 4.9 - Ellipse diameter results from the pressure films for the double armored cable.	60
Figure 4.10 - The relation between the ellipse diameters from the pressure films and applied force for a double armored cable.	61
Figure 4.11 - The relation between the compression and force for a double armored cable by using the ellipse diameters and applied force.	62
Figure 4.12 - Total compression for the bundled cable by using FEM.	63
Figure 4.13 - Divide the total compression into the local compression between roller and cable and between holder and cable for the bundled cable.	64
Figure 4.14 - Ellipse diameters result from the pressure films for the bundled cable.	65
Figure 4.15 - The relation between ellipse diameters and force for different load angles for a bundled cable.	66
Figure 4.16 - The relation between compression and force for a bundled cable in different load angles by using the ellipse diameter and the applied force.	66
Figure 4.17 - Force registered by the force sensor for the load case 6000N and load angle 0° for a bundled cable.	67
Figure 4.18 - Total compression registered by the displacement sensor for load case 6000N and load angle 0° for a bundled AC cable.	67
Figure 4.19 - Total compression from the sensor result for the different load angles for a bundled cable.	68
Figure 4.20 - Compression between roller and cable and holder and cable for the different load angles for a bundled cable.	68
Figure 5.1- The comparison between the methods for describing the relation between compression and force for a double armored cable	70
Figure 5.2 - Comparison between the methods for describing the relation between compression and force for the bundled cable in load angle 0°.	72
Figure 5.3 - Comparison between the methods for describing the relation between compression and force for the bundled cable in load angle 30°.	73
Figure 5.4 - Comparison between the methods for describing the relation between compression and force for the bundled cable in load angle 60°.	73
Figure 5.5 - Load angle for the bundled cable.	74
Figure 5.6 - Rotating of the cable during the loading will increase the larger ellipse diameter.	75
Figure 7.1 - Force sensor film with load cells.	77
Figure 7.2 - Radial force sensor applied on the roller support.	78
Figure 7.3 - Transition temperature for elastomers and crosslinking thermosets.	79

Figure A.1.1 - Solving the eccentricity $e$ by using a restricted random guess in an iterative process.	82
Figure A.3.1 - Cable compressed by a roller.	85
Figure A.3.2 - Plane YX Cable compressed by a roller.	86
Figure A.3.3 - Plane YZ cable compressed by a roller.	86
Figure A.3.4 - Contact area of a cable compressed by a roller.	86
Figure A.3.5 - Larger compression in the middle of the contact area.	87
Figure A.3.6 - Pressure distribution of two crossed cylinders. (inspired by (MHZ'as, 2009))	88
Figure A.4.1 - Force vs maximum pressure for two unequal crossed steel cylinders by using Hertzian's theory.	90
Figure A.4.2 - Force vs Compression for two unequal crossed steel cylinders by using Hertzian's theory.	91
Figure A.4.3 - Force vs Contact area for two unequal crossed steel cylinders by using Hertzian's theory.	91
Figure A.4.4 - Pressure distribution for Measurement 1 by using Hertzian's theory.	92
Figure A.5.1 - Two crossed linked steel cylinders in INVENTOR and ABAQUS.	93
Figure A.5.2 - Boundary conditions in ABAQUS for two crossed steel cylinders.	94
Figure A.5.3 - Force vs Pressure max for two unequal crossed steel cylinders by using FEM.	95
Figure A.5.4 - Force vs Compression for two unequal crossed steel cylinders by using FEM.	96
Figure A.5.5 - Force vs Pressure max: Comparison between Hertzain's theory and by a FEM model.	96
Figure A.5.6 - Force vs compression: Comparison between Hertzain's theory and by a FEM model.	97
Figure A.6.1 - Boundary condition and mesh for the no armored cable.	98
Figure A.7.1 - The relation between compression $\alpha$ and force $P$ for the no armored cable.	99
Figure A.7.2 - Relation between stiffness modifying parameter $S_{mp}$ and force $P$ for the no armored cable.	99
Figure A.7.3 - Schedule over the simulation and solving process.	100

# 1 INTRODUCTION

*This chapter describes the background, problems statement, purpose and delimitations within the project.*

## 1.1 Background

### 1.1.1 Organization of NKT

NKT is a world-leading supplier of high-voltage cable systems and installation services for all types of submarine and underground power transmission applications. Drawing on more than 140 years of cable expertise, NKT has an unrivalled track record of delivering high voltage AC and DC cable system solutions. NKT is a Danish owned concern and is presence in 18 countries and employ approximately 3400 people. In the year of 2017 NKT acquired ABB HVC cables in Karlskrona, Sweden. (NKT, 2018)

### 1.1.2 Cable compositions

A high voltage submarine cable consists of a conductor which is made of copper or aluminium and make the electric conductivity possible. The conductor screening, insulation and insulation screening are extruded to give a smooth dielectric surface. The insulation is either paper lapped (MI) or Cross-Linked Polyethylene (XLPE). To protect the cable from water ingression, the high voltage submarines cables are extruded with lead. The outer layer of the high voltage cable is the armouring, which is normally made of steel. The purpose of the armouring is to protect the cable against surroundings and to give a stability in the cable (Malm, 2018). (see Figure 1.1).



*Figure 1.1 - Cable compositions and cable types.*

Two different types of cable are usually produced, either bundled cable (AC) or single part cable (DC). The bundled cable has plastic profiles that are laid between each part cable. The profiles are installed as fillers to make the cable round and are utilized for wire fibre optics.

### 1.1.3 Background to the problem

During production and installation of high voltage cables, the cable is exposed to mechanical loads such as radial forces and tensile forces such as bending and twisting moments. An important part of the engineering for production and installation of these cables is to analyse the different steps of the planned operations to ensure that the cable limitations are not violated.

One of these operations are for example when the cable is transported throughout the factory from the first machine to the second one. Every specific cable has different compositions and therefore it must go in a specific order through every machine. By using roller supports (see Figure 1.2) combined with a pulling machine so called caterpillar (see Figure 1.3) makes it possible for the cable to travel through the factory.

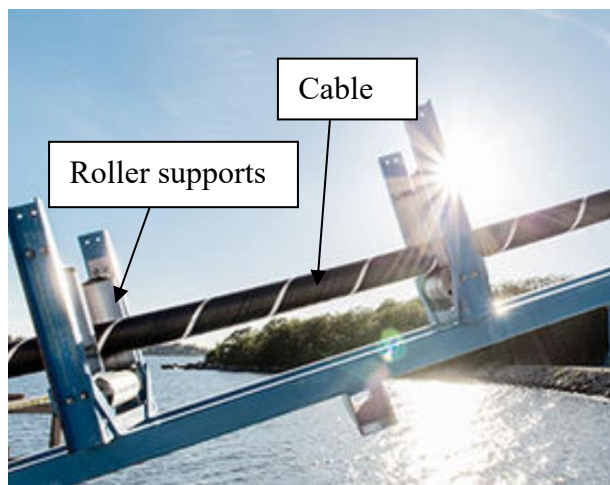


Figure 1.2 - Cable and roller supports.

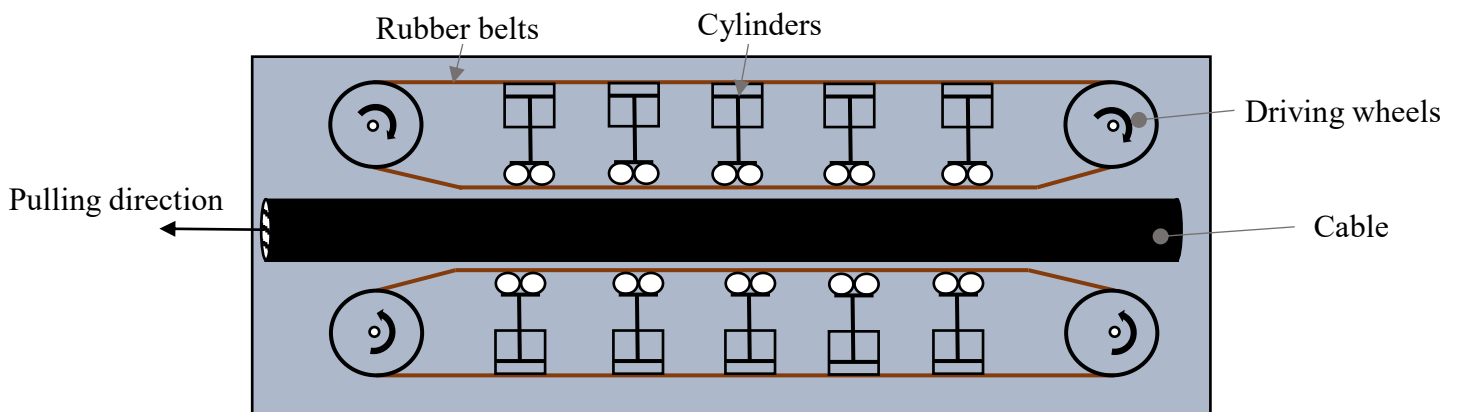


Figure 1.3 - Caterpillar makes it possible to transport the cables through the roller support track in the factory.

The problem is when the cable must go in a turning roller support track. Because the cable is pulled by a caterpillar it wants to take the shortest way between the machines. The bending stiffness also wants to straighten the cable. But when the roller supports are there, they will force the cable to follow the roller support track and no cable will be bent within its natural state.

In the radius of these curves it will be a radial force on the cable from the roller support that will create a sidewall pressure (see Figure 1.4). In several cable industries the sidewall pressure can also be expressed as force and force per length, which is a bit confusing. In this thesis the sidewall pressure is the pressure and radial force is the force.

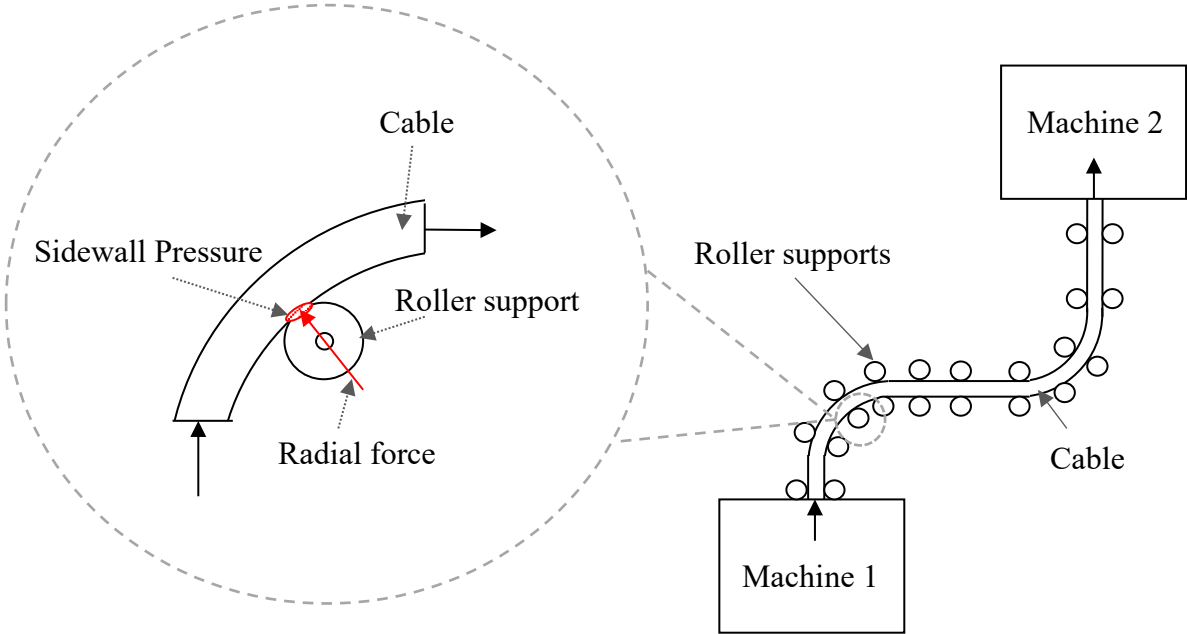


Figure 1.4 - Sidewall pressure accruing in the radius of the roller support track.

In theory the roller supports should be constructed in such way that they will take up equally amount of force from the cable, but in reality some of the roller supports are going to take up more of the radial force than others. This generates two problems:

- 1) Not equal distributed force on the rollers can create failure on some specific roller supports cause by fatigue.
- 2) Too high radial forces on the cable will make it plasticize, which can damage the cable's conductivity.

## **1.2 Problem statement**

Extend the knowledge on the sidewall pressure that is occurring between the roller supports and the cable. The sidewall pressure can deform the cable which will damage the cable's conductivity. The roller support can also get damage in the long run. This pressure need to be studied and in some way be measured to ensure that the cable limitations is not violated.

## **1.3 NKT's Interests**

NKT is interested to measure how large radial force it becomes on the rollers to ensure that the maximum radial force in cable is not exceeded. This limit is already known by NKT for each specific cable. By measuring the radial force between the roller and the cable it makes it possible to shims the rollers to distribute the force more equally between them, and therefore reduce the sidewall pressure.

## **1.4 General Interests**

Contact mechanics is a common area and can be useful in several applications not only in cable industries but also for example metal rolling, tires, bearings, hardness tests etc. The general interests of this thesis work are to get a better knowledge about the relation between radial forces and compression and how it will affect a cylindrical object that contain different layers of materials.

The basic concept is to show how to implement an easy general theory combined with FEM simulation and experimental test to be able to describe the relation between the compression and the radial force in a HVC. By using this method, it will be possible to discretize the complex system. That will give more of an overview but still generate a useful result that is easier to implement and understand for others. A better knowledge about radial force and its effect, makes it possible to reduce failures in several technical applications in our society.

## **1.5 Sustainability aspects**

Regarding sustainability, this thesis can reduce material resources on NKT. Because they can then ensure the cable limitations are not violated and therefore will reduce the risk of damaging the cable during the manufacturing and less waste will be produced. The economic and time advantages are that it saves money and time on less reworks and the recycling costs for the wastes.

## **1.6 Ethical aspects**

In an ethical point of view this thesis work will present different measuring methods to determine the radial force between cable and roller, which are two moving parts and risks of crushing injury is high. Therefore, shall a risk assessment always be performed before a measuring method is implemented and used in the real roller support track. NKT's norm is that they will always prioritize safety first. High safety on the workplace will always be an advantage for the society in general to make the work environment safe for all the employers.

## **1.7 Aim, objectives**

The aim of this project is to come up with a method to further validate which radial force that is occurring between the roller supports and the cable. The objective is to ensure that the cable limitations are not violated.

## 1.8 Delimitations

The limitation of this thesis work is it that the study will only be implemented on high voltage cables with Cross-Linked Polyethylene (XLPE) insulation and the radial forces that are produced is from the roller supports. The bending of cable will be assumed small and will not affect the radial force. Following theoretical models and simulations will be assumed that the cable will only deform elastic.

The Figure 1.5 and Figure 1.6 below shows the difference between an elastic deformation and plastic deformation of a cable:

Elastic case:

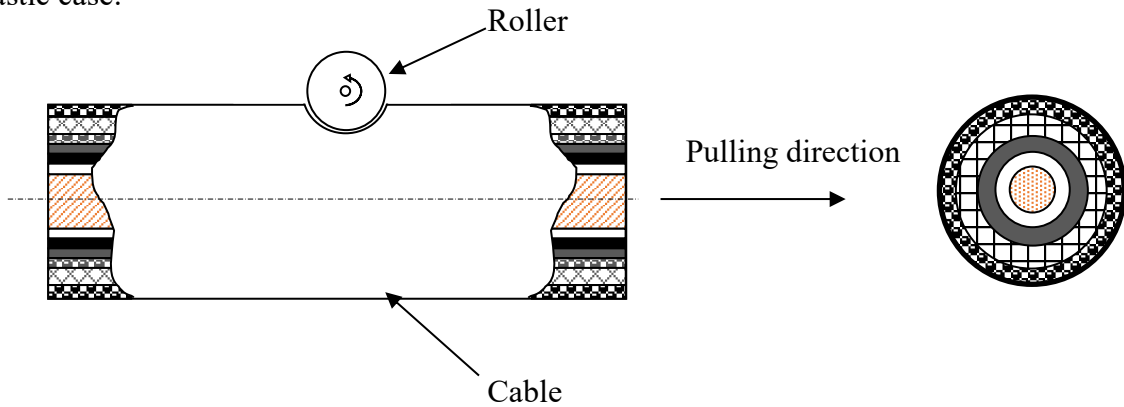


*Figure 1.5 - Elastic deformation of a cable.*

Plasticity case:

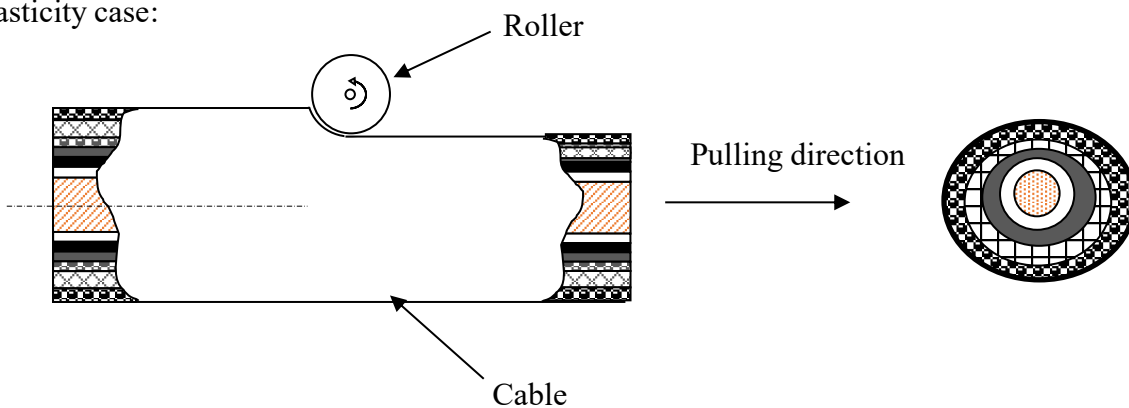


*Figure 1.6 - Plastic deformation of a cable.*

Other delimitations and following assumption is made:

- The temperature is constant and will not affect the material properties of the cable.
- The compression will only accrue in the cable and not in the roller.
- It is possible to describe a nonhomogeneous cylinder (a cable) with several homogenous cylinders that have a specific stiffness for each specific load case.

- The velocity of the cable is small and will not have impact on the compression in the cable.

The radial force can be determined in several different ways. In this project two different ways of determining radial force are chosen:

- Determine the radial force by using the pressure film.
- Determine the radial force by measuring the compression.

These are chosen because of NKT wants to investigate and see if it is possible to use these less costly methods for determine the radial force. This will be valuable basis for making decision about if the more expensive measuring methods are going to be needed or not.

## **1.9 Thesis Questions**

Following thesis questions have been stated for these two ways of determining the radial force to ensure that the cable limitations are not violated.

- 1) How can the pressure film be used to measure the radial force between a roller support and high voltage cable?*
  - 2) By measuring the compression in cable how can the radial force be determined?*
- SQ2) How can a relation between radial force and compression (produced by roller support) of two different types of high voltage cables (DC and AC) be described?*

## 2 THEORETICAL FRAMEWORK

---

*In this chapter will the theories and information about measuring method that are the foundation of this work be presented and described.*

### 2.1 Hertzian's theory

Hertzian's theory from 1882 is associated to contact mechanics and is describing how the stress will behave when two elastic solid come in contact and deform slightly by an imposed load. This theory has been useful for example to study bearing and locomotive wheel-rail contact stresses. A detail derivation of the Hertzian's theory can be found in the book Contact Mechanics by K.L Johnson. (Johnson, 2012)

Hertzian theory use the following assumptions:

- Elastic deformation, in other words the elastic limits of the materials is not exceeded.
- Homogenous materials.
- Small deformations.
- No friction between the contact surfaces.
- Perfectly smooth surfaces.
- Adhesion is neglected.

Further theories like DMT (Derjaguin Muller Toporov), Maugi Dugdale and JKR (Johnson Kendall Roberts) are also including adhesion which is more important to consider when the adhesion have a larger impact on the contact behaviour, for example when softer materials interact with each other. Many of these theories and Hertzian's theory are tested experimentally for very smooth surfaces and these theories models are describing it well. (ME 597 Lecture 8: Introduction to Contact Mechanics, 2010)

Hertzian's theory will be used in this thesis to get fundamental knowledge about contact pressure and will later in the work be adjusted practically to describe the sidewall pressure between the roller and a high voltage cable.

In a technical paper (M.J Puttock E.G Thwaite, 1969) they describe different types of cases based on Hertzian's theory. One of cases are two cylinders with unequal diameter that are 90 degrees crossed. Another case is when the cylinders are crossed with arbitrary angle. The second case will not be considered in this work because the contact area is in the worst case scenario smallest when the cylinders are 90 degree crossed. Later will also the theory of two parallel cylinders be used. Based on this technical report, calculations and examples will be made to verify the theory. Notice that in this reference they are using gram force (gf) instead of newton (N) so the equations have been rewritten in this thesis to be able to use newton as input unit.

### 2.1.1 Hertzian's theory for crossed cylinders

Unequal diameter cylinders crossed with their axes at right angle see Figure 2.1:

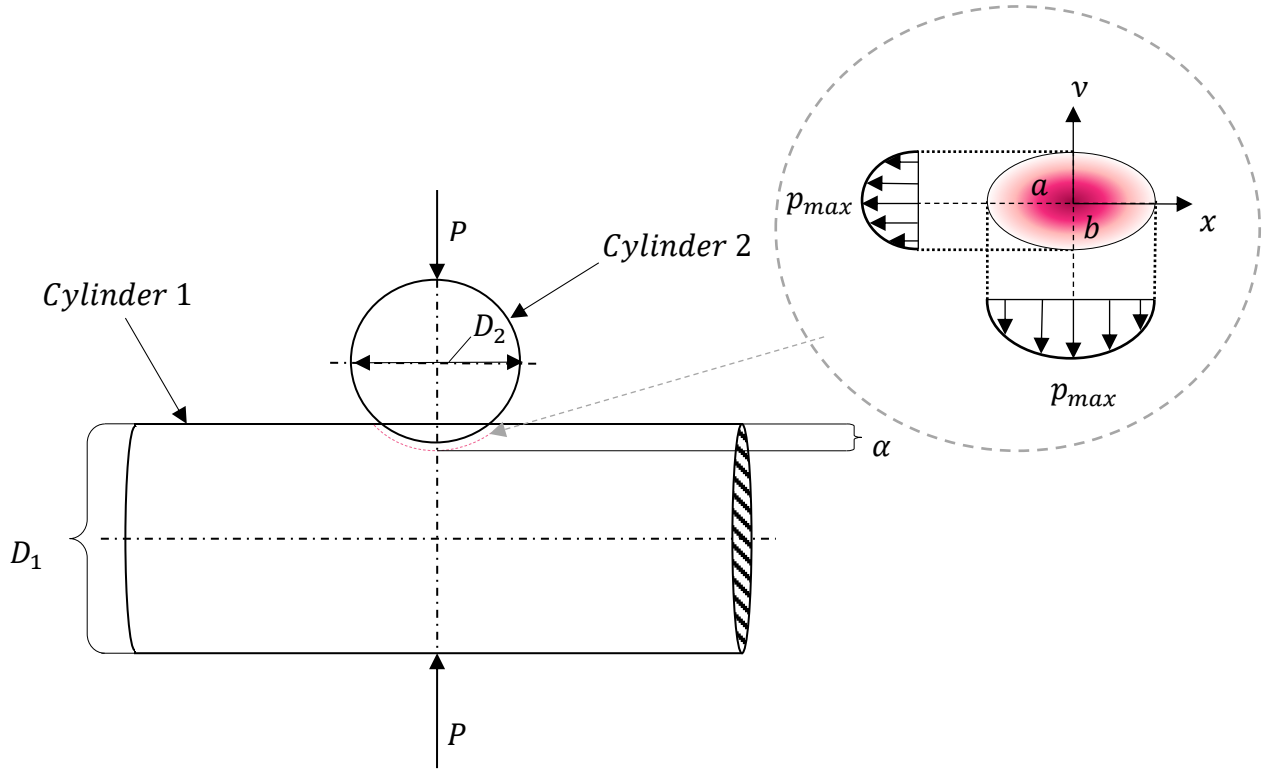


Figure 2.1 - Unequal diameter cylinders crossed with their axes at right angle.

The total elastic compression  $\alpha$  in two unequal diameter crossed cylinder is described in the following equation:

$$\alpha = 2K(10^6 \cdot P \cdot Q)^{\frac{2}{3}} \cdot \left( \frac{1}{2D_1 \cdot \left( -\frac{1}{e} \frac{dE}{de} \right)} \right)^{1/3} \quad (2.1)$$

where  $P$  is applied force,  $Q$  is material parameter for dissimilar materials and  $D_1$  is the large diameter.  $K$  and  $E$  describes the complete elliptic integral of the first and second class respectively with the eccentricity  $e$ . These two last mentioned parameters are related to the diameters of the cylinders.

The pressure distribution for the contact surface of an ellipse is described in equation (2.2):

$$p(x, y) = \frac{3P}{2\pi ab} \left( 1 - \frac{x^2}{a^2} - \frac{y^2}{b^2} \right)^{1/2} \quad (2.2)$$

where  $a$  is the large ellipse radius and  $b$  is the small ellipse radius of the elliptical contact surface. The  $x$  and  $y$  are the coordinates with the origin in the middle of the ellipse (see pressure distribution in Figure 2.1). For example if  $x$  and  $y$  is zero in Equation (2.2) it will be the maximum pressure at the centre of the ellipse.

The material parameter for dissimilar materials  $Q$  is described in equation (2.3).

$$Q = \frac{3}{4}(V_1 + V_2) \quad (2.3)$$

where  $V_1$  and  $V_2$  is the material parameter for respective cylinder. This material parameter  $V$  is dependent on the Poisson's ratio  $\nu$  and elastic modulus  $E$  in following way:

$$V = \frac{1 - \nu^2}{\pi E} \quad (2.4)$$

In the equation (2.5) the eccentricity  $e$  is describing the ratio between small ellipse radius  $b$  and the large ellipse radius  $a$  of the contact area of an ellipse.

$$e = \left(1 - \frac{b^2}{a^2}\right)^{\frac{1}{2}} \quad (2.5)$$

The equation (2.6) describes the elliptic integral of first class.

$$K = \int_0^{\frac{\pi}{2}} \frac{d\theta}{(1 - e^2 \sin^2(\theta))^{\frac{1}{2}}} \quad (2.6)$$

The equation (2.7) describes the elliptic integral of second class.

$$\frac{1}{-e} \frac{dE}{de} = \int_0^{\frac{\pi}{2}} \frac{\sin^2(\theta)}{(1 - e^2 \sin^2(\theta))^{\frac{1}{2}}} d\theta \quad (2.7)$$

To get the ellipse radiuses  $a$ ,  $b$  and elliptic integrals of first class  $K$  and second class  $\frac{1}{-e} \frac{d\mathbf{E}}{de}$  the eccentricity  $e$  must first be known. By combining the following equations:

$$\frac{d\mathbf{E}}{de} = -e \int_0^{\frac{\pi}{2}} \frac{\sin(\theta)^2}{(1 - e^2 \sin(\theta)^2)^{\frac{1}{2}}} d\theta \quad (2.8)$$

$$\frac{dK}{de} = e \int_0^{\frac{\pi}{2}} \frac{\sin(\theta)^2}{(1 - e^2 \sin(\theta)^2)^{\frac{3}{2}}} d\theta \quad (2.9)$$

$$Aa^3 = -\frac{2QP}{e} \cdot \frac{d\mathbf{E}}{de} \quad (2.10)$$

$$Ba^3 = \frac{2QP}{e} \cdot \frac{dK}{de} \quad (2.11)$$

The equation can then be written like following equation:

$$\frac{A}{B} = \frac{\int_0^{\frac{\pi}{2}} \frac{\sin(\theta)^2}{(1 - e^2 \sin(\theta)^2)^{\frac{1}{2}}} d\theta}{\int_0^{\frac{\pi}{2}} \frac{\sin(\theta)^2}{(1 - e^2 \sin(\theta)^2)^{\frac{3}{2}}} d\theta} \quad (2.12)$$

Where  $A = \frac{1}{D_1}$ ,  $B = \frac{1}{D_2}$  and  $\theta$  is the angle of the ellipse integral.

$$\frac{D_2}{D_1} = \frac{\int_0^{\frac{\pi}{2}} \frac{\sin(\theta)^2}{(1 - e^2 \sin(\theta)^2)^{\frac{1}{2}}} d\theta}{\int_0^{\frac{\pi}{2}} \frac{\sin(\theta)^2}{(1 - e^2 \sin(\theta)^2)^{\frac{3}{2}}} d\theta} \quad (2.13)$$

The eccentricity  $e$  is now only related to the diameters of the cylinders and can now be solved from the equation (2.13) (see Appendix A.1 how it was solved in this thesis).

When  $e$  is known it is possible to get the large ellipse radius  $a$  by using equation (2.14):

$$a = \left( -\frac{2QP}{Ae} \cdot \frac{dE}{de} \right)^{\frac{1}{3}} \quad (2.14)$$

And by using equation (2.15) it is possible to get the small ellipse radius  $b$ :

$$b = (a^2(1 - e^2))^{\frac{1}{2}} \quad (2.15)$$

The elliptic integral of first class  $K$  and second  $\frac{1}{-e} \frac{dE}{de}$  can now be solved according to the equations (2.6) and (2.7).

### 2.1.2 Hertzian's theory for two cylinders in contact with axes parallel

The Figure 2.2 below presents two cylinders in contact with axes parallel. (M.J Puttock E.G Thwaite, 1969):

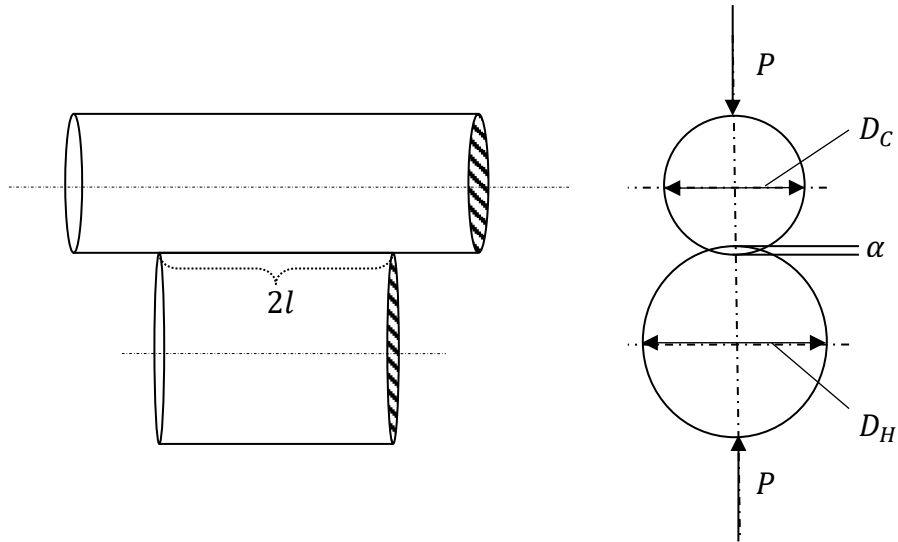


Figure 2.2 - Two cylinders in contact with axes parallel.

The compression  $\alpha$  for two parallel cylinders is described as following equation:

$$\alpha = 10^6 \cdot \bar{P} \cdot (V_1 + V_2) \cdot \left( 1 + \ln \left( \frac{8l^2}{10^6 \cdot \bar{P}(V_1 + V_2)} \cdot \left( \frac{1}{D_H} + \frac{1}{D_C} \right) \right) \right) \quad (2.16)$$

where  $\bar{P}$  is the force per contact length. In equation (2.17)  $2l$  is the contact length,  $V_1$  and  $V_2$  is the material parameter for the cylinders and  $D_H$  and  $D_C$  is the diameter of the cylinders.

$$\bar{P} = \frac{P}{2l} \quad (2.17)$$

By setting the diameter  $D_H$  to negative will instead give bowl formed holder like Figure 2.3 below (Bamberg, 2006):

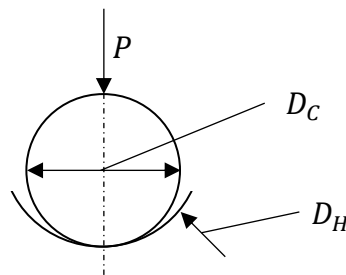


Figure 2.3 - Bowl formed contact.

## 2.2 Finite element method (FEM)

FEM is a numerical method to solve partial differential equation in form of boundary value problems. FEM is a method that will discretize the structure in to small elements there each element interacts with each other by nodes. In an analogy of spring system, it can simplified explained for mechanical structures as following (see Figure 2.4). (A. Josefsson / rev M.Herman, 2014)

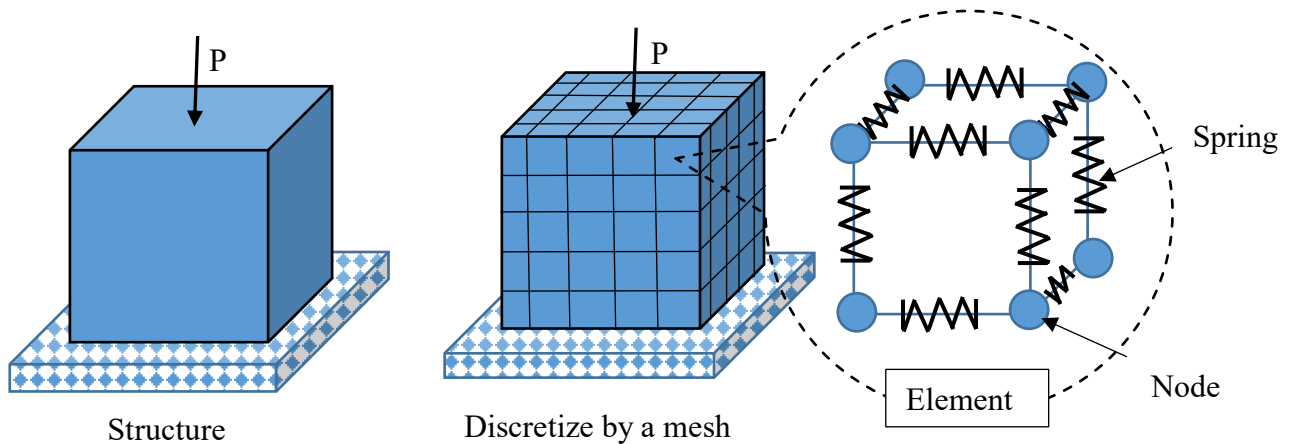


Figure 2.4 - The theory of FEM.

The force  $P$  for one dimensional spring can be described by the spring characteristic and  $k$  multiplied with the distance change  $\Delta u$  of the spring:

$$P = k \cdot \Delta u \quad (2.18)$$

Hooke's law describes the stress  $\sigma$  by the modulus of elasticity  $E$  and strain  $\epsilon$ :

$$\sigma = E \cdot \epsilon \quad (2.19)$$

The stress  $\sigma$  can also be described by force  $P$  and area  $A_A$ :

$$\sigma = \frac{P}{A_A} \quad (2.20)$$

By combining these two equations (2.19) and (2.20) it is possible to describe the spring characteristic  $k$  by modulus of elasticity  $E$  and geometrical properties like area  $A_A$  and length of the spring  $u$ :

$$P = \frac{A_A E}{u} \cdot \Delta u \quad (2.21)$$

By connecting several springs together a representation of the structure can be made, an example of two springs are presented in Figure 2.5:

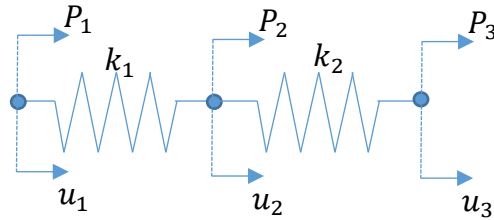


Figure 2.5 - Two springs in series.

The two springs in series can in matrix form be written:

$$\begin{Bmatrix} P_1 \\ P_2 \\ P_3 \end{Bmatrix} = \begin{bmatrix} k_1 & -k_1 & 0 \\ -k_1 & k_1 + k_2 & -k_2 \\ 0 & -k_2 & k_2 \end{bmatrix} \cdot \begin{Bmatrix} u_1 \\ u_2 \\ u_3 \end{Bmatrix} \quad (2.22)$$

This simple spring system can then be scaled up to a larger spring system for example in three dimensions. There  $K_{stiff}$  is the global stiffness matrix of the structure.

$$\{P\} = [K_{stiff}]\{u\} \quad (2.23)$$

The stiffness matrix  $[K_{stiff}]$  is depending on the geometry and material properties for the model that going to be analyzed. By setting specific boundary conditions for example in translation for  $\{u\}$  makes the equation system (2.4) solvable. To make a good representation of the structure and to get more accurate result, many elements are needed. The equation system will then be larger and take longer time to solve. Today software like for example ABAQUS are used to create and solve this equations system for different structures.

### 2.3 Pressure films

Pressure film from Fujifilm is a film that change colour tone depending on how large pressure it is on the film. That can later be compared in a sheet or with help of a scanner which contain a colour spectrum that are connected to a specific pressure level. This can be used inter alia in this case to measure the surface pressure that will accrue between the roller and the cable. These films have different spectrum of pressure ranges which can measure low to high pressures depending on film model (see Figure 2.8). According to Fujifilm the accuracy of these films are about  $\pm 10\%$ , they are also sensitive to sunlight and the results is depending on the temperature and humidity. A following example is presented in the Figure 2.6.

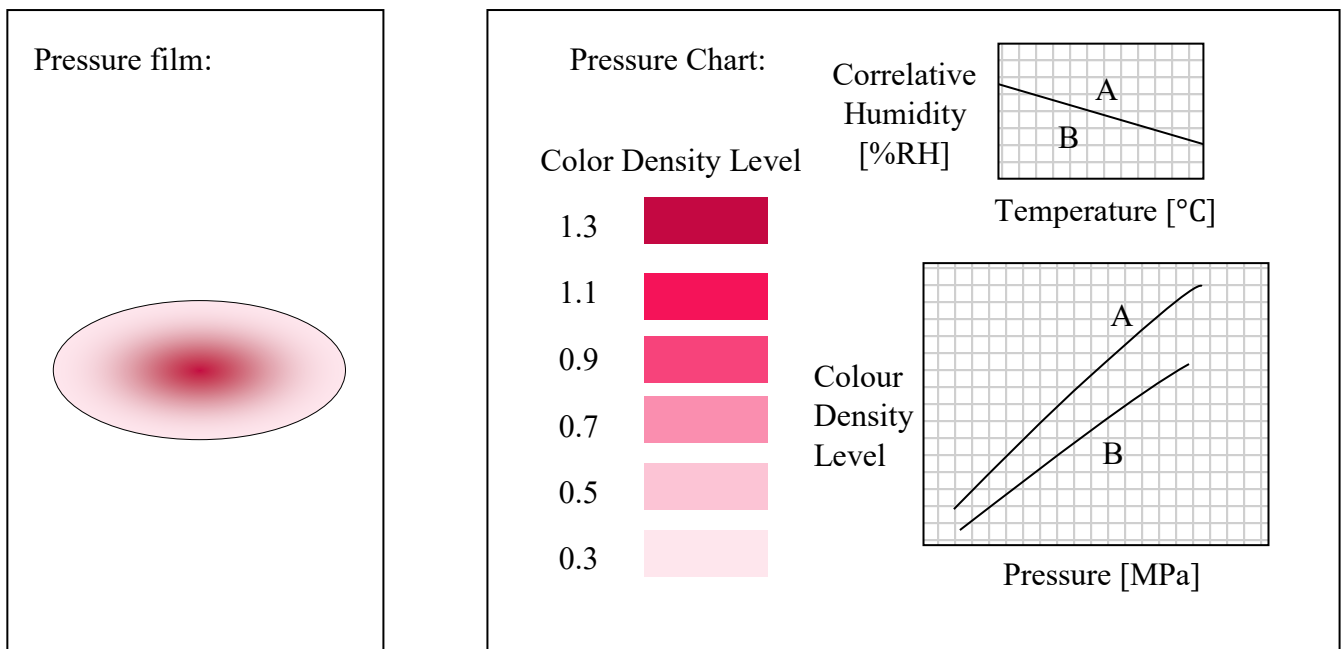


Figure 2.6 - Example of used pressure film and pressure chart. Inspired by (FUJIFILM, 2018)

To the left in *Figure 2.6* it is an example of a pressure film that has been used and by comparing it to the pressure chart it is possible to check the colour Density Level on the specific area of interest on the film. For example, in the middle of the ellipse area it is about 0.9 in colour density. By also knowing the correlative humidity, the temperature and depending on that check on line A or B to be able to translate the Colour Density Level to pressure. (FUJIFILM, 2018)

### 2.3.1 How the pressure films work and their pressure ranges

These pressure films contain three layers there one of them contain microcapsules. When these microcapsules breaks, they react with the colour-forming material that creates a red colour tune on the colour-developing layer. These microcapsules are designed to break according to the pressure so the colour density level correspond to correct pressure level. (see Figure 2.7). (FUJIFILM, 2018)

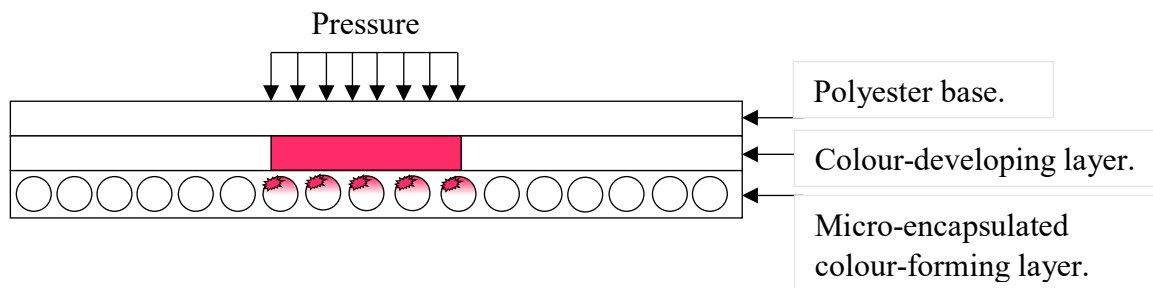


Figure 2.7 - The pressure film's different layers. Inspired by (FUJIFILM, 2018)

There are different ranges of these pressure films, everything from very low to high pressures. The Figure 2.8 show different film types that have specific ranges of pressures that the films can measure. (The bold marked ones will be used in this thesis)

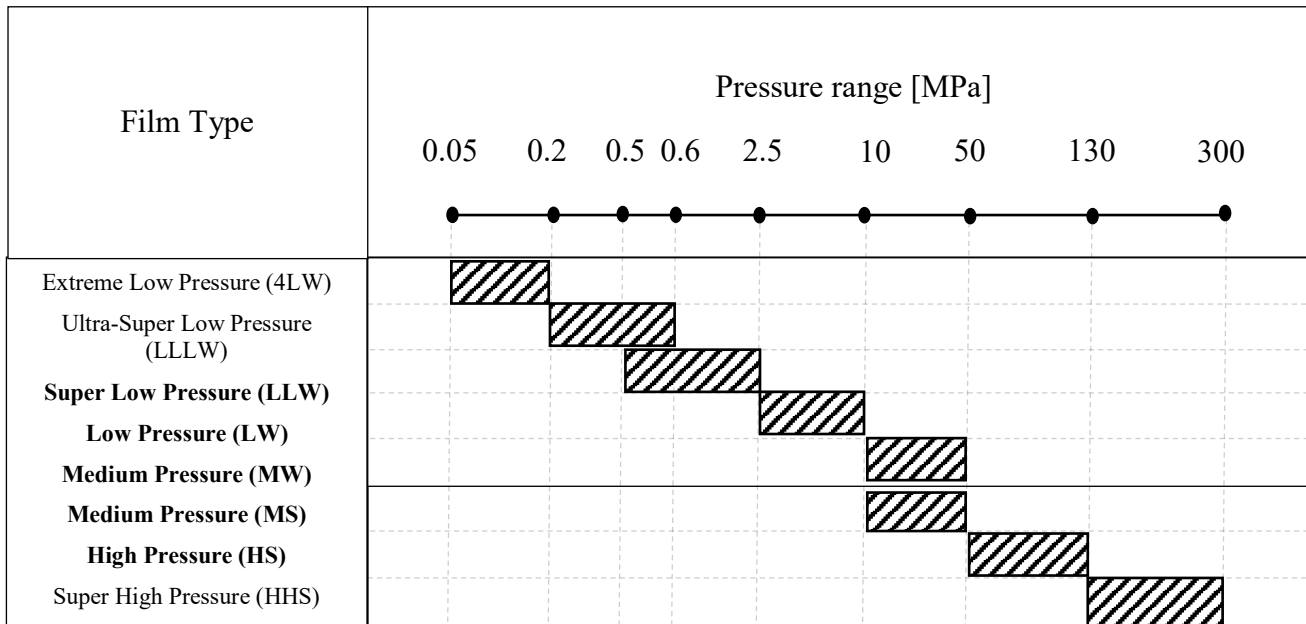


Figure 2.8 - Pressure ranges for different types of pressure films. Inspired by (FUJIFILM, 2018)

## 3 METHOD

---

*This chapter describes the general methods and the working processes that have been used to perform and to come up with a result.*

### 3.1 General methods

#### 3.1.1 Risk analyse

Risk analyse is a method to reflect on the risk that can accrue and how to reduce them. This method can be performed on many different types of applications. The risk analyse contain two main categories (Häring, 2018):

- 1) Risk assessment – Identify the risk, measuring and evaluating the probabilities and consequences of the risks.
- 2) Risk management – do arrangements to reduce the risks.

A risk analyse has been made in the beginning of the project to reflect about which possible risks that can accrue (see in Appendix A.2) to avoid possible failures in the project.

#### 3.1.2 Planning schedule

Planning schedule method is used to set up specific sub goals in a schedule in a limited timeframe to obtain the main goal of a project. The advantage using this method is to reflect about in which order things should be made and to be able to finish in the given timeframe. Planning schedule utilizes with maximum efficiency the available time and resources. This will give a good overview over project. In this thesis a planning schedule is made and have been useful for example:

To be able to perform experimental tests in this project some specific equipment will be needed therefore also be constructed and manufactured. This will take time and can also cause delays therefore it was planned to do in the early stage of the project.

#### 3.1.3 Five Whys

To understand what is the problem 5 Whys method is used to explore the cause and effect relationships for the particular problem (Serrat, 2009). In this project this method is used to ask following five whys:

In the roller support track the cable's conductivity and the roller can get damage. Why?

- 1) To high sidewall pressure between cable and the roller support. Why?
- 2) The roller supports are not shimmed in an appropriate way. Why?
- 3) Not knowing how much each roller support generate in in radial force. Why?
- 4) Do not have a measuring method to determine the radial force.

This make it possible to understand that the cable's conductivity and roller are getting damaging cause of not having a measuring method to check how much each roller support generates in radial force.

### 3.2 Complex system describing

To describe a complex system, like in this case sidewall pressure between cable and a roller support it is possible to use different approaches to describe the system see Figure 3.1.

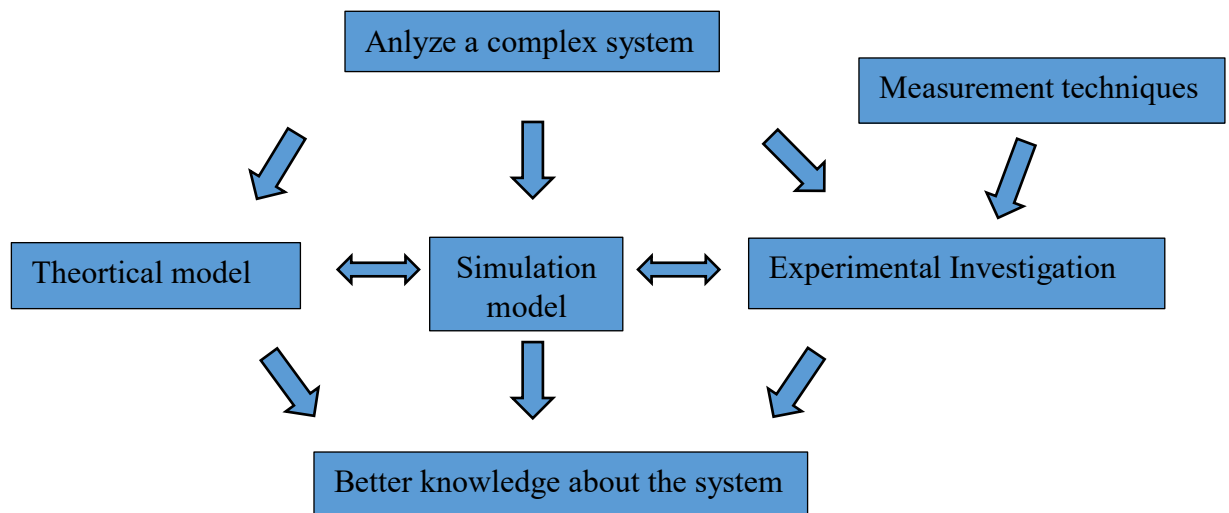


Figure 3.1 - Analyze a complex system. Inspired by (Broman, 2003)

- Theoretical model is often an analytical model that include for example equations or differential equations, which describe the essential part of the system. The advantage of using a theoretical model is that it is often easy to implement and is not expensive to use. In this project the Hertzian's theory will be used as theoretical model.
- Simulation model is often a numerical and discretized method for example FEM to describe the system by using several computational calculations. Depending on the software, it can include complex interactions that are difficult to describe with just an analytical model. In this project cable models have been created in SOLIDWORKS and later been used to set up a simulation model in ABAQUS.
- Experiment investigation is good to perform to capture the real behaviour and to check if the theoretical models and simulations are describing the system in an appropriate way. An experiment test can also be made to get a specific data that is unknown from the system. The disadvantages by performing an experimental test is that it can be expensive to perform and it is often dependent on a specific measurement technique that can give measuring faults. In this project two different experiment tests have been made to perform experiment investigation there sensors and pressure films are used as measuring techniques.

It is important to reflect about these approaches, what they will consider and what they do not.

It is possible to combine all these three to come up with a useful model of the specific system. Which will be done in this project.

### 3.2.1 Critical thinking

Before exploring well known theories in this case the contact mechanics, it is good to reflect and try to understand its behaviour yourself to get the fundamental knowledge about the system. The advantage of doing this before study different well-known theories is that it will establish a basic knowledge that can be used to check known theories and see if they are reasonable. (Ennis, 1962) A simple model can give the essential parts to understand the system. In the *Variety of Men* in 1969, C.P. Snow is writing about thought experiments there he describes Einstein:

*“It looks as though he had reached the conclusions by pure thought, unaided, without listening to the opinions of others. To a surprisingly large extent, that is precisely what he had done.”* (Snow, 1969, pp.100)

#### 3.2.1.1 Logical reasoning

The method of using logical reasoning is based on giving reasons to consider the assertion as true or least likely. In other words, logical reasoning is any reasoning that give any kind of reason for believing in an assertion. Intuitive logic are assertions that are necessarily true and should be objective. By using logical reasoning, it possible to improve the skills of draw conclusions, find errors in your own and other peoples reasoning but also become less naive and more critical. (Rosling, 2006)

In this project this logical reasoning was used for example to:

- Study the behaviour of the relation between compression and contact area of two crossed cylinder. This was also made to be able to get basic knowledge about how the system works and to criticise other sources of the well-known theories of Hertz contact mechanics. (see Appendix A.3)
- Describe possible ways by using the pressure films together with Hertzian’s theory to measure the radial force between the cable and the roller support. (see chapter 3.3.1)
- Describe how the result of using stacked pressure films on moving cable against a rolling roller support. (see chapter 3.3.2)
- Combine the Hertzian’s theory and ellipse diameter from the pressure films to describe the compression between roller support and cable (see chapter 3.4.2)
- Divide the total compression in the cable into local compression between holder and cable and between roller and cable. (see chapter 3.4.4)

#### 3.2.1.2 Check the produced result

This method is used to check the produced result. Because some errors can have been made during the process of getting the result. Therefore, it is good to use other solving methods to be able to compare the result and see if it is reasonable. It is also important to reflect about how the implementation is made and know how to check it so it works like it is attended to do.

In the project this method was used for example:

- To see if the Hertzian's theory was implemented in a correct way an example of two crossed steel cylinders were made and compared with corresponding FEM model. (see Appendix A.4)
- In simulations software the forces are assigned but is not clear this force is individual applied in each node or if it is distributed equally over each node. But applying the force and run simulation it is possible to check this by looking on the reaction forces.
- The result of this project the FEM simulation, sensors and the pressure film is compared with each other to see if they are showing the same result.

### **3.2.1.3 Start with a simple model and improve it step by step**

To analyse a complex system, it is always an advantage to start with a simple model and thereafter improve the model step by step if its needed (Ameisen, 2018). Because if something is going wrong during the implementation it is then easier to evaluate what has caused the error. In each step new knowledge will be obtained that will be useful to progress further to the more advance steps.

In this project this method was used to perform and increase knowledge of doing this types of simulations in ABAQUS:

- First model was two crossed steel cylinders. (see Appendix A.4)
- Second model was roller support and no armoured cable. (see Appendix A.6)
- Third model was roller support and double armoured DC cable. (see chapter 3.4.1.3)
- Fourth model was roller support and bundled AC cable. (see chapter 3.4.1.4)

### **3.2.1.4 Discretization of a complex system**

To be able to describe a complex system it is possible to discretize an advanced problem into several easier problems (Tirthankar, et al., 2011). The most known theory of using this method is the finite element method which is described in chapter 14.

In this project the discretization of a complex system was used to describe a nonhomogeneous cable with several homogenous cylinders by theoretical calculation from Hertzian's theory. (see Appendix 3.4.3)

## **3.2.2 Conversation**

During the thesis several discussions have been done with the supervisors from NKT and BTH to be able get different point of views before making some decisions. This makes it possible to reduce the risk of making wrong decisions by using other people's experience and knowledge.

### **3.2.3 Idea generation**

Brainstorming is an idea generating method where the objective is to come up with different ideas to fulfil specific needs. In this project this method was used to come up with appropriate equipment for the squeeze rig in upcoming experiments (see chapter 3.5.2).

### 3.3 Working process of answering first thesis question

This chapter describes how the working process has been done to answer first thesis question:

- 1) *How can the pressure film be used to measure the radial force between a roller support and high voltage cable?*

#### 3.3.1 Usage the pressure film to determine the radial force in static case

The pressurefilms will give a specific result when they are used between in a static loadcase between a roller and a cable. By using logical reasoning following assertion can be stated:

- A radial force produced by the roller support on the cable will give specific compression in the cable.
- According to the Hertzian's theory of two crossed cylinders will the contact area is a ellipse with two ellipse diameters there maximum pressure is the middle of the ellipse.
- The pressure film will register the pressure.
- By using a lower range pressure film stacked with a high range pressure film the lower range pressure film will register approximately the ellipse diameters and the high range pressure film will register the maximum pressure.
- Depending on the stiffness of the cable the same ammount of froce will give different ammount of compressions, different withs of the ellipse diameter and levels of maximum pressure.

By combining what pressure film can register and the Hertzian's theory of describing the pressure it is possible to determine the force for a static load case.

Two possible ways to calculate the force in theory by using the information from the pressure films:

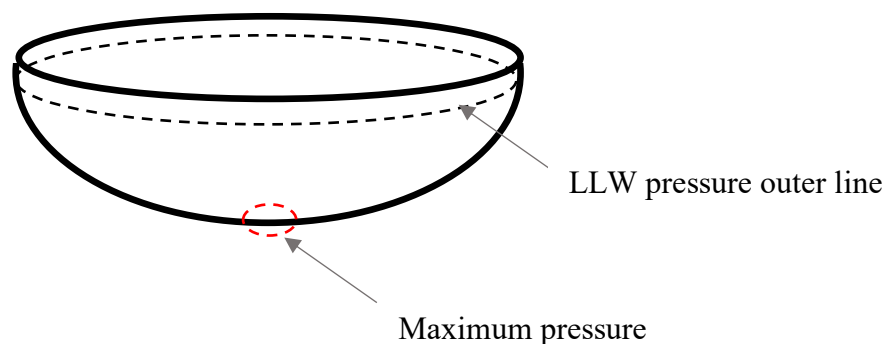


Figure 3.2 - Determine force by using the maximum pressure and ellipse diameter from the pressure film LLW.

The first one is by using the biggest ellipse diameters from LLW combined with the maximum pressure from example HS it is possible by the Hertzian's theory (see Equation (3.2) and Figure 3.2) to translate it to force (see detail MATLAB script in Appendix A.12).

$$p(x, y) = \frac{3P}{2\pi ab} \left( 1 - \frac{x^2}{a^2} - \frac{y^2}{b^2} \right)^{1/2} \quad (3.1)$$

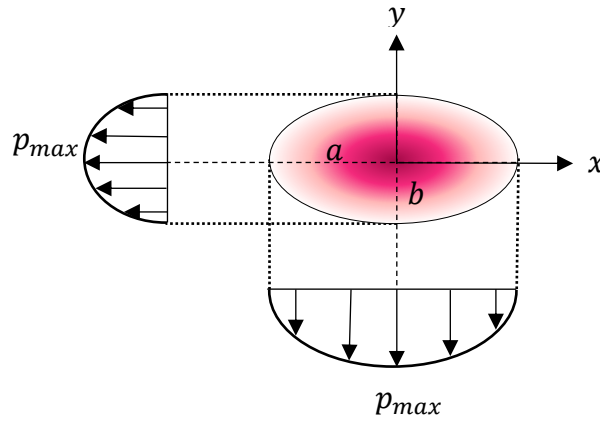


Figure 3.3 - Pressure distribution for ellipse contact.

By measuring the maximum pressure (in other words  $x = 0$  and  $y = 0$ ) and the ellipse diameters with the pressure film it is then possible to calculate the force by following equation:

$$P = \frac{2\pi \cdot a_{LLW} \cdot b_{LLW} \cdot p_{maxHS}}{3} \quad (3.2)$$

To reduce the error of reading the maximum pressure from pressure chart it is possible to use the second method that is based on the outer line of the ellipse marks (which show automatically the lowest pressure level the film can register) from the pressure films LW and LLW to predict the maximum pressure by using the Hertzian's theory (see Equation (3.3) and Figure 3.4) and thereafter determine the force  $P$ .

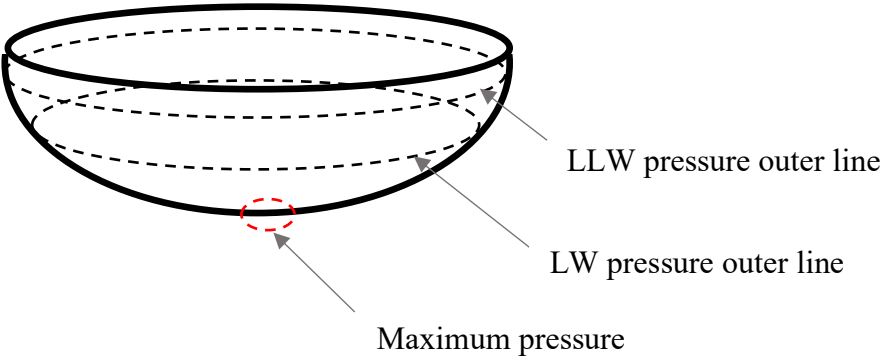


Figure 3.4 - Determine the maximum pressure by pressure film LLW and LW.

Lowest pressure level LW can register =

$$2.5MPa = \frac{3P}{2\pi a_{LLW} b_{LLW}} \left( 1 - \frac{x_{LW}^2}{a_{LLW}^2} \right)^{1/2} \tag{3.3}$$

or

$$2.5MPa = \frac{3P}{2\pi a_{LLW} b_{LLW}} \left( 1 - \frac{y_{LW}^2}{b_{LLW}^2} \right)^{1/2} \tag{3.4}$$

### **3.3.2 Usage of the pressurefilm to determine the radial force in dynamic case**

In the real roller support track the cable is moving against the roller support and is not possible to perform pure static load case to determine the force. By using the logical reasoning more assertion can be stated:

- When pressure film is mounted on the moving cable the roller must roll over the the whole pressure film to be able to remove the pressurefilm afterwards and read the pressure result.
- The pressure film will register the pressure of the whole rolling distance. Therefore will the result on the pressure film become a strip. In other words the contactarea of a ellipse will be presented several times on the pressure film and presenting a strip of pressure distribution.
- By using a low range pressure film stacked with high range pressure film, it is possible to measure the approximatelty largest ellipse diamater with lower range pressure film and the maximum pressure with the higher range pressure film.
- The velocity is small therefore it should be possible to calculate the radial force in a same manner as at the static case (see chapter 3.3.1)

A hypothetical model how the pressurefilms will generate the pressure distribution based on logical reasoning for a moving single part cable is presented below (see Figure 3.5):

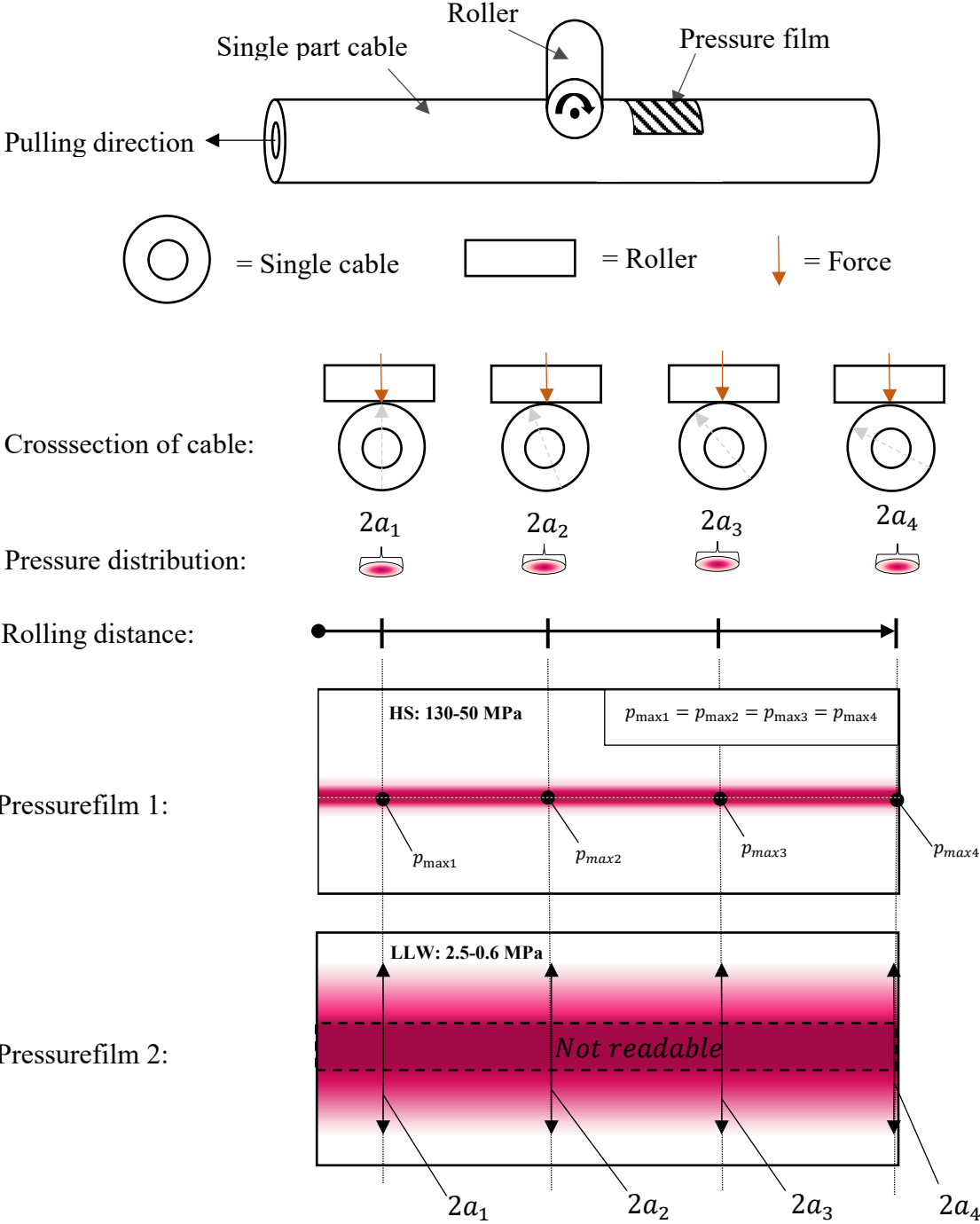


Figure 3.5 - Single part cable rolling over pressure films.

The pressurefilms will give another result when they are used between the bundled cable and the roller, when the roller is rolling against a moving cable. Because of the cable is bundled and it has a pitch that will make the compression varies during the moving of the cable. A hypothetical model how the pressurefilms will generate the pressure distribution is presented below (see Figure 3.6): Notice that the assumption is made: The internal parts in bundled cable can not move relative to each other and the plastic profiles have a lower stiffness than the part cables.

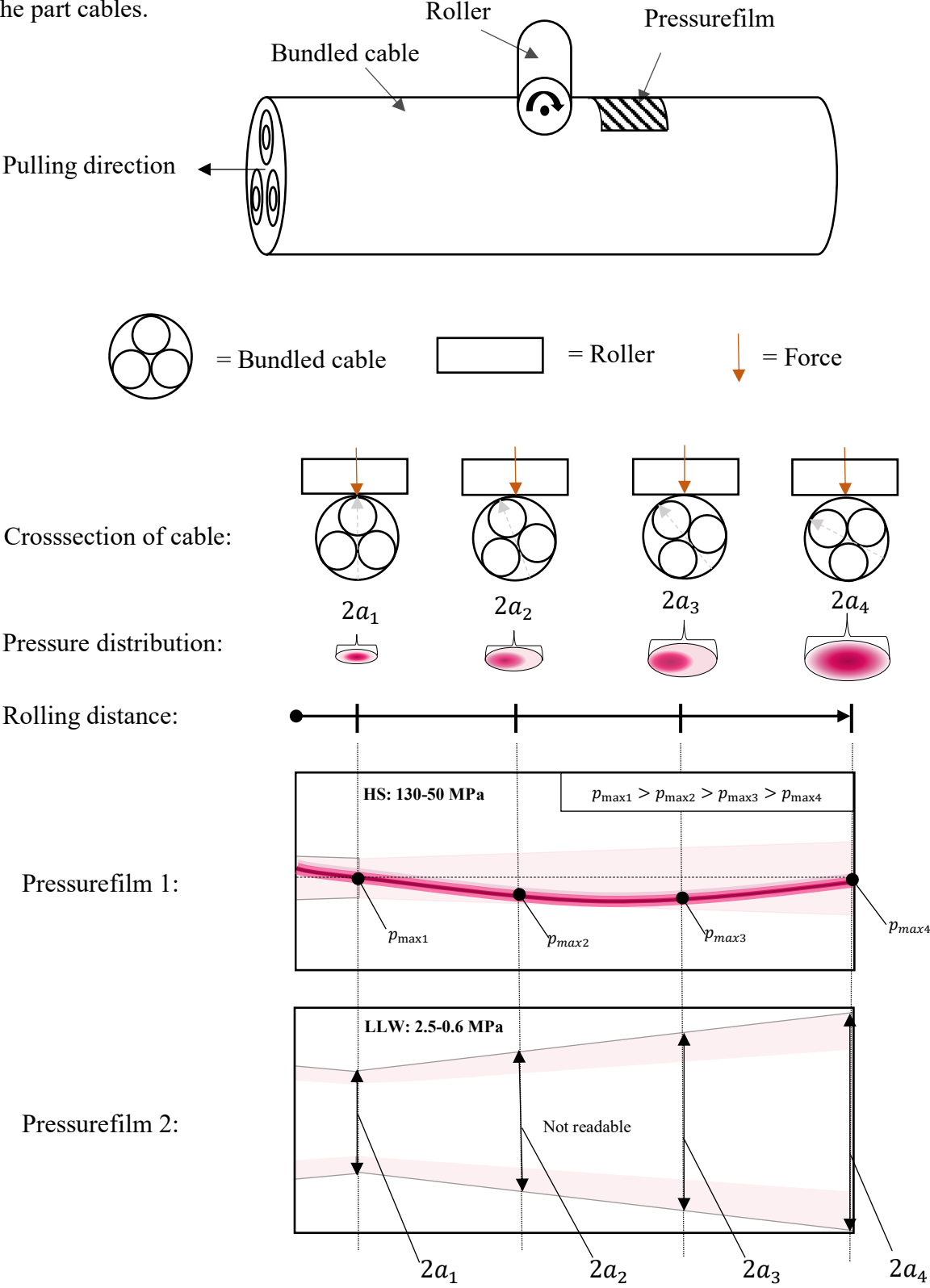


Figure 3.6 - Bundled cable rolling over pressure films.

Notice that the two middle  $p_{max2,3}$  will be moved down from the centreline because the bundled cable will behave stiffer on the left side of the force (because of the higher stiffness on the part cable) compared to the right side (plastic profile) and therefore the maximum pressure will be a little bit offset among these load cases. This will make it probably less accurate to calculate the force with this Hertzian theory at these points. But it is important to also consider the cable is armoured then the pressure will spread over a larger area of the cable. Which will make the  $p_{max2,3}$  get closer to the centerline.

### **3.3.1 Verify the method of determine the radial force by experimental test**

In the experimental chapter 3.5 one dynamic test and one static test will be performed to verify this way of using the pressure films together with Hertzian's theory to determine the radial force.

### **3.4 Working process of answering second thesis question**

This chapter describes how the working process has been done to answer second thesis question:

2) *By measuring the compression in cable how can the radial force be determined?*

*SQ2) How can a relation between radial force and compression (produced by roller support) of two different types of high voltage cables (single part and bundled) be described?*

#### **3.4.1 FEM to determine the relation between compression and radial force**

To be able to perform finite element analysis to describe the relation between compression and the radial force for a specific cable a model of the cable is needing to be created and material properties must be found. Also because of interesting of study this relation, several simulations are needed to be performed and therefore an automatic simulation process is a good method to make simulations run automatically after each other.

### 3.4.1.1 Finding material properties for the FEM model

To find the material properties for each material for the upcoming FEM models for every cable composition the CES EDUPACK software has been used together with discussion with NKT's calculating department. The software includes much information about several materials like elastic modulus, Poisson's ratio, yield strength etc. The stress-strain curve for the materials are presented in Figure 3.7 for the cable composition (Note that these shows only the relation not any exact values)

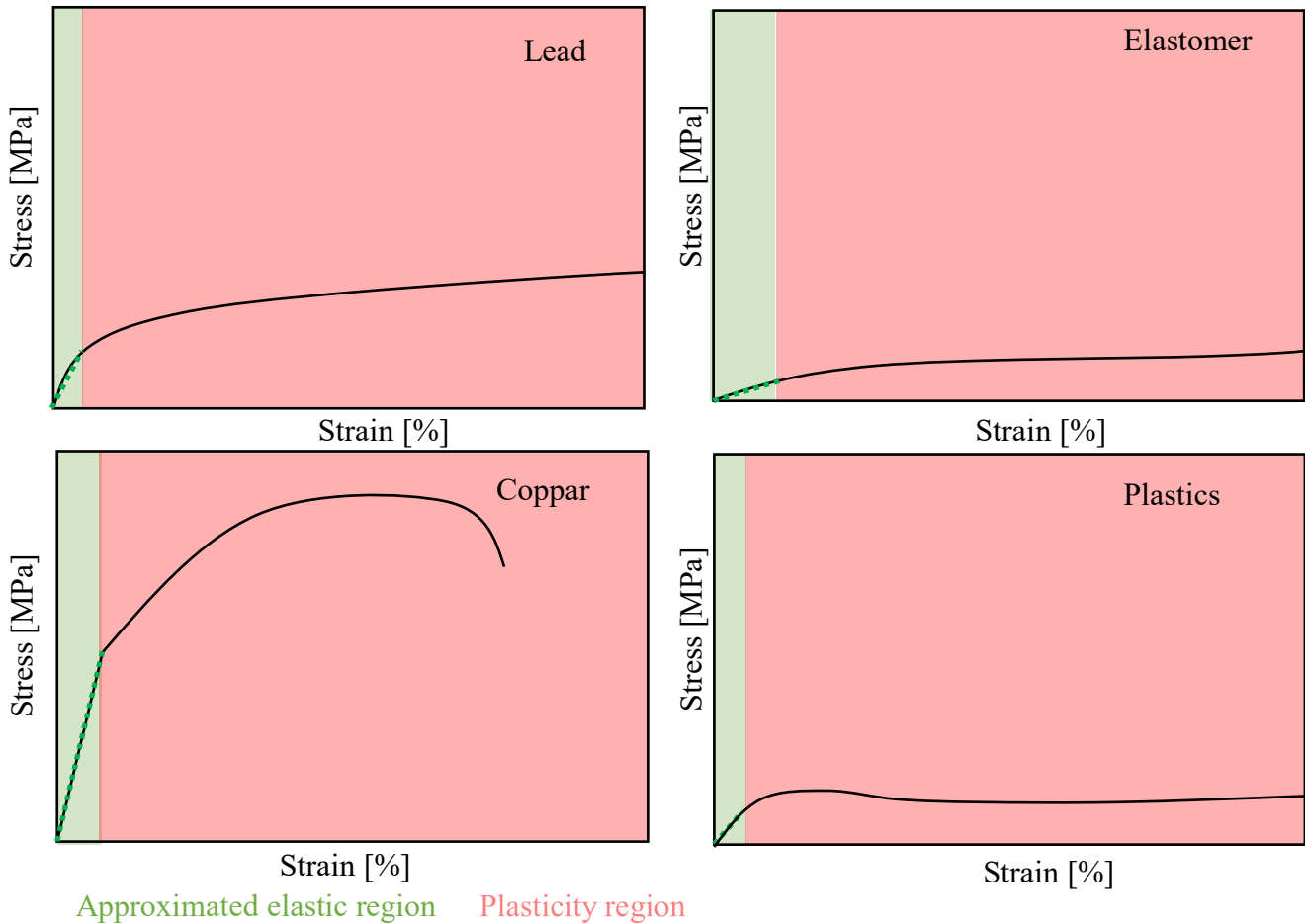


Figure 3.7 - Stress-strain curve for different materials.

One assumption that have been made in this project is that the cable will be only deform elastic. The elastic regions (see green area) will only then be considered.

A generalized material properties is presented for a cables in the Table 3.1:

Table 3.1 - Material properties for a cable.

Material	~Yield strength (MPa)	~Elastic modulus (GPa)	~Poisson's ratio
Copper	120	117	0.345
Steel	300	210	0.3
Lead	10	16	0.44
Plastic	20	0.55	0.45
Elastomer	0.01	0.15	0.49

### 3.4.1.2 Simulation automation process

To perform several FEM simulations with different levels of loads to determine the relation between compression and radial force can be very time consuming. But this can be solved by using MATLAB as server to control ABAQUS as a client. (Wall, 2017) The Figure 3.8 describes the main steps of using this method. See a detail script in (see Appendix A.13).

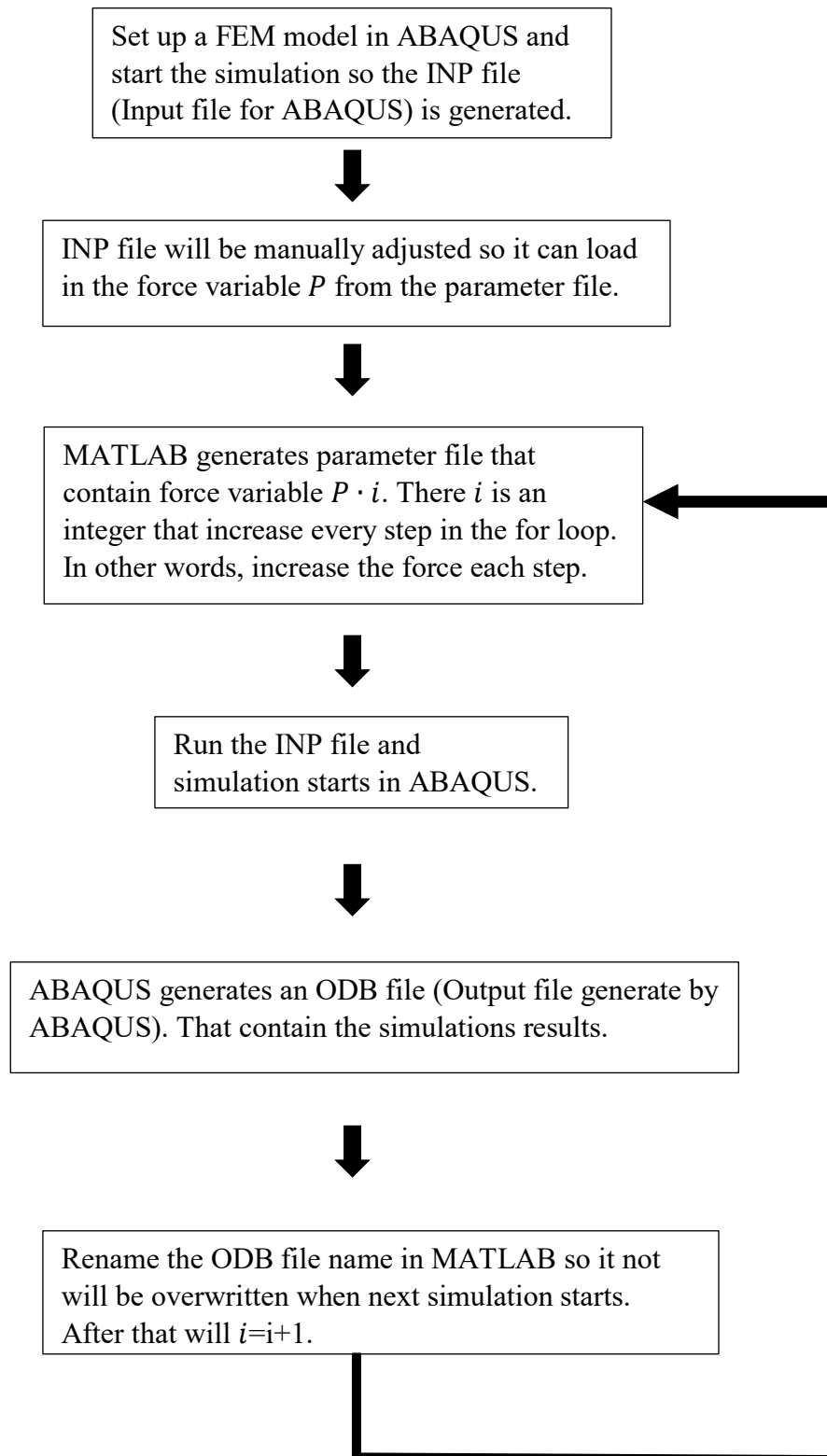


Figure 3.8 - Using MATLAB as a server and ABAQUS as a client.

### 3.4.1.3 Cable model and FEM setup for double armoured DC cable

A double armoured cable contains two types of layers of armouring wires, often made of galvanized steel or stainless steel to protect the cable from example anchoring. The armouring wires are layered crossed each other with a specific pitch angle to spread the load impact in to larger area of the cable. The advantage of having it crossed armouring is that it will reduce the effect of torsion in the cable when the cable gets affected by a tension.

A CAD model of the cable have been made in SOLIDWORKS (see Figure 3.9). A holder has been added also to make it possible to compare the FEM result with the upcoming experiment. The holder is needed to be able to perform the experiment in the squeeze rig (see chapter 3.5.2 ).

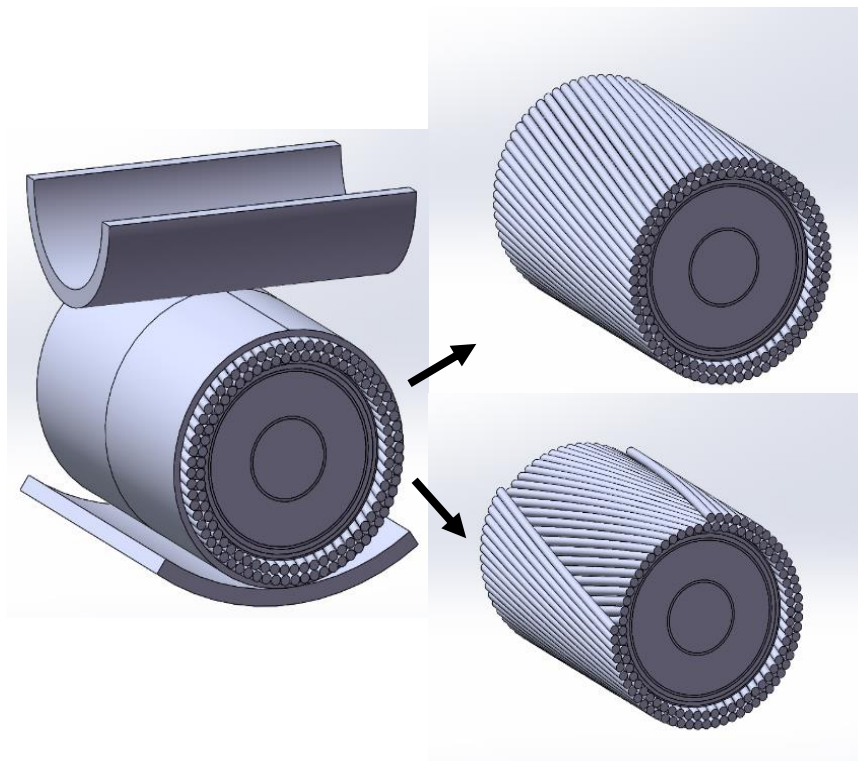


Figure 3.9 - Double armoured DC cable.

To set up a FEM model for double armoured cable following simplifications have been made, to reduce number of elements and simulation time:

- The roller is a halfpipe and is a rigid body.
- Small piece of the cable.
- Every material layer in the cable are tied together.
- Contact is accruing between the roller and the cable but also between the cable and the holder. These have the interactions of finite sliding and a friction constant of 0.1.

For the double armoured cable following boundary conditions are used:

- The roller is constrained with no translation in Y and X, no rotation around the axis X, Y and Z.
- The holder's bottom surface is fixed in all translation directions and rotations directions.
- The conductor's end is constrained with no translation X and Y and no rotation.
- The force is equally applied in 12 nodes on the roller (see yellow arrows in Figure 3.10).
- A nonlinear implicit solver is used in ABAQUS to solve this FEM model.
- Mesh type: Linear brick element type.

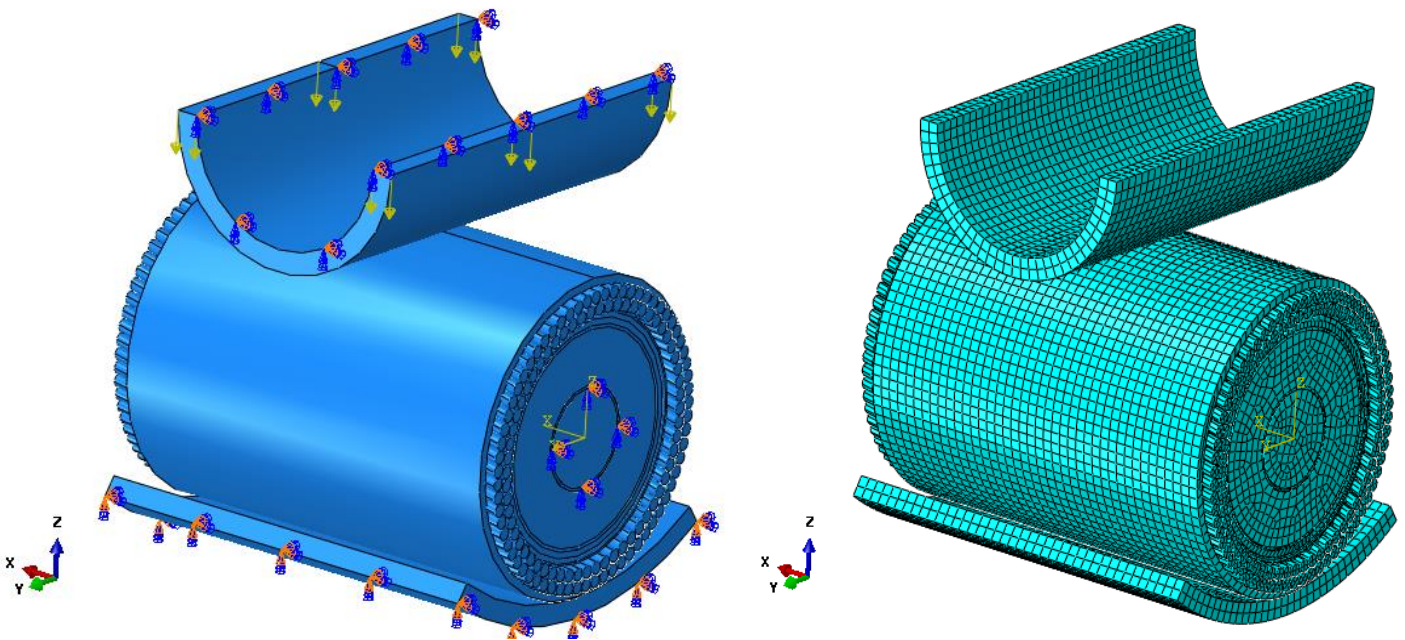


*Figure 3.10 - Boundary condition and mesh for a double armoured DC cable.*

Forces is applied in a intervall of 3000-33000N for this double armoured cable and the automatic simulation process is also implemented.

#### 3.4.1.4 Cable model and FEM setup for bundled AC cable

A bundled single armoured cable contains three part cables with plastic profiles between each of them. The part cables and the plastic profiles are bundled with specific pitch, to avoid a large torsion and give a protection on the cable an armouing layer have been added in opposite pitch direction. Like the Figure 3.11 shows.

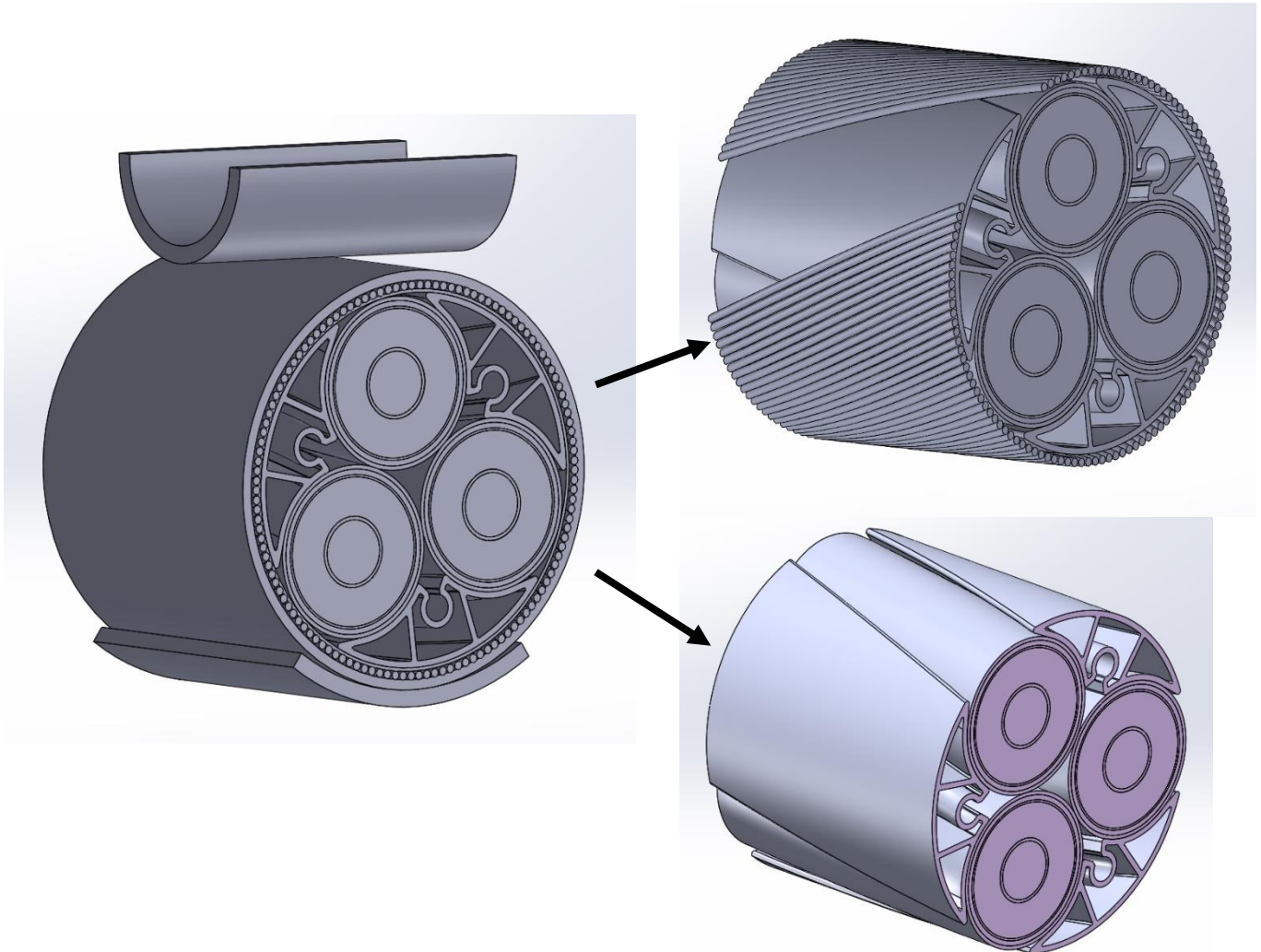


Figure 3.11 - Bundled AC cable.

A CAD model of the cable have been made in SOLIDWORKS. The FEM model have been created in ABAQUS to study the relation between the compression and the radial force in this specific cable.

To set up a FEM model for bundled cable following simplifications have been made, to reduce number of elements and simulation time:

- The roller is a halfpipe and set to be rigid body.
- Small piece of the cable.
- Every material layer and internal parts in the cable are tied together.
- Contact is accruing between the roller and the cable and between the cable and the holder, it is also accruing between each internal part cable. These have the interactions of finite sliding and a friction constant of 0.1.

For the bundled cable, following boundary conditions are used:

- The roller is constrained with no translation in Y and X, no rotation around the axis X, Y and Z.
- The holder's bottom surface is fixed in all translation directions and rotations directions.
- The conductor's end is constrained with no translation in X and Y direction and no rotation.
- The plastic profiles are constrained with no translation in X direction and rotation around X direction.

The force is applied in 12 nodes on the roller (see yellow arrows in Figure 3.12).

A nonlinear implicit solver is used in ABAQUS to solve this FEM model.

Mesh type: Linear brick element type.

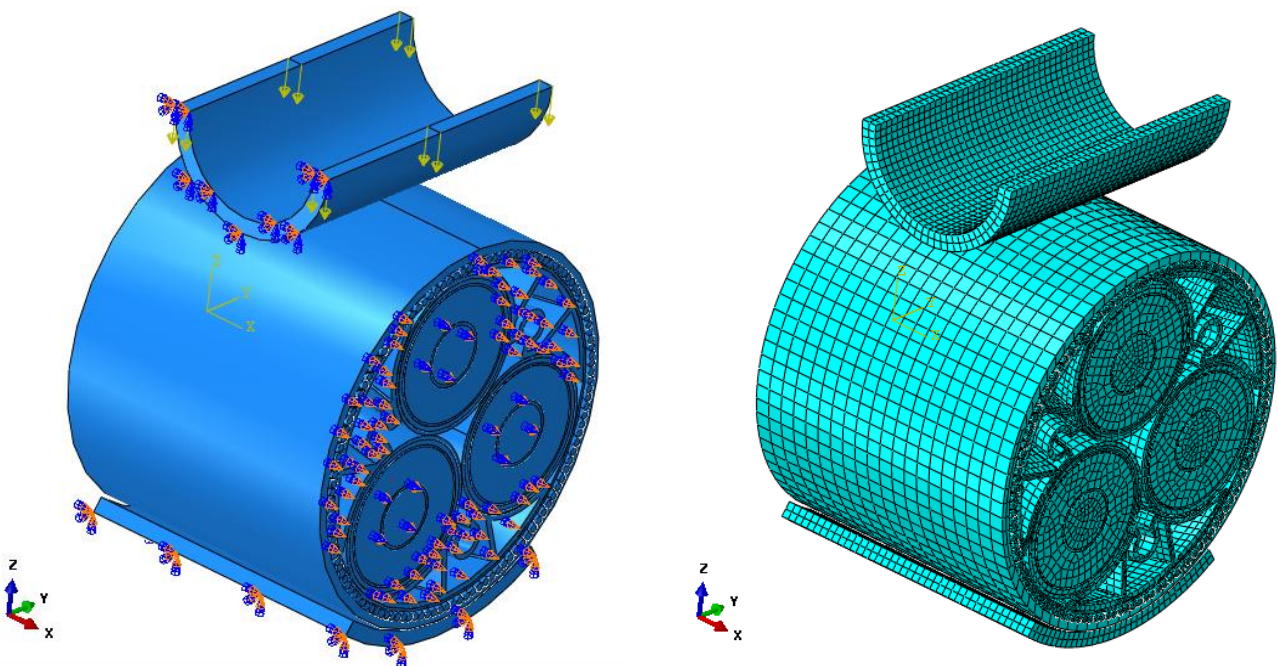


Figure 3.12 - Boundary condition and mesh for a bundled AC cable.

Forces is applied in a intervall of 6000-15000N is going to be simulated in three different load angles (based on the cable behave stiffer depending on where the load is applied) on the bundled cable see Figure 3.13. In a similar way as the double armored cable MATLAB is used as server and ABAQUS as client to perform the automatic simulation process.

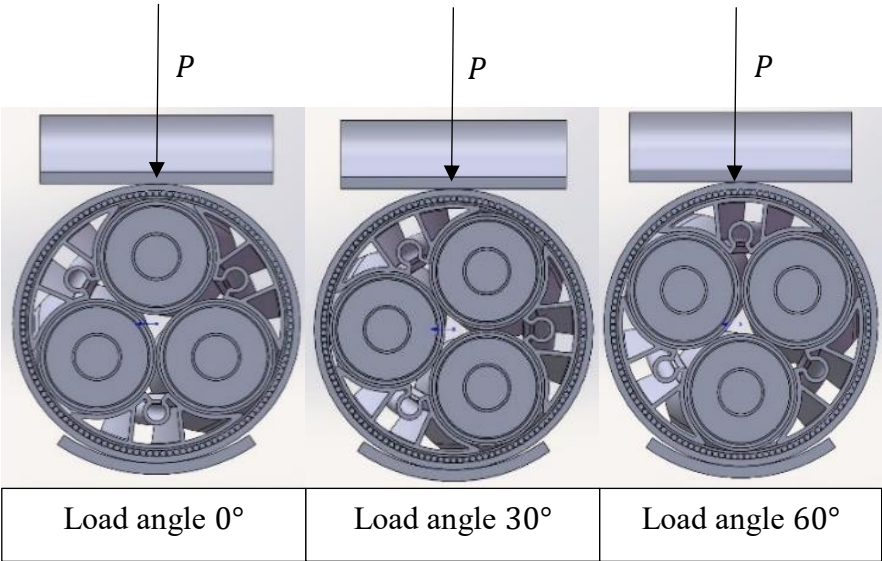


Figure 3.13 - Different load angles for the bundled cable.

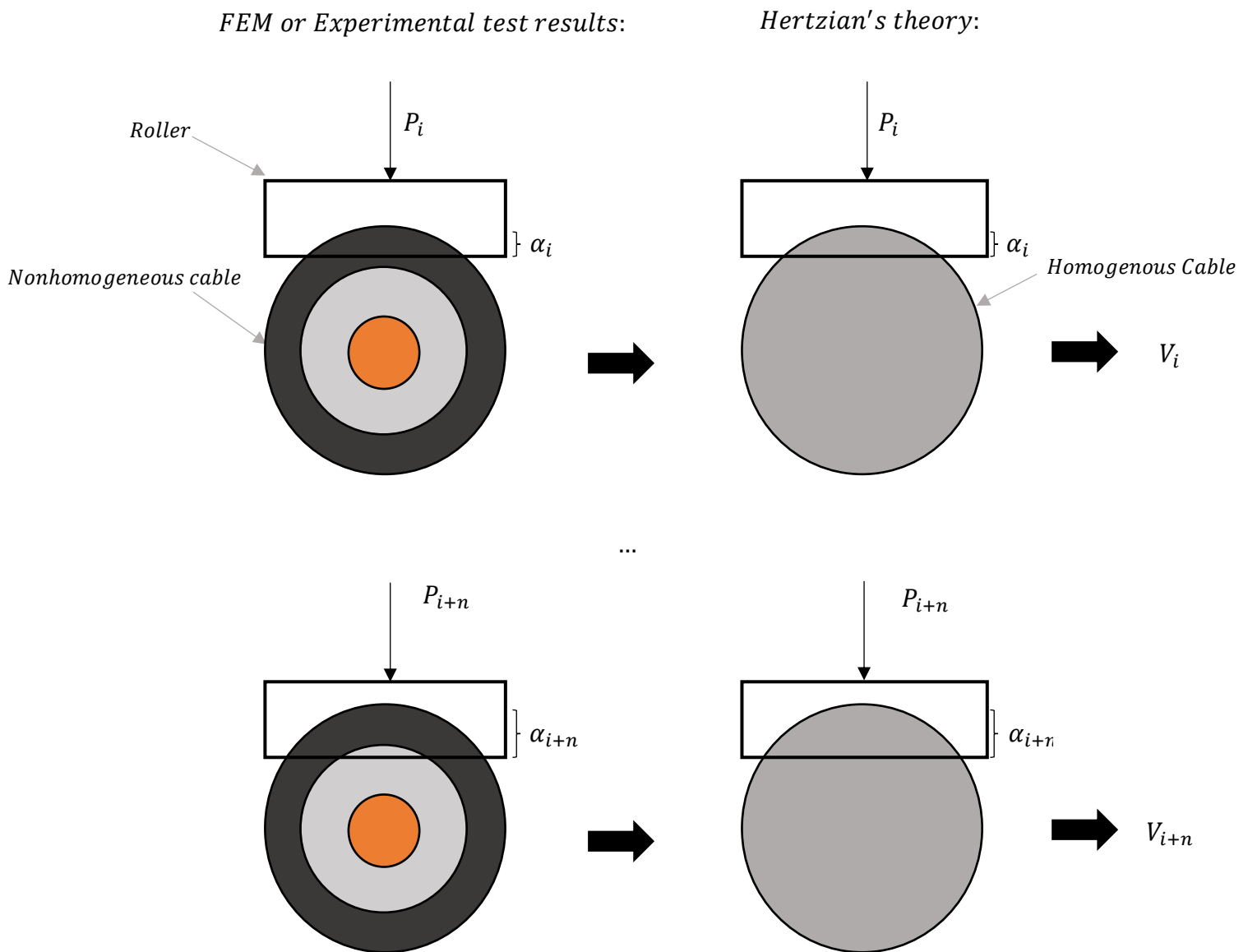
**3.4.2 By using experiment tests**

Another method to determine the relation between radial force and the compression of a cable is to use an experiential setup that have sensors that can register the force and the compression in cable. This will be described more in detail in the chapter about squeezerig (see chapter 3.5.2).

### 3.4.3 Describing the stiffness of a nonhomogeneous cable

The material parameter  $V_2$  in Hertzian's theory will be useful further in this project to divide the total compression in the cable into local compression for the FEM model and experimental result. But also, to use pressure film combined with Hertzian's theory and knowing the applied force to describe the relation between compression and radial force.

By using, the Hertzian's theory combined several FEM simulations results or experimental results it is possible theoretically for each specific load case define how material parameter  $V_2$  for the cable is related to force. The assumption is that for every specific load case on a nonhomogeneous cable it is possible to replace the real cable with a homogenous cable with specific material parameter  $V_2$  that will give the same compression result as the nonhomogeneous cable. In the Figure 3.14 is a representation of this.



where  $n$  is an integer.

There  $V_i \rightarrow V_{i+n}$  describe how the theoretical material parameter changes for a nonhomogeneous cable.

Figure 3.14 - Nonhomogeneous cable translated to homogenous cable for every specific load case.

The material parameter  $V_2$  will no longer only describing the material properties for the cable. It describes the changing of the stiffness of the cable by including the material parameters, all interactions, moving parts and other parameters in the cable that will affecting the compression result. Therefore, it will be called stiffness modifying parameter  $S_{mp}$  instead further in this project.

### 3.4.4 Theoretically divide the total compression into local compressions

To consider that the displacement will accrue both between the roller and cable and between the cable and the holder in both FEM model and upcoming experiment, following method will be used to split up the total compression into these two local compressions. Notice that the interesting part is the local compression between the roller and the cable. To be able to do this the assumption of describing a nonhomogeneous cable with several homogeneous cables combined with Hertzian's theory is needed.

The Figure 3.15 describe the local compression between roller and cable between cable and holder in upcoming experiment.

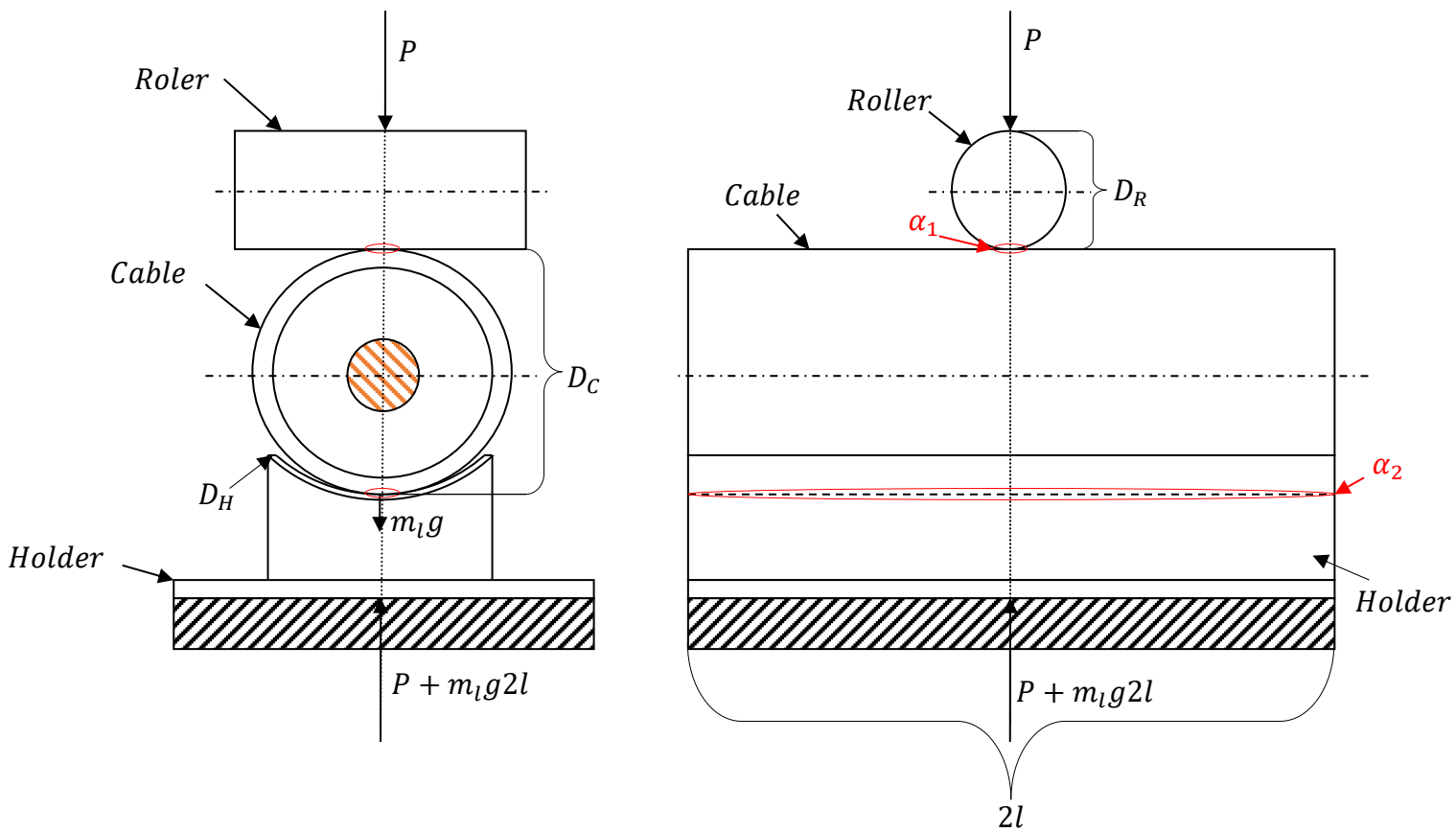


Figure 3.15 - Local compression of a cable in the upcoming experiment.

$\alpha_1$  is the local compression between roller and cable.

$\alpha_2$  is the local compression between cable and holder.

$\alpha_{\text{tot}} = \alpha_1 + \alpha_2$  is the total compression.

By combining these two theories:

- Unequal diameter cylinders crossed with their axes at right angles
- Two cylinders in contact with axes parallel

it is possible to divide this measured total displacement  $\alpha_{tot}$  into local compression  $\alpha_1$  and  $\alpha_2$  by following the schedule in Figure 3.16 below (see detail in the MATLAB script in Appendix A.10):

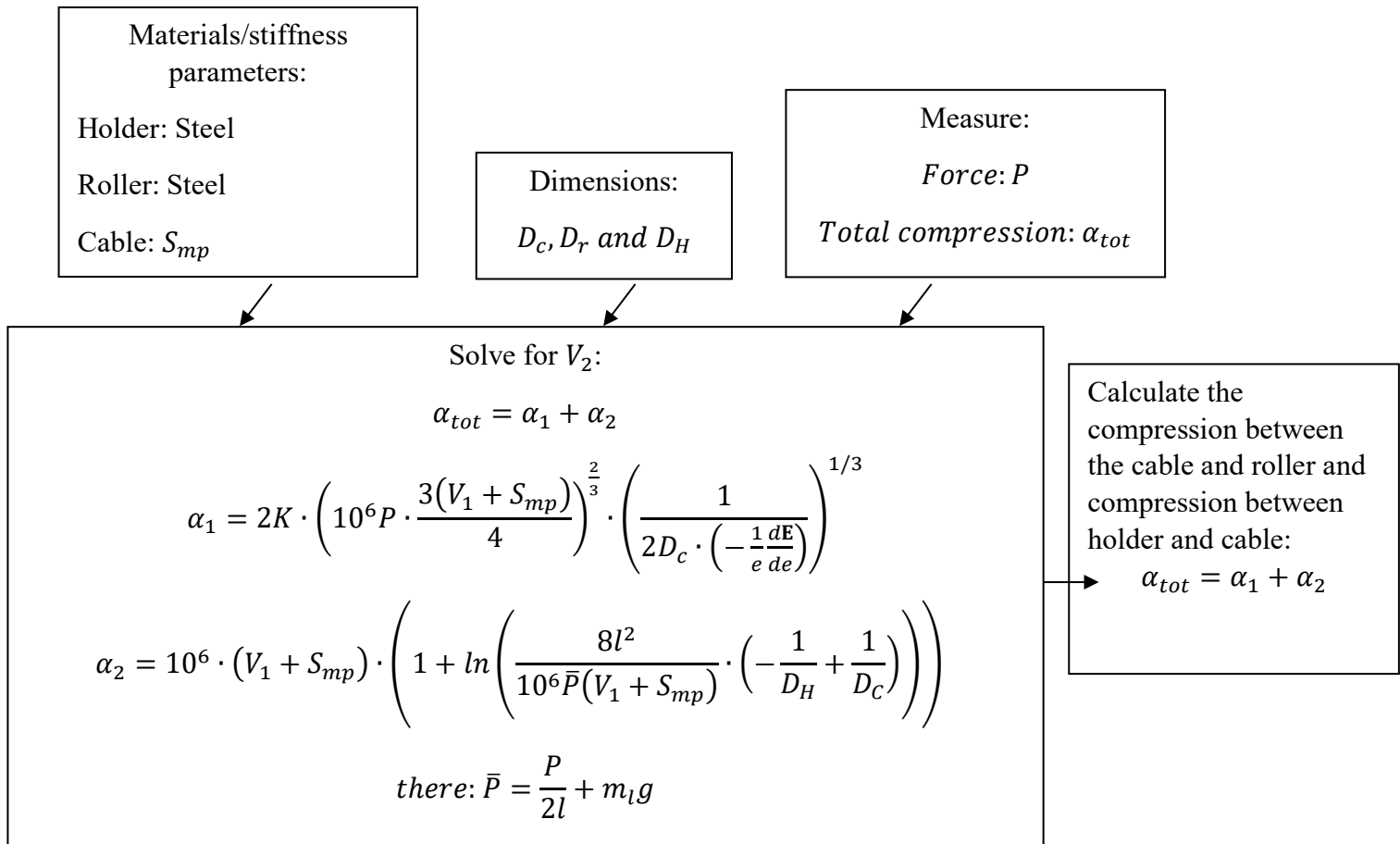


Figure 3.16 - Theoretical divide the total compression.

This method is used to be able to divide the total compression in the cable into local compression between roller and cable and between the holder and the cable. In the reality the total compression will also go to change geometrical shape of the cable which this method not consider. In other words, if the total compression is only divided into only local compression like in this case, it will make these a local compression larger than what they are in the reality.

### 3.4.5 Using the ellipse diameters, Hertzian's theory and applied force

To use the both ellipse diameters from the pressure film and the applied force from the upcoming static experiment in Squeeze rig (see chapter 3.5.2) to describe the relation between compression and radial force, following calculation is made (see MATLAB script in Appendix A.11).

First calculating the eccentricity for each load case, there  $a$  is the large ellipse radius and  $b$  is the small ellipse radius measured from the pressure film:

$$e = \left(1 - \frac{b^2}{a^2}\right)^{\frac{1}{2}} \quad (3.5)$$

By using the equations (3.6), (3.7) and (3.8) to solve the stiffness modifying parameter  $S_{mp}$  for the cable both in (3.9) and (3.10). After that do average on these two values on material parameter  $S_{mp}$  for the cable:

$$\frac{1}{-e} \frac{dE}{de} = \int_0^{\frac{\pi}{2}} \frac{\sin(\theta)^2}{(1 - e^2 \sin(\theta)^2)^{\frac{1}{2}}} d\theta \quad (3.6)$$

$$\frac{1}{e} \frac{dK}{de} = \int_0^{\frac{\pi}{2}} \frac{\sin(\theta)^2}{(1 - e^2 \sin(\theta)^2)^{\frac{3}{2}}} d\theta \quad (3.7)$$

$$Q = \frac{3}{4}(V_1 + S_{mp}) \quad (3.8)$$

$$Aa^3 = -\frac{2QP}{e} \cdot \frac{dE}{de} \quad (3.9)$$

$$Ba^3 = \frac{2QP}{e} \cdot \frac{dK}{de} \quad (3.10)$$

$$\text{There: } A = \frac{1}{D_1} \text{ and } B = \frac{1}{D_2}$$

Using the equation (3.11) below to calculate the compression in the cable:

$$\alpha = \frac{2QP}{a} \cdot K \quad (3.11)$$

Notice that the applied force must  $P$  be known.

There  $K$  is the ellipse integral.

$$K = \int_0^{\frac{\pi}{2}} \frac{d\theta}{(1 - e^2 \sin^2(\theta))^{\frac{1}{2}}} \quad (3.12)$$

This makes it possible to describe compression by using the pressure film together with Hertzian's theory. And because the radial force is known in upcoming test it is possible describe the relation between the compression and the radial force.

### 3.5 Experimental test

The FEM model will not include everything for example adhesion, the correct layer interactions and high nonlinear material properties which materials like plastics and leads have. Therefore, an experimental test will be able to capture a more realistic relation between compression and force between the roller and the cable. But also, to verify the method of using the pressure film to determine the force.

#### 3.5.1 Pointload test

The pointload test is performed to study how much damage in this case a small diameter (compared to the other cables that is tested in the squeeze rig) single armoured DC cable will take when it is affected by a point load. Because the test also includes an interaction between a roller support and the cable it is also for this thesis work interesting to see if it is possible to use the pressure films to determine the radial force.

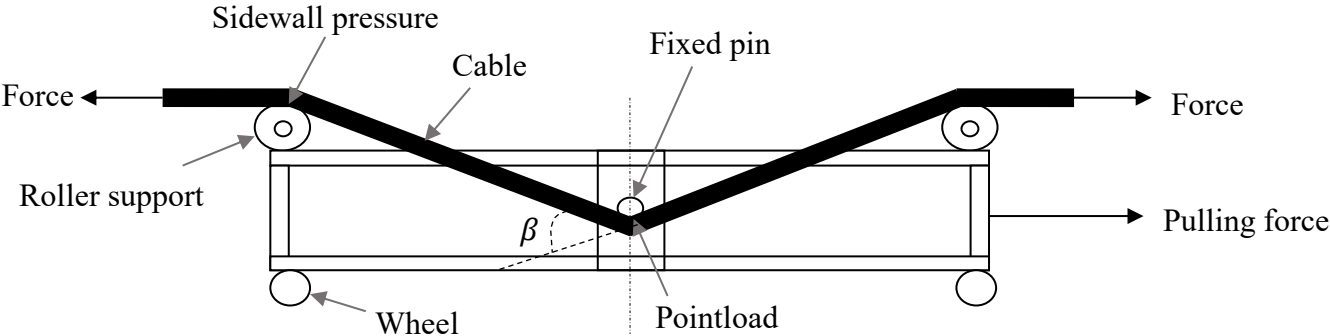


Figure 3.17 - Theoretical model of the Pointload test.

The Figure 3.17 show the pointload test there the cable is tensed up by an equal force in both ends (in other words the cable is not moving) and after that the wagon is getting pulled some distance. The test was performed in two different angles on  $\beta$ . In the Figure 3.18 shows how several pressure film is stacked together and mounted on the cable to using the method of using the result of the pressure film and combine it with Hertzian’s theory to determine the radial force.

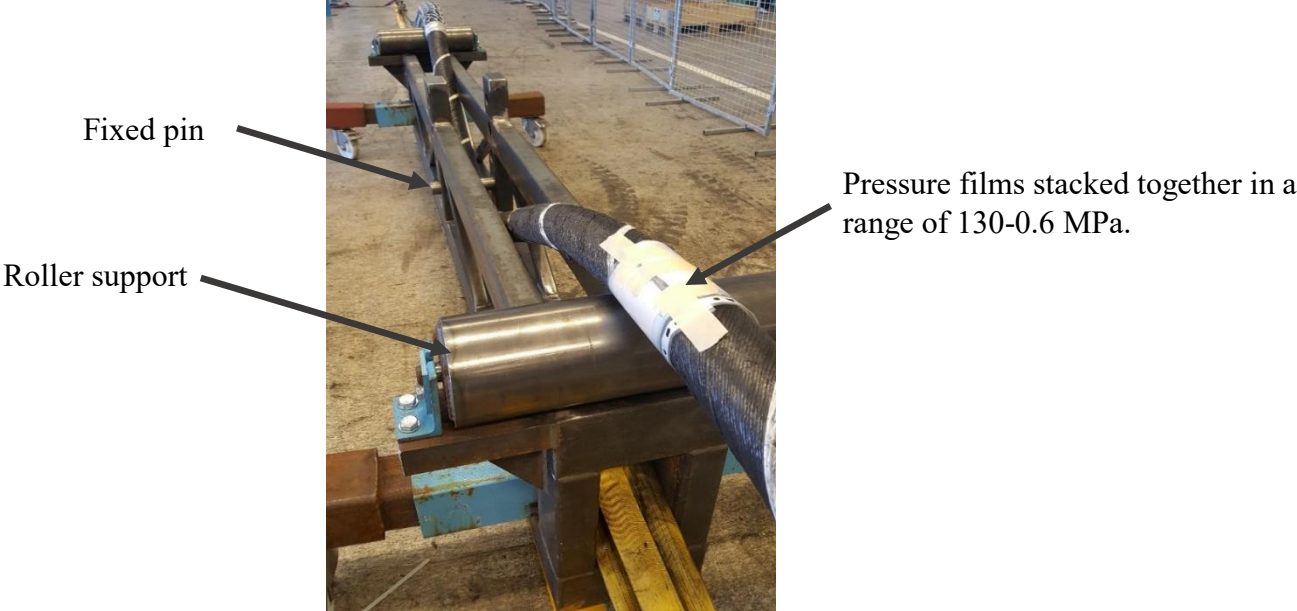


Figure 3.18 - Pointload test in reality.

### 3.5.1.1 Theoretical model of the pointload test

To get a knowledge about the radial force to see if the pressure film is giving a corresponding result between the cable and roller a simple theoretical model has been made, where the cable assumed to be a rope (see Figure 3.19 and equation (3.14)):

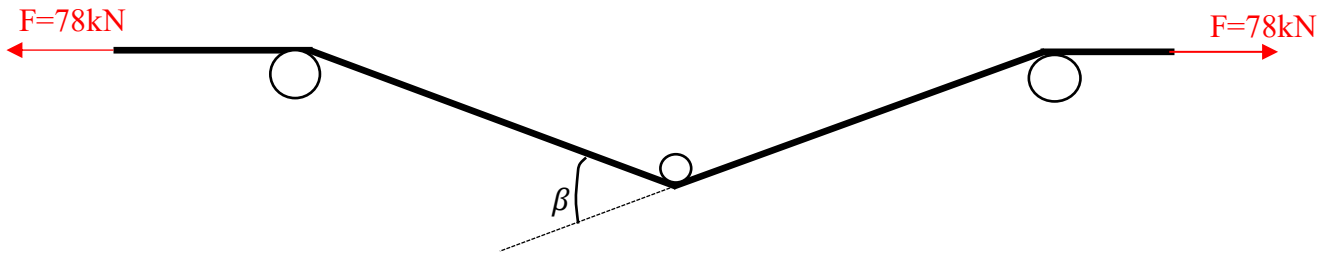
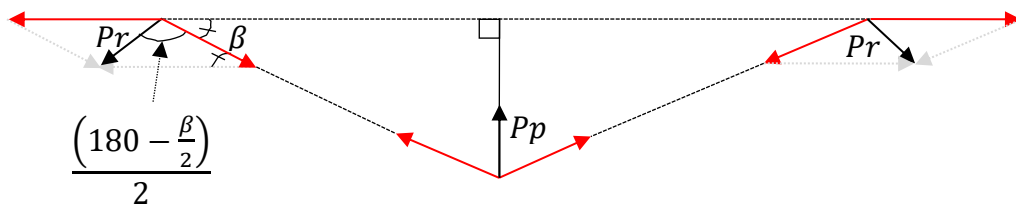


Figure 3.19 - Theoretical model of point load test.



$$P_p = 2 \cdot F \cdot \cos\left(90 - \frac{\beta}{2}\right) \quad (3.13)$$

By using law of sines:

$$P_r = \sin\left(\frac{\beta}{2}\right) \cdot \frac{F}{\sin\left(\frac{180 - \frac{\beta}{2}}{2}\right)} \quad (3.14)$$

**3.5.1.2 FEM model of the pointload test in ORCAFLEX**

The bending stiffness in the cable will generate a larger radial force between roller and the cable, therefore a simulation in ORCAFLEX (see Figure 3.20) have been made together with supervisor from NKT to simulate the real load case. In a similar way as the theoretical model it will be compared to see if similar result of radial force can be determined with the pressure film.

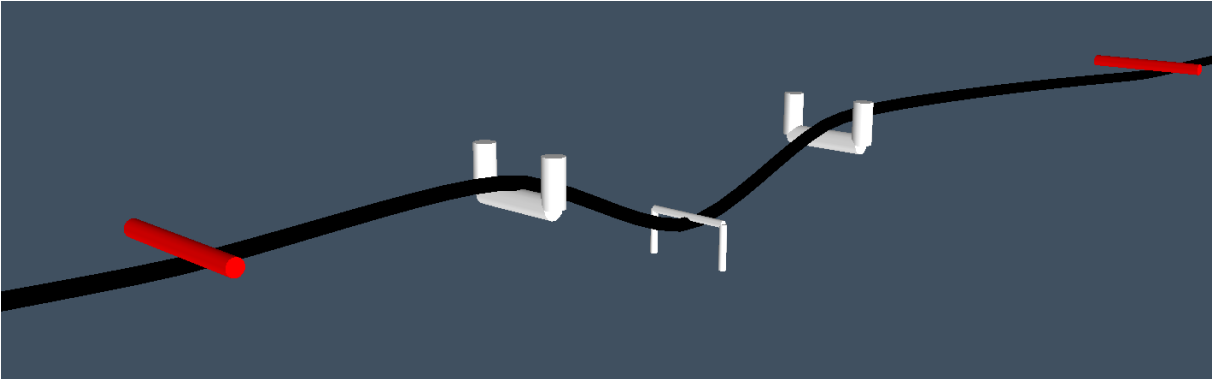


*Figure 3.20 - Simulation of pointload test in ORCAFLEX.*

### 3.5.2 Squeeze rig test

NKT's test lab department have so called squeeze rig there they can squeeze the cable with hydraulic cylinders (see Figure 3.21). The advantage of using this rig is that it can measure the applied force and the total displacement in the cable. This experiment makes it possible to compare the result of using the pressure film to determine the force with the actually applied force. But also describing the relation between the radial force and the compression in the cable by using the sensors and pressure films.

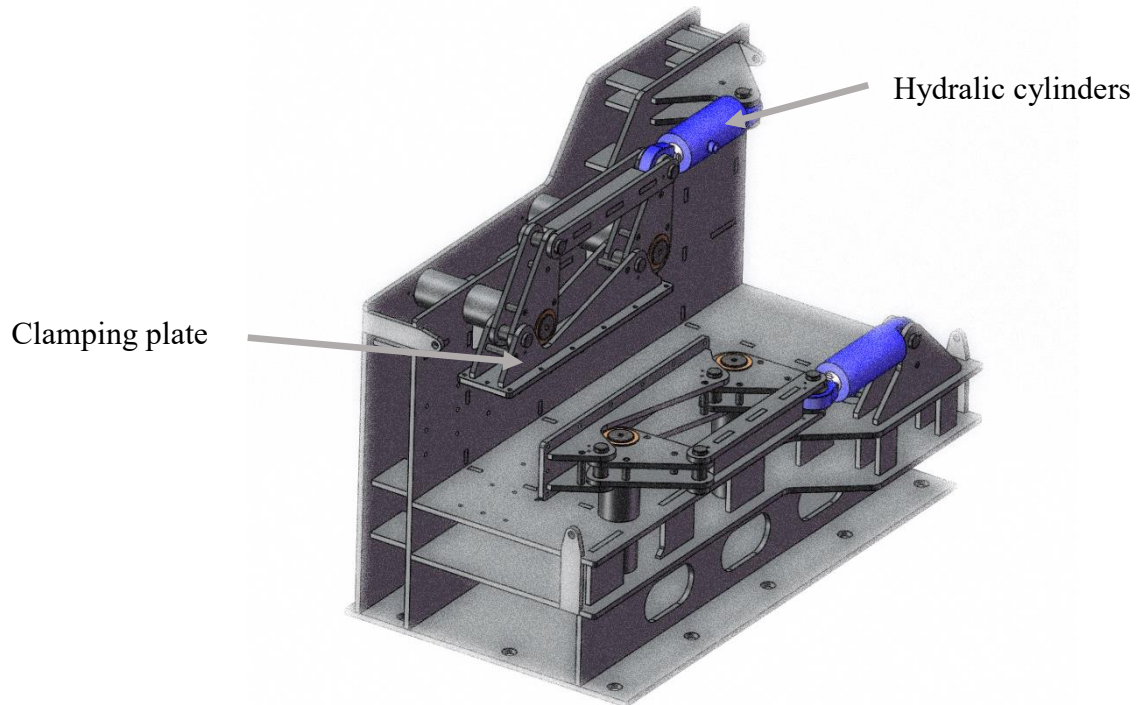


Figure 3.21 - The squeeze rig.

Two types of sensors are used on the squeeze rig, one of them is used to measure the force on cylinder and other is a displacement sensor which show the total displacement of the clamping plate. The displacement (total compression) will be distributed as local compression at the contact between the roller and the cable but also between the cable and the holder. But also in the reality it will change the geometry of the cable. Theoretically will the total compression will be divided according to chapter 3.4.4 into local compression between roller and cable which is of interest but also local compression between holder and cable.

To perform the sidewall pressure test on cable some equipment are needed.

One roller support and two cable holders have been designed and constructed from ideas generated with brainstorming. Production documentation and calculation on abrasion resistance have been also be done in this part of project. (see Figure 3.22).

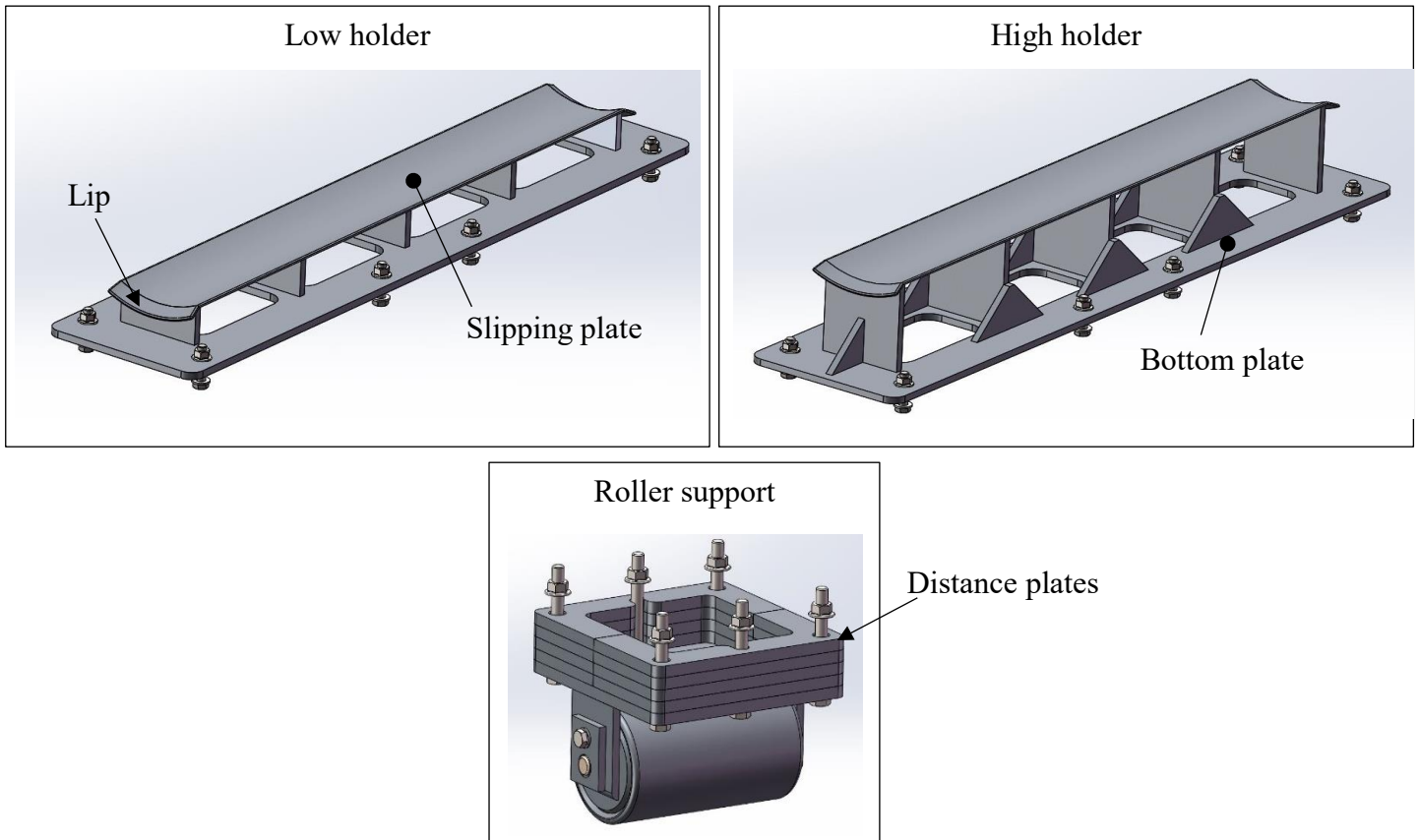


Figure 3.22 - Equipment for the squeeze rig.

The equipment is constructed in following way:

- The number of different type of components are minimized for example for the holder the bottom plate and the slipping plate is the same for both types of holders to reduce the changeover time in following manufacturing process.
- The holders and the distance plates is made in such way that it is possible to combine these in a way that different sizes of cables can be tested. The distance plates can easily be removed and added if it is needed without removing the whole roller support each time.
- The slipping plate is bowl formed to minimize the risk that the cable is moving sideways when the cable is getting loaded. To minimize the local compression of the cable at the contact with holder a large contact surface was made to distribute the force on a large area of the cable.
- The slipping plate have lips to reduce the risk that the cable threads get hooked by the holder if the cable is getting pulled in future tests (after this thesis work).
- Every component is slightly over dimensioned to minimize the risk of affecting the measurement result of displacement.

The Figure 3.23 and Figure 3.24 shows the equipment in the reality and how they will be mounted in the squeeze rig.

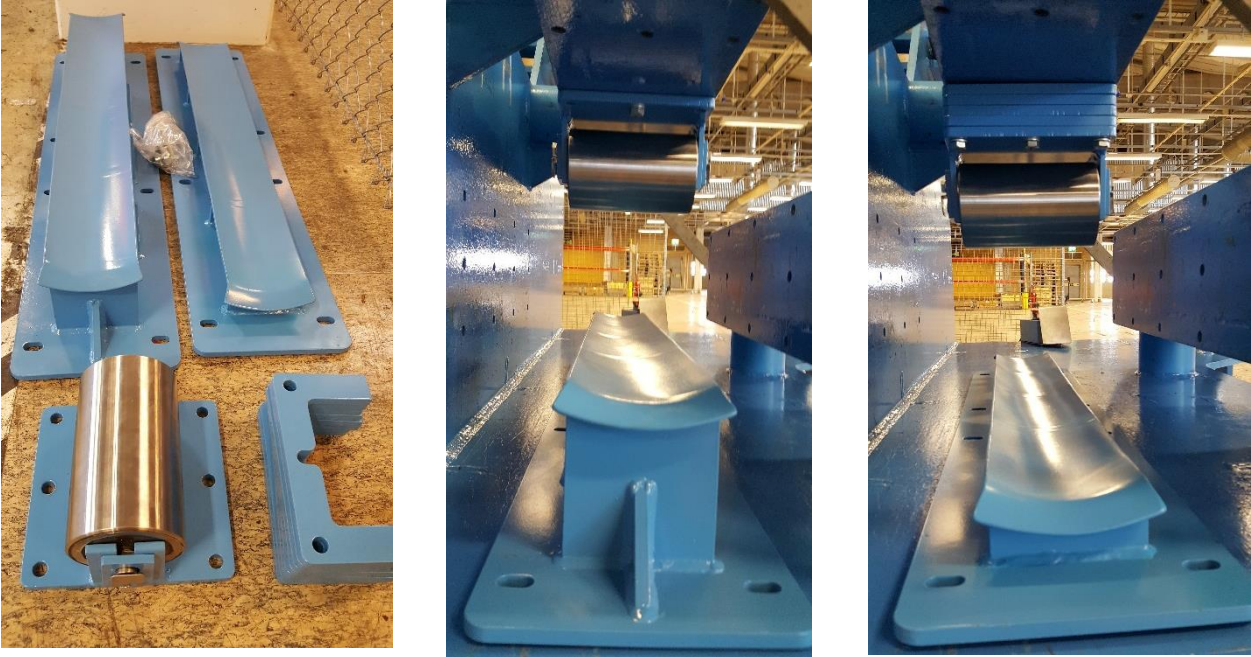


Figure 3.23 - Equipment mounted in Squeeze rig.



Figure 3.24 - Roller support mounted in the middle of the Squeeze rig's clamp.

### **3.5.2.1 The experiment for the double armoured DC cable**

The double armoured cable is placed in the holder (see Figure 3.25) and the pressure films are attached on the cable upper side under the roller support. In an interval of 3000N – 40 000N ten forces are applied. Between each measurement the cable was moved a bit so the compression will be performed on a new and not already compressed surface on the cable.



*Figure 3.25 - A double armoured cable in the squeeze rig.*

### 3.5.2.2 The experiment for the bundled AC cable

The bundled cable is placed in the holder and the pressure films are attached on the cable upper side under the roller support (see Figure 3.26). In an interval of 3000-12000N, four forces are applied and are repeated in three different load angles (see Figure 3.27). Between each measurement, the cable was moved a bit so every compression is being performed on a new and not already compressed surface on the cable.

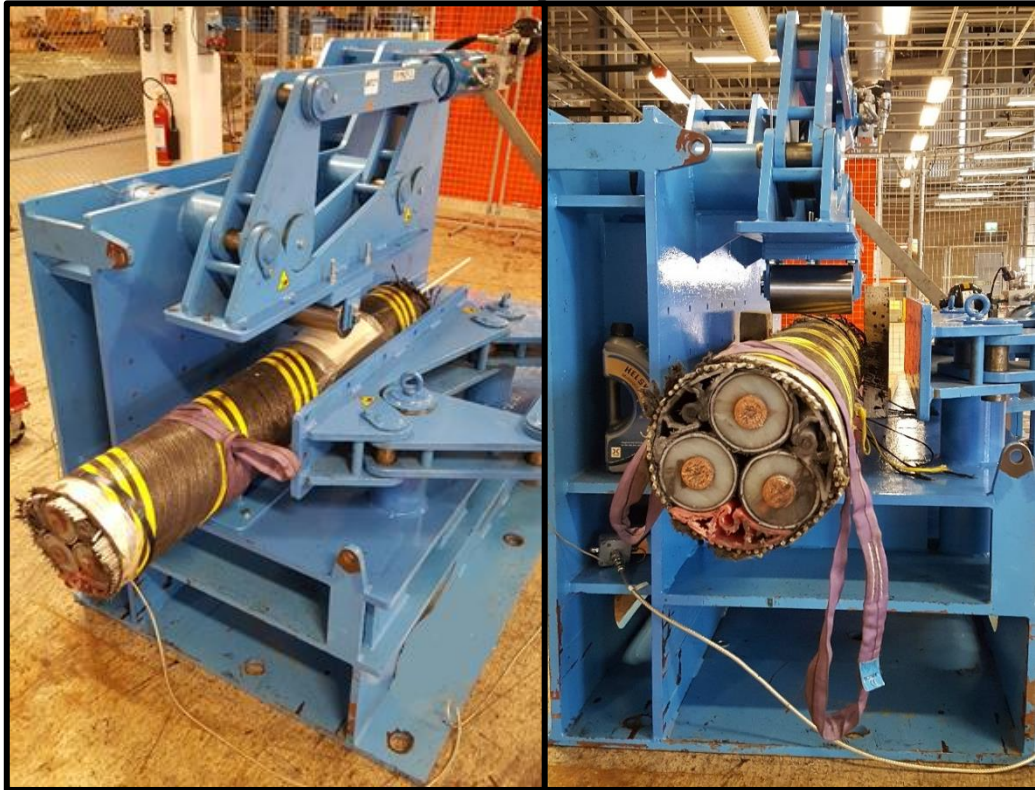


Figure 3.26 - The experiment for a bundled cable.

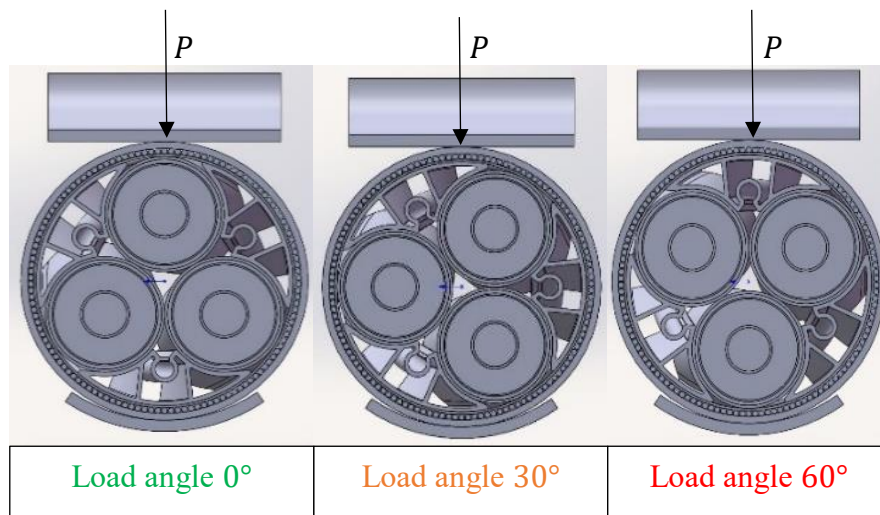


Figure 3.27 - Different load angles.

# 4 RESULT

In this chapter will the results be presented.

## 4.1 The result of using the pressure film to determine the radial force

### 4.1.1 Small single armoured DC cable used in Pointload test

The result of using the pressure film for determine the applied force on a small high voltage cable in pointload test is presented in Figure 4.1 below:

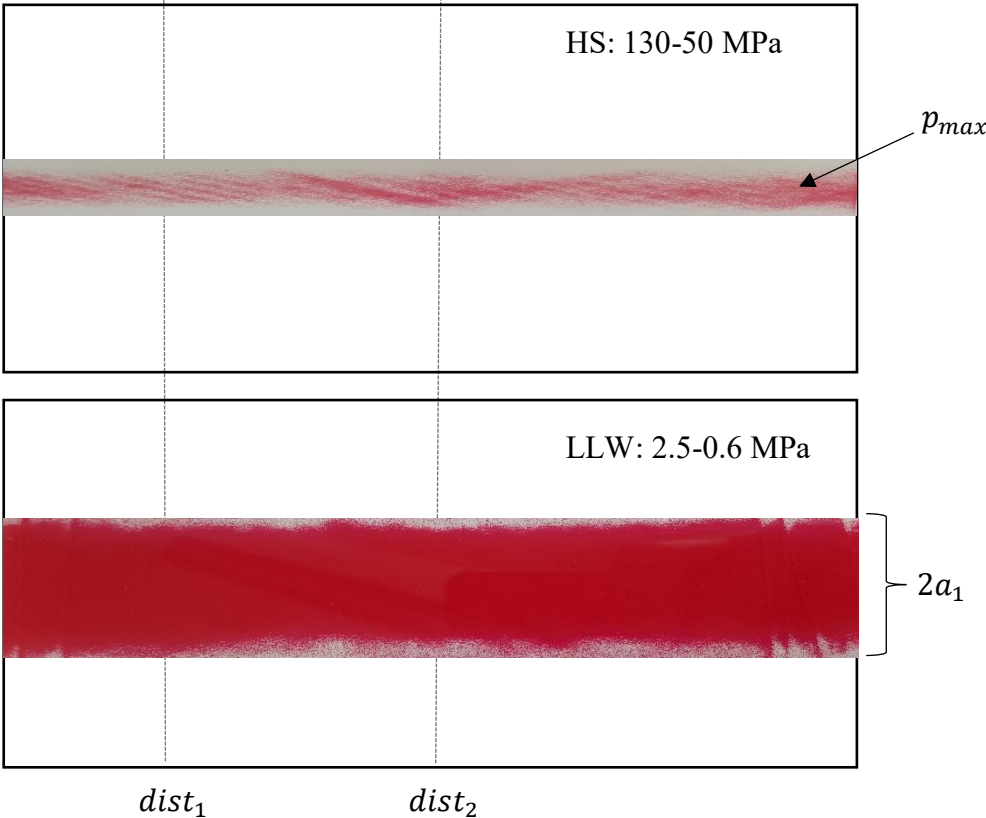


Figure 4.1 - The result from the pressure films at point load test.

In the high-pressure film HS it is possible to see the armouring wires (see stripes in the Figure 4.1) made it difficult to translate the colour density level to pressure. In the Table 4. below the maximum pressure and the ellipse diameter are presented.

Table 4.1 – Measured data from the pressure films for the pointload test.

Load case	Angle $\beta$ [°]	Maximum Pressure $p_{max}$ [MPa]	Ellipse diameter $2a_1$ [mm]
1	31.6	~80	30
2	39.6	~80	34

The table shows the maximum pressure and largest ellipse diameter result from the pressure films for different angles  $\beta$ . By using the maximal pressure and the ellipse diameters combined with Hertzian's theory the radial force is determined (see Table 4.2).

Table 4.2 – Comparison between the theoretical, ORCAFLEX and pressure films generated force.

Pointload test with tensile force $F = 78\text{kN}$				
Load case	Angle $\beta$ [°]	Theoretically $P_r$ [kN]	Orcaflex $P_r$ [kN]	Pressure films $P_r$ [kN]
1	31.6	20.2	26.8	26.4
2	39.6	25.0	32.5	34.0

The Table 4.2 shows that it becomes a small difference between the ORCAFLEX result and pressure film result.

**4.1.2 Double armoured DC cable and bundled AC cable in Squeeze test**

In the squeeze rig test for the larger diameter cables (double armoured DC cable and bundled AC cable) it was difficult to read the value of the pressure on the pressure films. Because of the armouring wires will spread out the maximum pressure but also show a local high pressure on each armouring thread (see Figure 4.2).



Figure 4.2 - Pressure distribution on the armouring wires

By using the maximum pressure on the armouring wires it will give a force that become much larger (by using the pressure film result combined with Hertzian's theory) compared to the forces that were applied in the experiment. And using the predicted maximum pressure by two pressure films to translate it to force it will become much smaller force compared to the real forces.

## 4.2 Relation between compression and radial force for a double armoured DC cable.

### 4.2.1 FEM result for double armoured DC cable.

The Figure 4.3 presents the result of the compression between the cable and the roller for double armoured cable by using a FEM model. The total compression was divided into local compression between roller and the cable according method mentioned in chapter 3.4.4. The curve shows that it has almost a linear behaviour at the larger force meanwhile at the lowest forces it will turn into the origin.

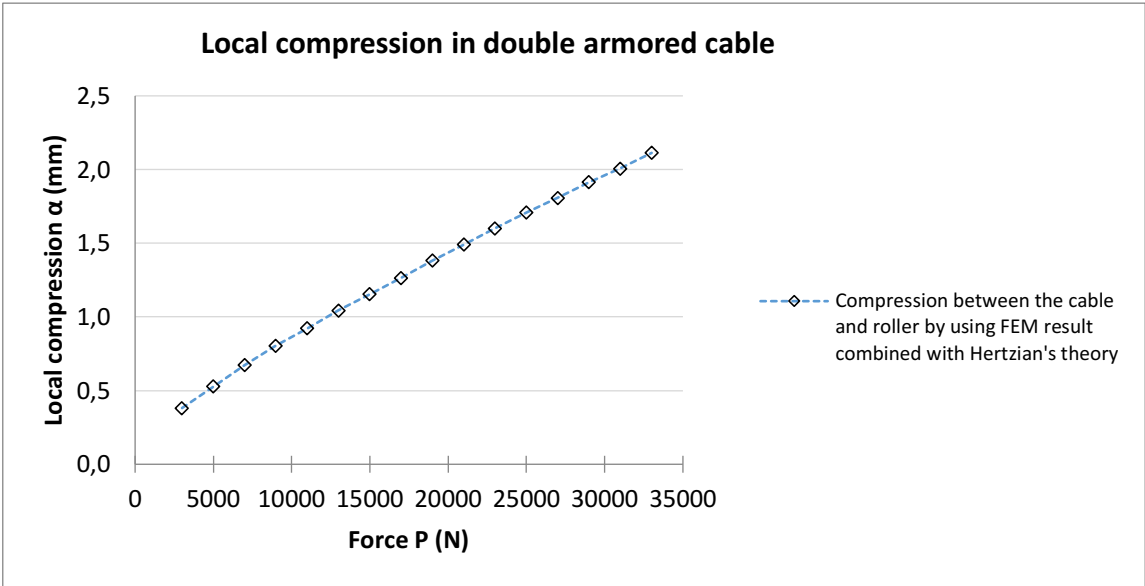


Figure 4.3 - Relation between compression and force for a double armored cable by using FEM.

#### 4.2.2 Result from force and displacement sensor for a double armoured DC cable

The Figure 4.4 and Figure 4.5 shows one of ten test results from the force and displacement sensors on the squeeze rig.

Figure 4.4 shows the example of what the force sensor has registered for the loadcase: 6000N. The peaks in the beginning of the force curve is because of the force sensor is calibrated on the pressure and the resistance in cylinder will then register some force when the cylinder is just moving down without having contact with the cable. At 01:00 the force starts to increase to the wanted force level (which are the time when it roller support starts to come in contact with the cable).

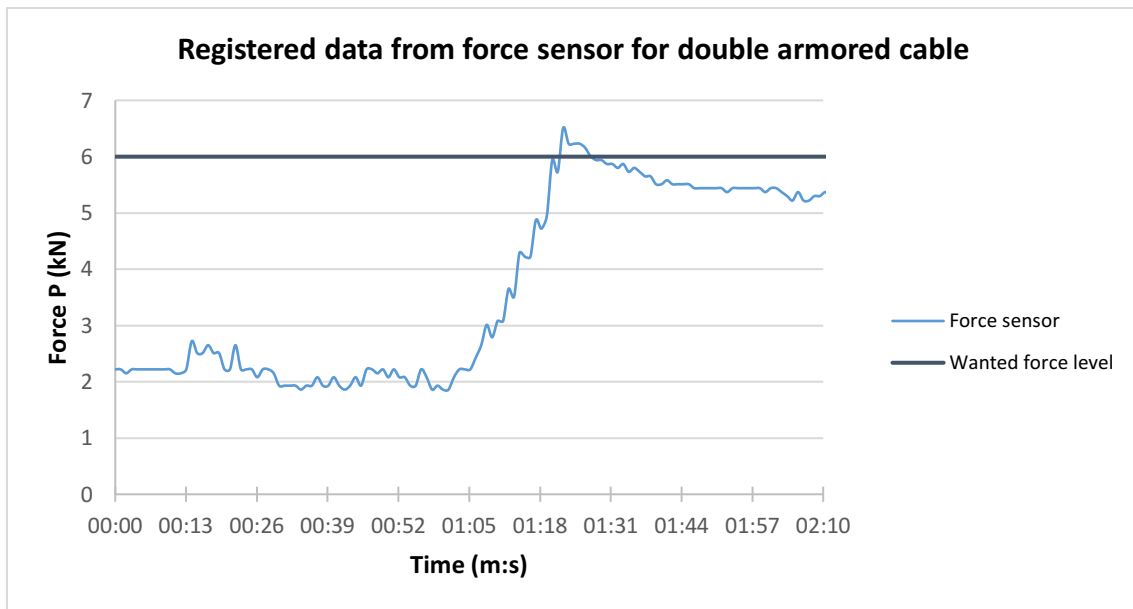


Figure 4.4 - Force sensor registered data for load case 6000N for double armored cable.

Figure 4.5 shows the total displacement of the movement of the roller. To calculate the total compression in the cable the end value of the compression (when the reaches the maximum force) must be subtracted with the start value of compression (when the cable has contact, which is the same as when the force is starting to increase).

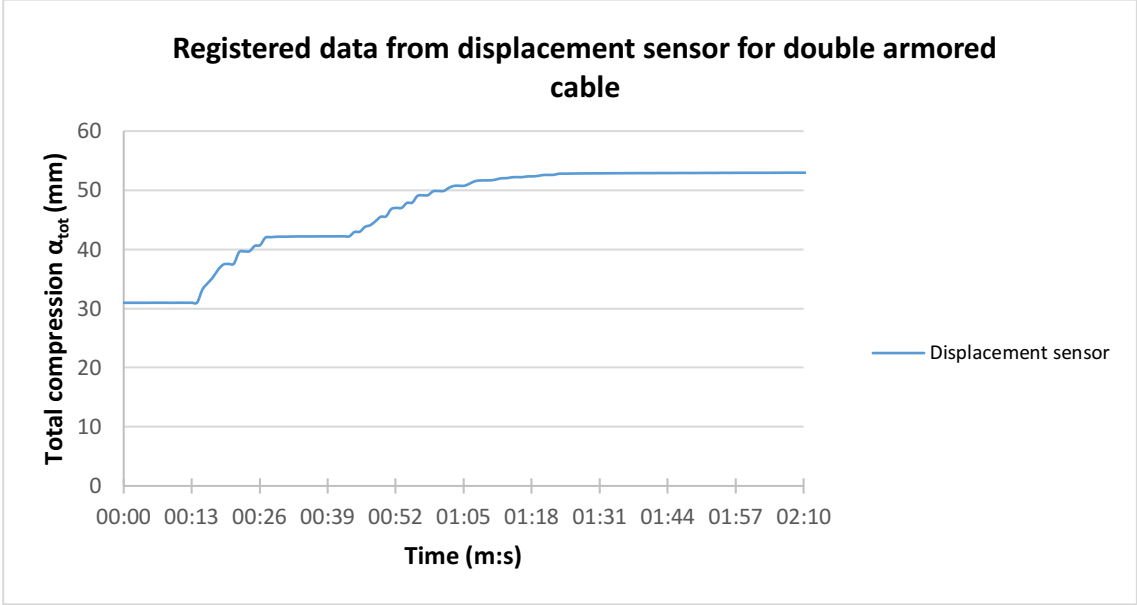


Figure 4.5 - Displacement sensor registered data for load case 6000N for the double armored cable.

The force was plotted relative to the total compression in the loading interval to be able to perform a linear approximation between the measuring points to filter the registered data. Thereafter an average slope has been calculated for all measurement results to be able to get a general and simplified result which are presented in the Figure 4.6.

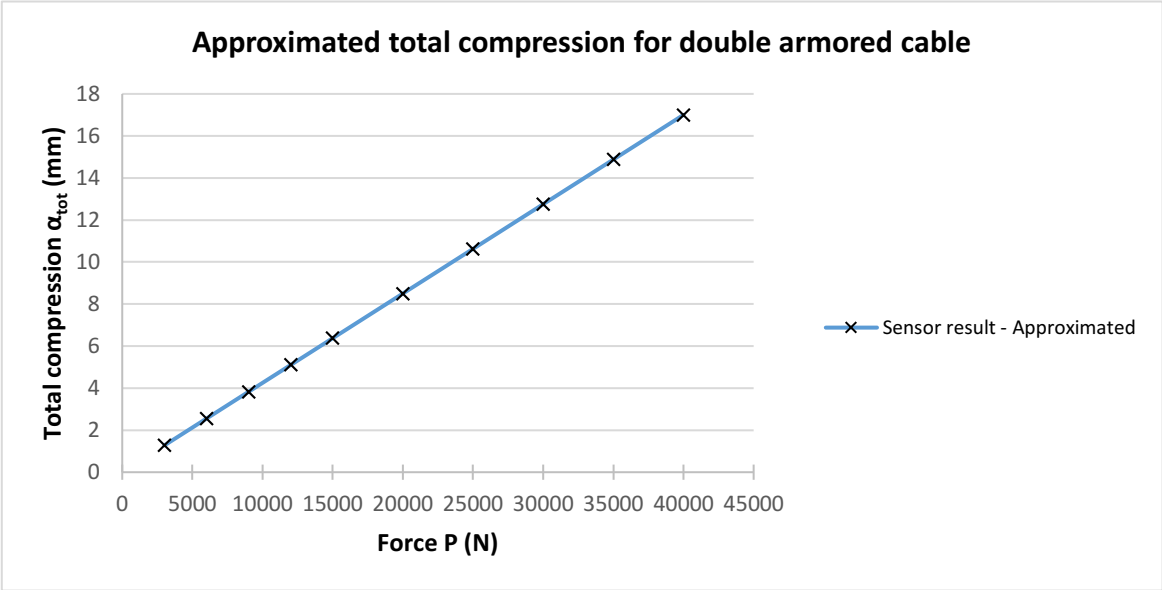


Figure 4.6 - Total compression in a double armored cable by using the sensor result.

The Figure 4.6 shows the total compression relative to force in the cable but the interesting part is the local compression between cable and roller. Therefore the total compression was divided into local compressions which was mentioned in chapter 3.4.4.

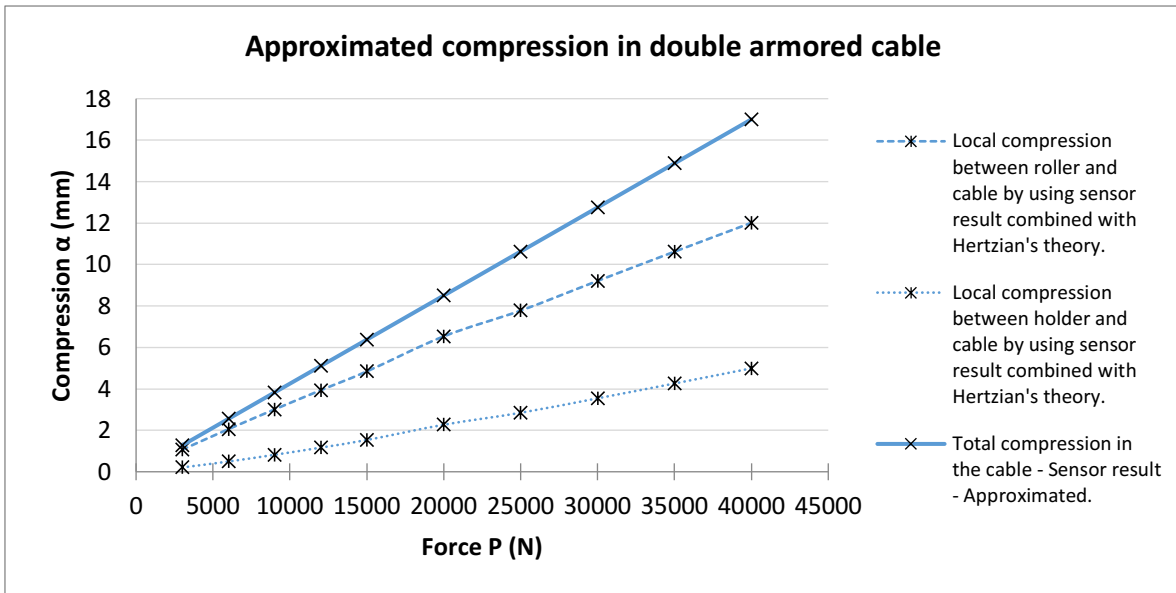


Figure 4.7 - Division of the total compression for double armored cable.

The Figure 4.7 shows the total compression is divided into local compression between roller and cable and between holder and cable.

The Figure 4.8 presents the result of the approximated compression between the cable and the roller for the double armored cable, by using the registered data from the force sensor and displacement sensor.

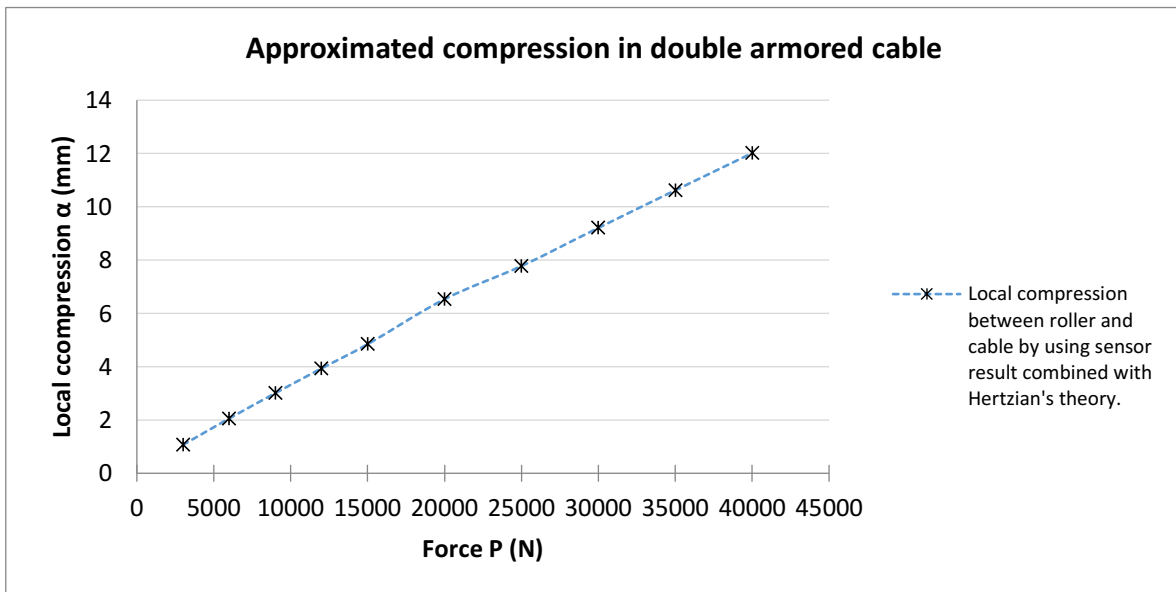


Figure 4.8 - The relation between the compression and force for a double armored cable by using the sensor result.

### 4.2.3 Pressure film result for a double armoured DC cable

The Figure 4.9 below shows the result from the pressure films, the ellipse contact and the pressure distribution for different forces on the double armoured cable. The forces are in interval of 3000N – 40 000N. Notice that the results on the MS film is only the red area. The purple around is the other pressure film behind that are shining through the MS film.

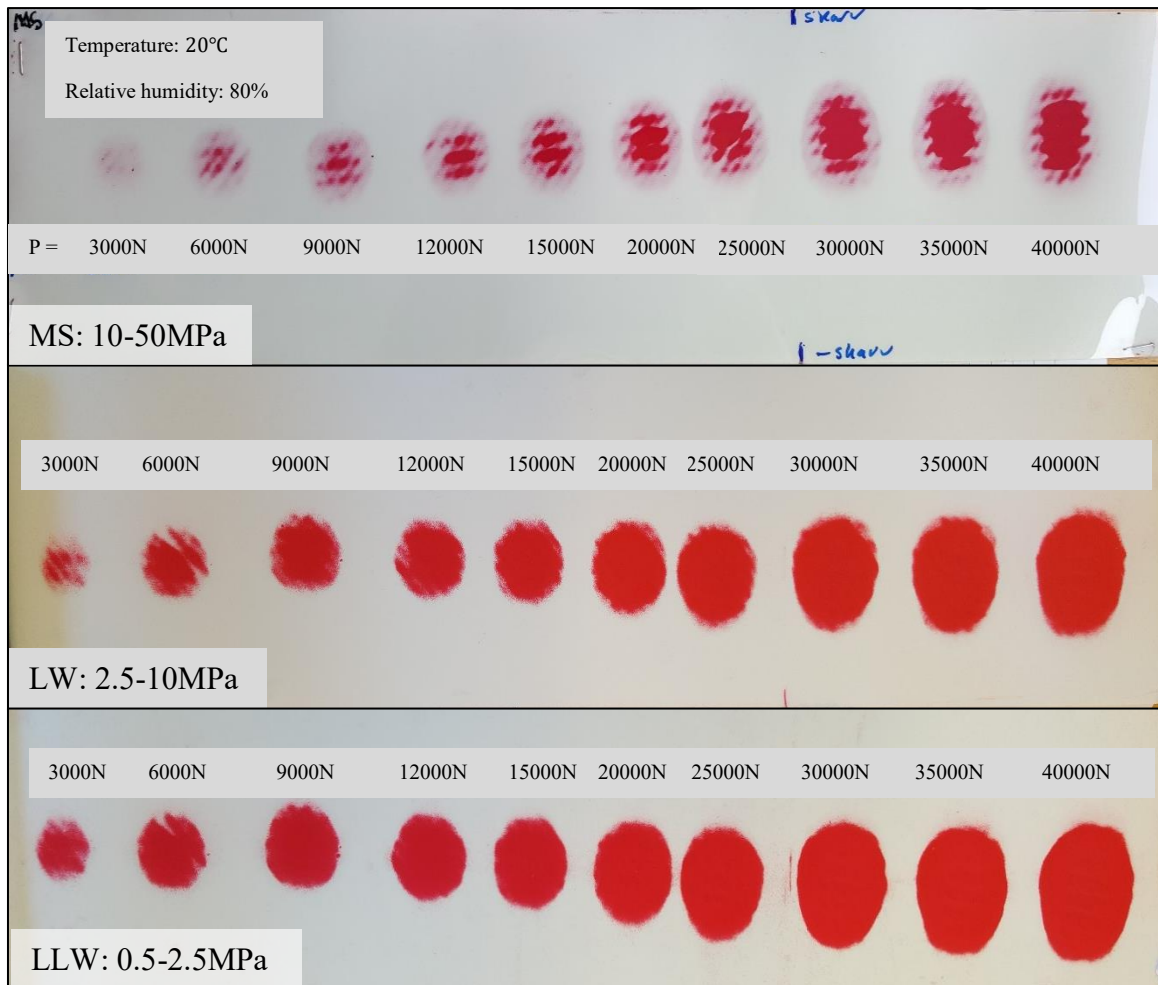


Figure 4.9 - Ellipse diameter results from the pressure films for the double armored cable.

In the Figure 4.10, the ellipse diameters from the LLW pressure film was plotted relative to the force for the double armoured cable.

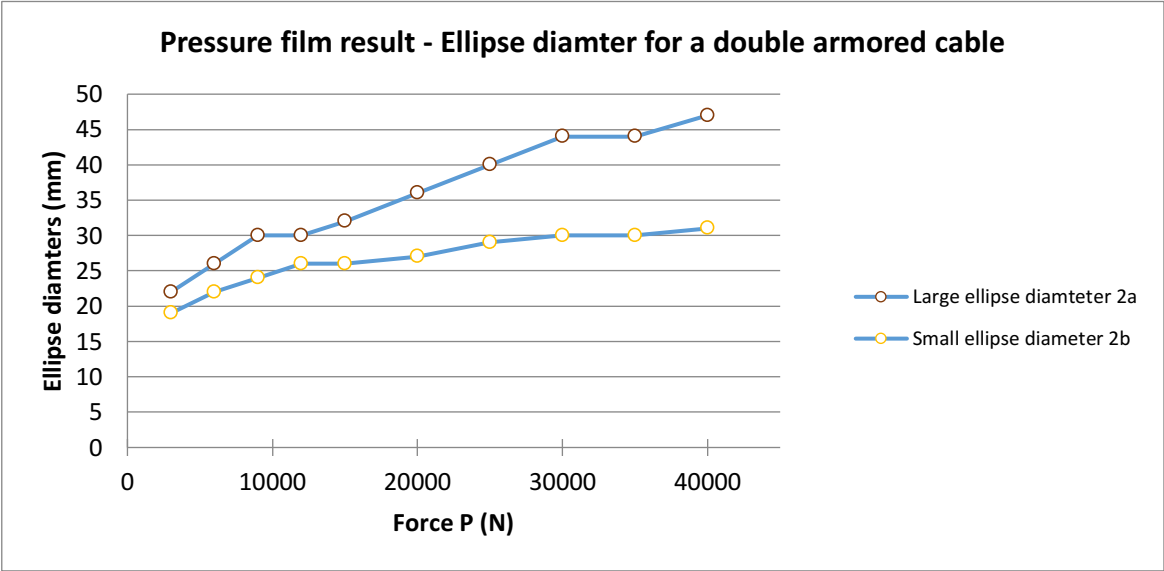


Figure 4.10 - The relation between the ellipse diameters from the pressure films and applied force for a double armored cable.

From the ellipse result combined with Hertzian’s theory according to chapter 3.4.5 it is possible to describe the local compression between the roller and the double armoured cable which is presented in the Table 4.3 and Figure 4.11.

Table 4.3 – The result of combining measured ellipse diameters with Hertzian’s theory

Ellipse Large diameter 2a (mm)	Ellipse Small diameter 2b (mm)	Eccentricity e	Force P (N)	Material parameter cable $S_{mp}$ (mm <sup>2</sup> /N)	Ellipse integral K	Compression $\alpha$ (mm)
25	20	0,600	3000	0,004	1,751	2,367
29	23	0,609	6000	0,003	1,758	3,179
33	25	0,653	9000	0,003	1,796	4,073
32	26,5	0,561	12000	0,002	1,722	3,911
34	27	0,608	15000	0,002	1,757	4,371
39	28	0,696	20000	0,002	1,841	5,619
42	30	0,700	25000	0,002	1,846	6,509
46	32	0,718	30000	0,002	1,868	7,762
47	32	0,732	35000	0,002	1,886	8,064
49	33	0,739	40000	0,002	1,896	8,744

The Figure 4.11 presents the result of the compression between the cable and the roller for double armored cable by using the ellipse diameters registered on the pressure films combined with Hertzian's theory and knowing the applied force. The curve shows that it can almost be described as a linear behaviour at the larger forces.

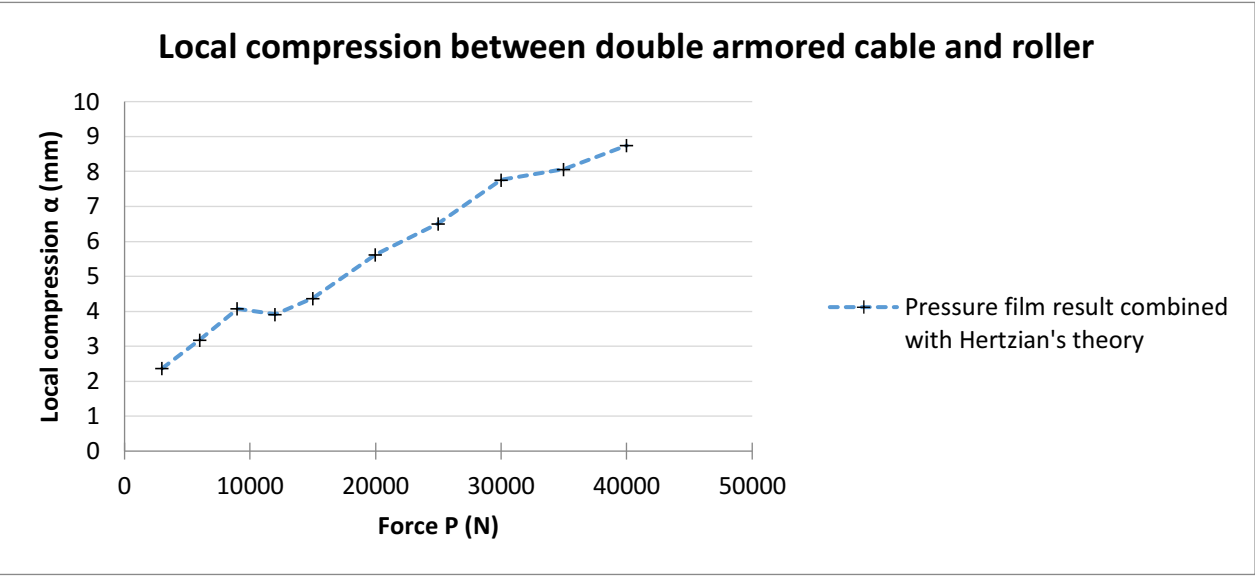


Figure 4.11 - The relation between the compression and force for a double armored cable by using the ellipse diameters and applied force.

### 4.3 Relation between compression and radial force for a bundled AC cable.

#### 4.3.1 FEM result for bundled AC cable.

The result of using finite element method to determine the relation between compression and radial force for a bundled AC cable is presented in Figure 4.12. The result shows a linear behaviour and in the 60° load angle it has be the largest compression.

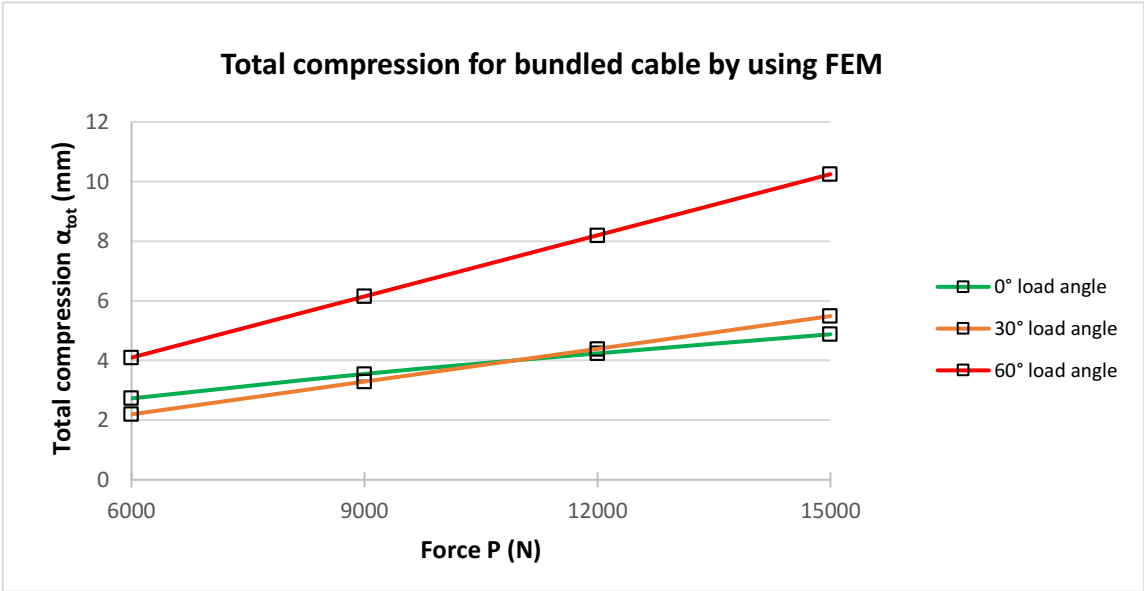


Figure 4.12 - Total compression for the bundled cable by using FEM.

In a similar manner as for the double armoured DC cable the bundled AC cable's total compression was theoretical divide into local compressions. The Figure 4.13 shows the local compressions between cable and roller and between cable and holder for the bundled cable in different load angles. The diagram show that the largest compression will be in the load angle 60 degrees and less for the 0 and 30 degrees load angle.

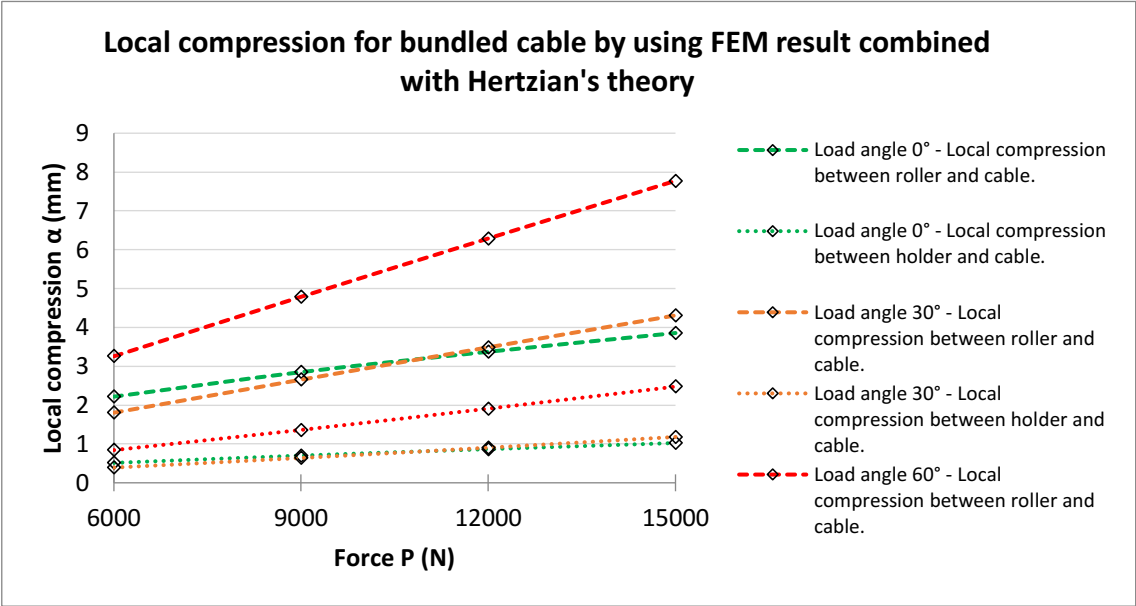


Figure 4.13 - Divide the total compression into the local compression between roller and cable and between holder and cable for the bundled cable.

### 4.4 Ellipse diameter result for bundled AC cable

The Figure 4.14 below shows the result from the pressure films, the ellipse contact and the pressure distribution for different forces in the three different load angles for the bundled AC cable. The forces are in interval of 3000N – 12 000N. It possible to see (especially in load angle 0° and 60°) that the smallest ellipse diameter is changing much less than the large ellipse diameter.

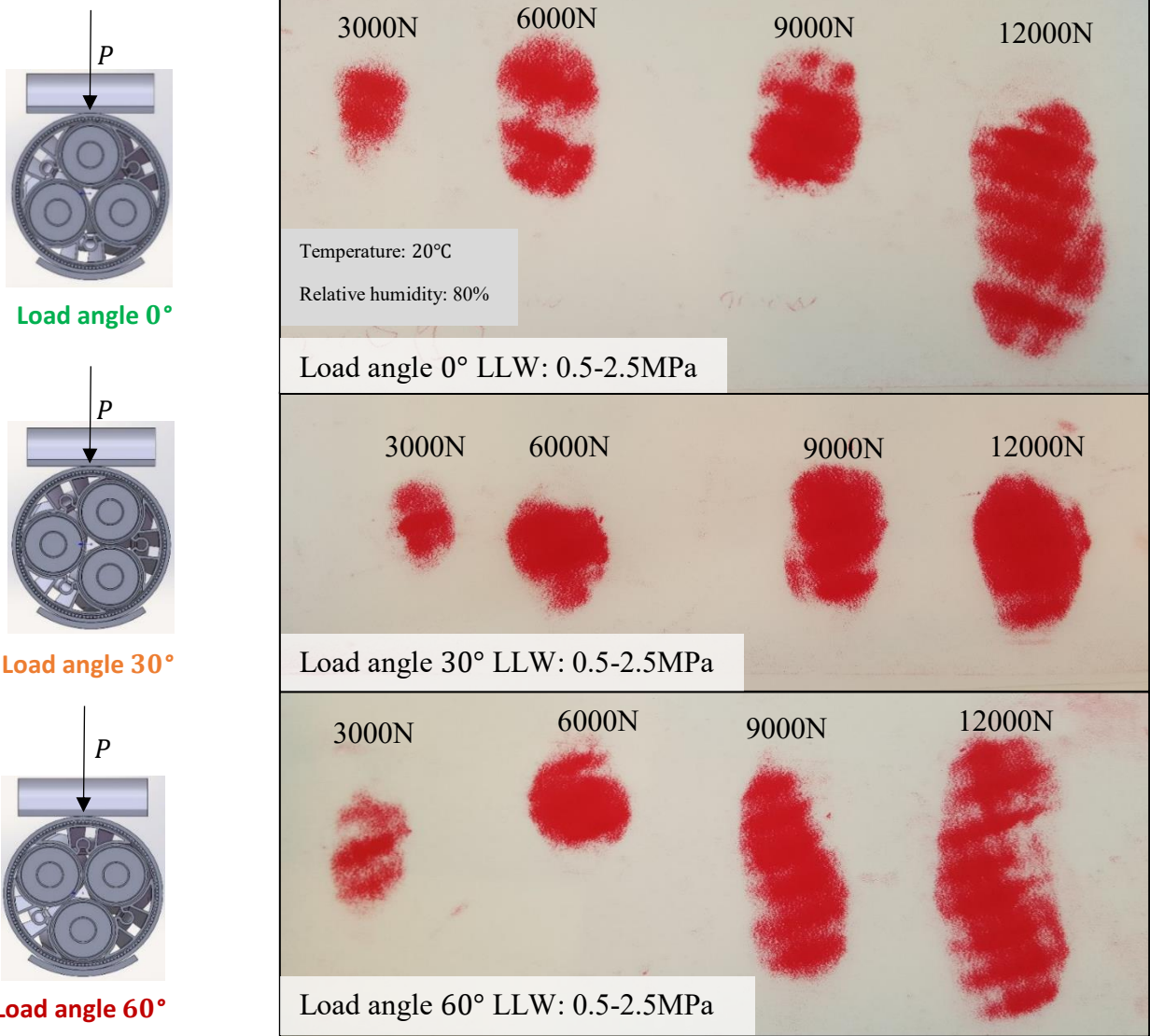


Figure 4.14 - Ellipse diameters result from the pressure films for the bundled cable.

The Figure 4.15 below is showing the measured result of the ellipse diameters in the diagram.

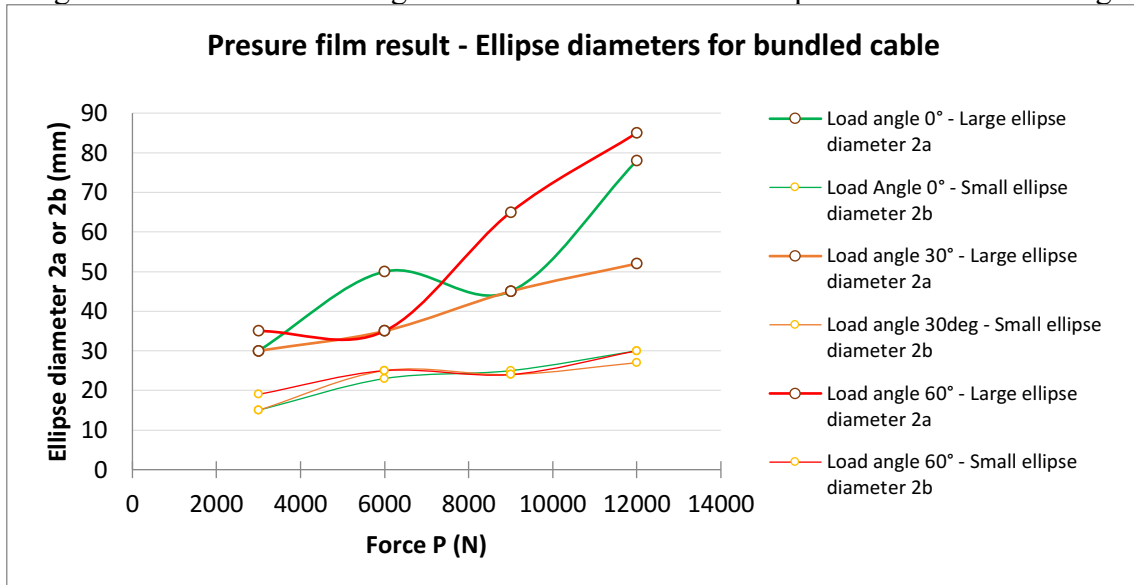


Figure 4.15 - The relation between ellipse diameters and force for different load angles for a bundled cable.

From the combination between ellipse diameters and Hertzian's theory according to chapter 3.4.5 the Figure 4.16 describes the local compression between roller and cable.

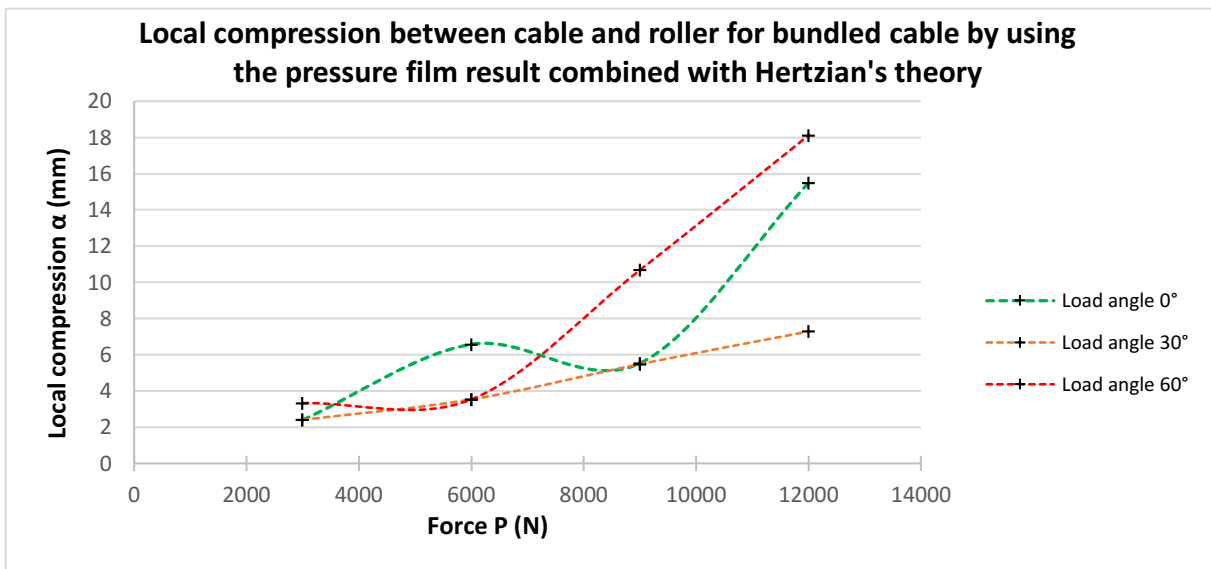


Figure 4.16 - The relation between compression and force for a bundled cable in different load angles by using the ellipse diameter and the applied force.

### 4.5 Result from force and displacement sensor for a bundled AC cable

The Figure 4.17 - Figure 4.18 shows one of twelve test results from the sensors on the squeeze rig.

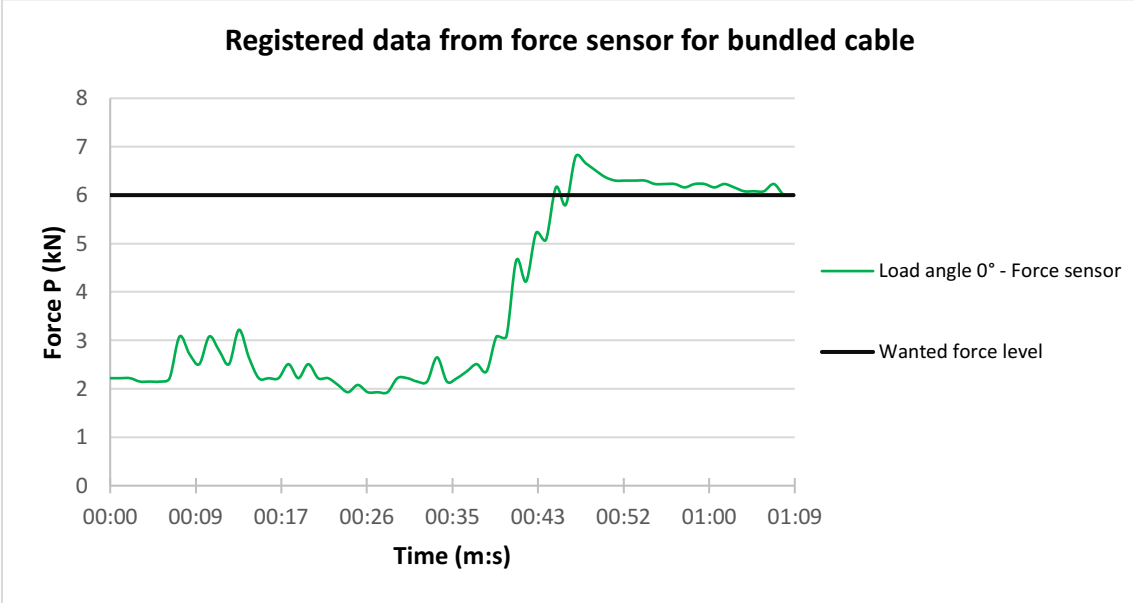


Figure 4.17 - Force registered by the force sensor for the load case 6000N and load angle 0° for a bundled cable.

Figure 4.17 shows what the force sensors has registered.

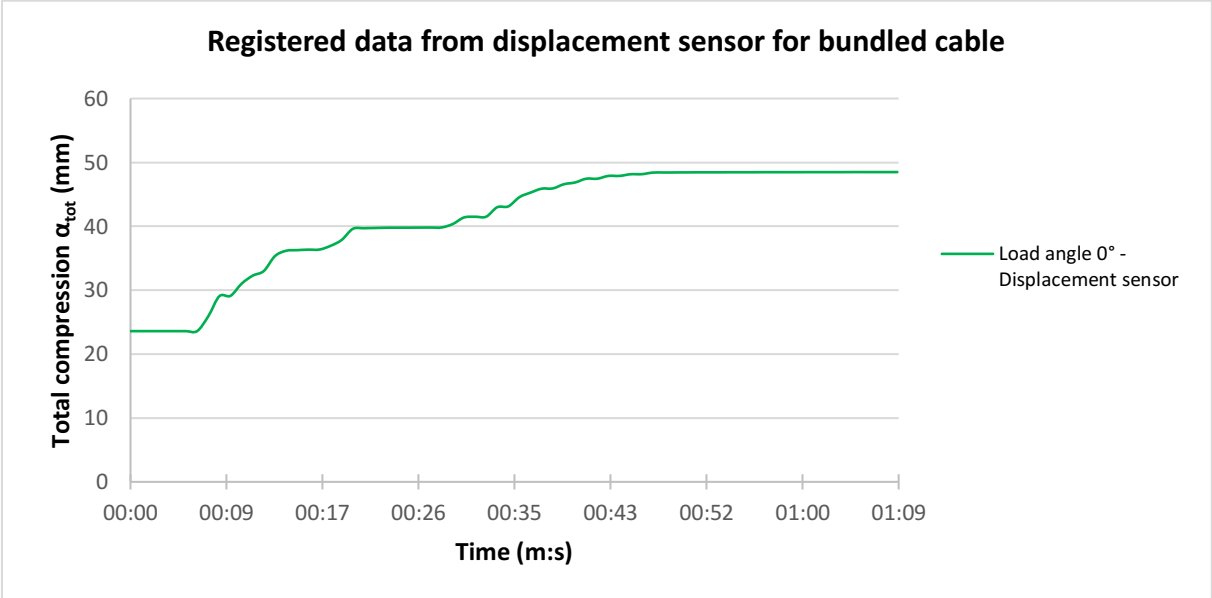


Figure 4.18 - Total compression registered by the displacement sensor for load case 6000N and load angel 0° for a bundled AC cable.

Figure 4.18 shows the total displacement of the movement of the roller. The approximated total compression was linear approximate and calculated in a similar way as for the double armoured DC cable.

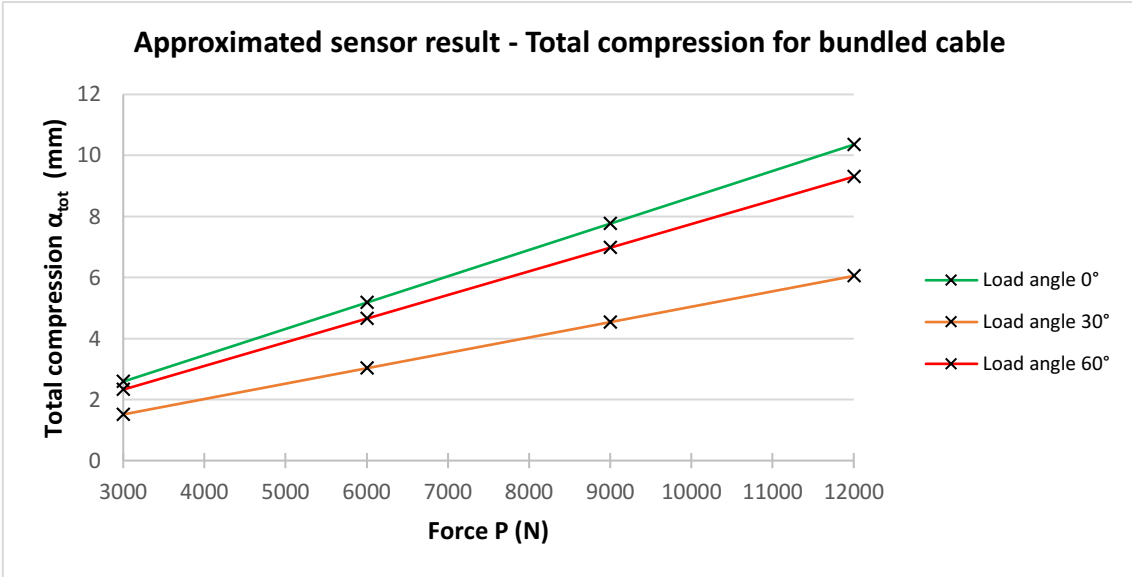


Figure 4.19 - Total compression from the sensor result for the different load angles for a bundled cable.

In similar way as for the double armoured DC cable the total compression is divided into local compression between roller and cable and between holder and cable. The Figure 4.20 shows the largest compression is in the load angle 0 degrees and less for the 60 degrees and 30 degrees load angle.

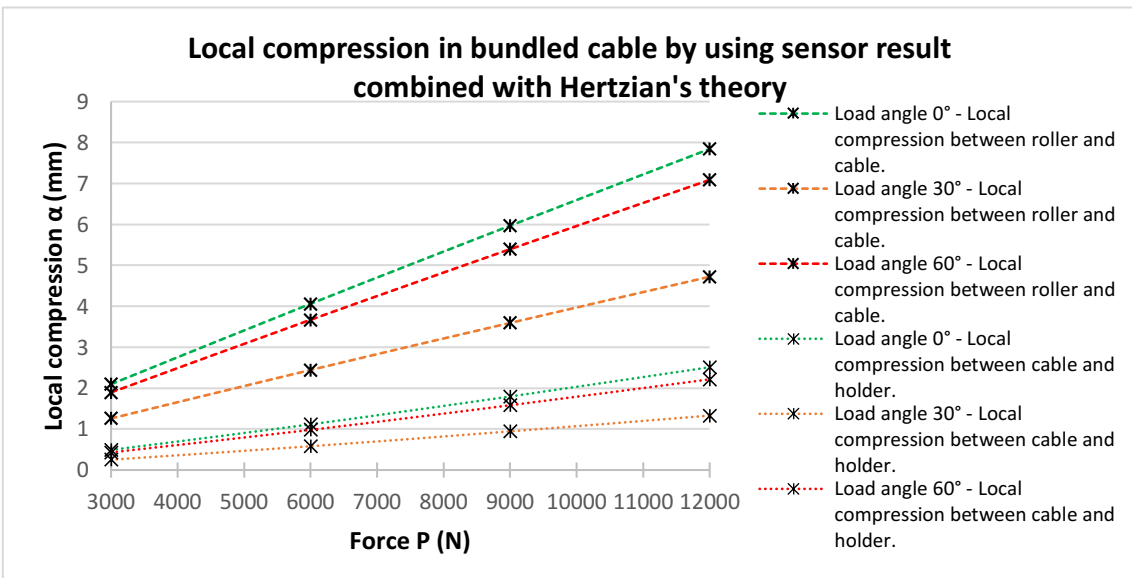


Figure 4.20 - Compression between roller and cable and holder and cable for the different load angles for a bundled cable.

## 5 DISCUSSION

---

*In this chapter discussion of the given results is found.*

### **5.1 Using the pressure film to determine the radial force**

To translate the colour density level to right pressure level is difficult and the accuracy is highly dependent on the translator. To reduce these types of error a scanner can be used to translate it to a more accurate pressure result. But it will not be a cost-effective method to use.

One of the goal was to be able see if it was possible to measure the radial force it becomes between cable and roller support by using these pressure films. When the armouring wires are affecting the pressure film result it becomes very difficult to translate colour density level to pressure and therefore also the force. The advantage of using the pressure film was that they could capture the ellipse diameters. To just measure the force, it exists better and easier measure methods which will be mentioned in the chapter of future works (see chapter 7).

In the pointload test the result of translating the pressure to force was possible. Probably because it was a smaller cable that had smaller armouring wires which effect the pressure distribution less. Any conclusion from this could not be stated because during this test only two measurement result could be generated. It is not a valid method to use if it is not working for all types of cables. For the large cables the double armoured DC and bundled AC cable which have larger armouring wires, it was not possible to translate pressure to force by using the pressure film together with Hertzian's theory.

## 5.2 Comparison between the results of using FEM, sensor and ellipse diameter result for describing the relation between compression and force for a double armored DC cable.

The Figure 5.1 presents the comparison between the result of using FEM, sensors and ellipse diameter to describe the relation between compression and force in a double armored cable.

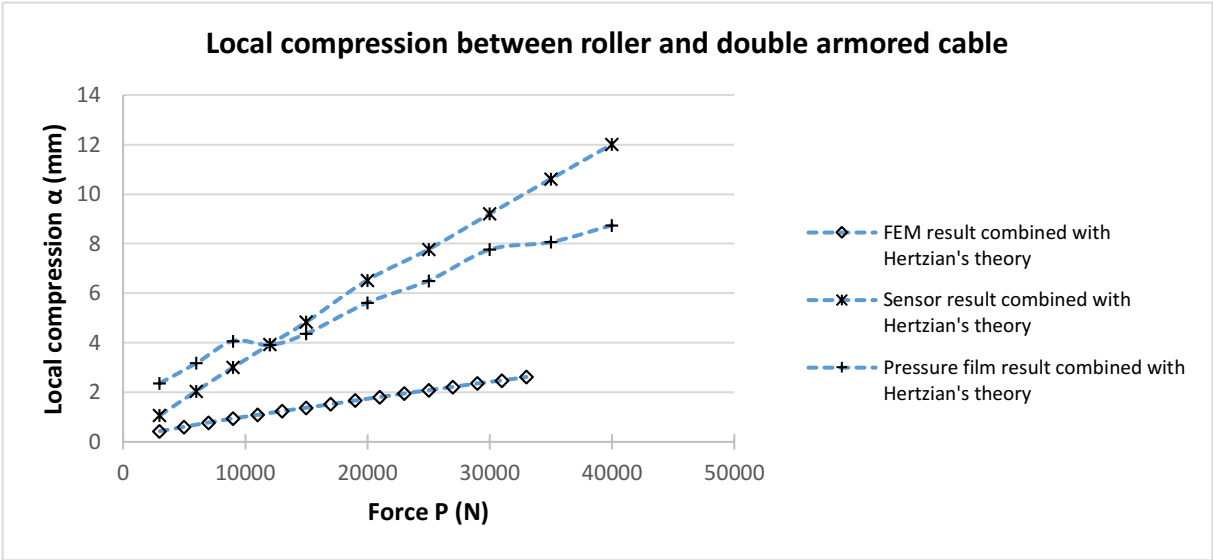


Figure 5.1- The comparison between the methods for describing the relation between compression and force for a double armored cable

The FEM result in Figure 5.1 is less than the ellipse and sensor results. This is probably because when the FEM model was made it was simplified, to reduce the calculation time. The material layers were tied together which in this case, for the double armored the cable behave much stiffer in the FEM model than in the reality.

The ellipse result and the sensor result is dependent on the applied force that was registered by the force sensor in the squeeze experiment. The force sensor was calibrated to the pressure of the cylinder which made it difficult to precisely get the force that was applied on the cable.

The pressure films were used to get the ellipse diameters and with Hertzian's theory used to calculate the compression in the cable. But the lowest pressure film, LLW can only registered at lowest 0.5 MPa. The Hertzian's theory uses the theoretical ellipse diameters that have in theory 0 MPa. In other words, will the LLW pressure film shows a smaller ellipse diameter than what it should do if for example 4LW (0.02-0.05 MPa) had been used. Therefore, would the compression also become a little larger than what it is show in the figure. But in practical it would not be possible to handle these super sensitive pressure films in an appropriate way.

Both the sensor and FEM result could only register the total compression in the cable. Later it was theoretically dived into local compression between roller and cable and between holder and cable. But in the reality, some of the total compression will also go to change the geometry of the cable which this method does not consider. In other words, will the sensor result and the FEM will show a little bit larger local compression than what it does in the reality.

The sensors results were linear approximated to be able to filter the registered data and an average on all measurement was made to easily describe a general result of the cable. This probably makes the result of the approximated sensors less accurate at the lower force ranges.

### 5.3 Comparison between the results of using FEM, sensor and ellipse diameter result for describing the relation between compression and force for the bundled AC cable.

All the simulations for 30° load angle and 60° load angle, were not completed because of convergence problem in ABAQUS this can be explained by the large displacement in the soft materials. But for each load angle some of the simulations went through which made it possible to perform a linear interpolation to approximately predict the other compressions. Linear approximation was chosen because of the 0° load angle had this behaviour in this force interval.

Figure 5.2 - Figure 5.4 presents the results of using FEM, sensors and ellipse diameter for a load angle of 0, 30 and 60 degrees to describe the relation between compression and force for the bundled cable.

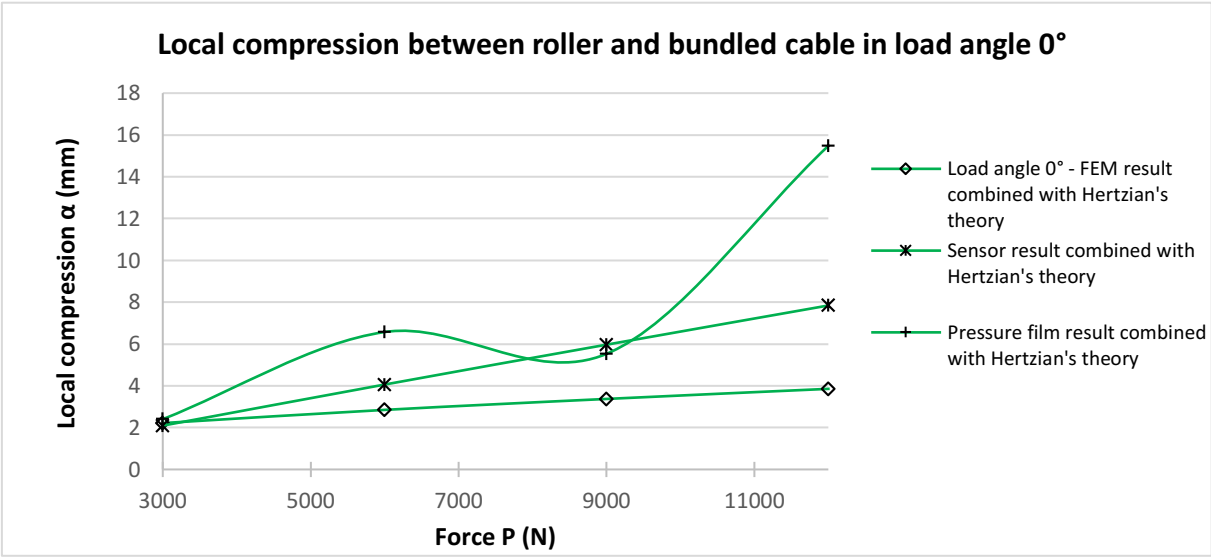


Figure 5.2 - Comparison between the methods for describing the relation between compression and force for the bundled cable in load angle 0°.

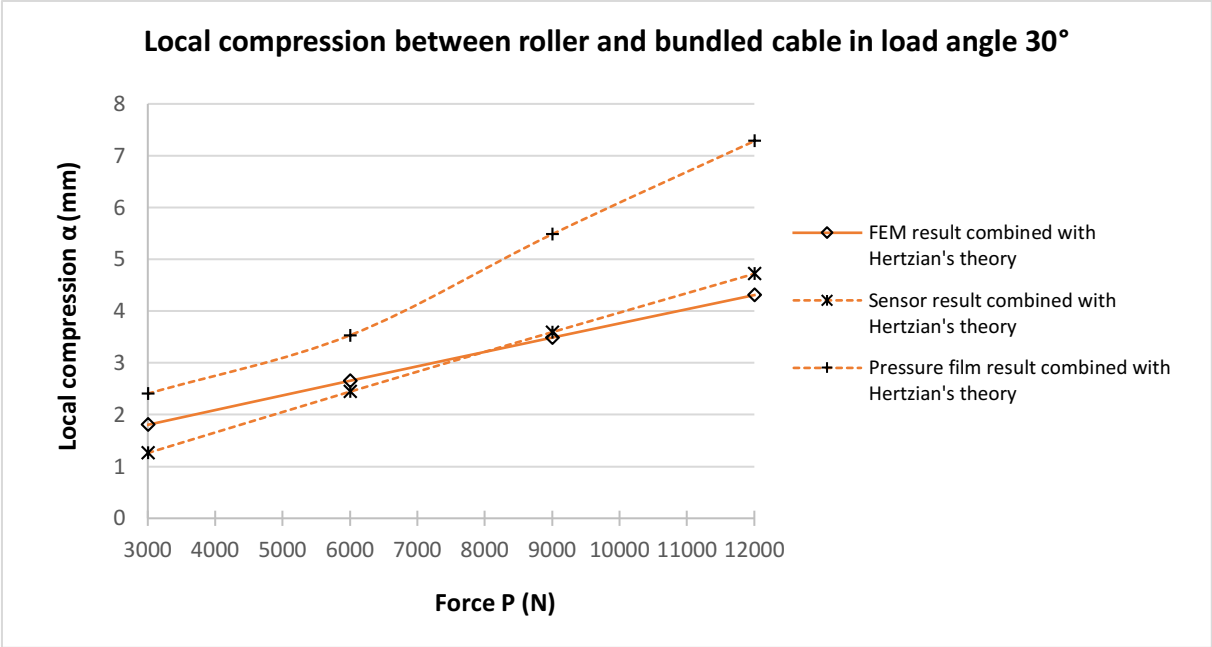


Figure 5.3 - Comparison between the methods for describing the relation between compression and force for the bundled cable in load angle 30°.

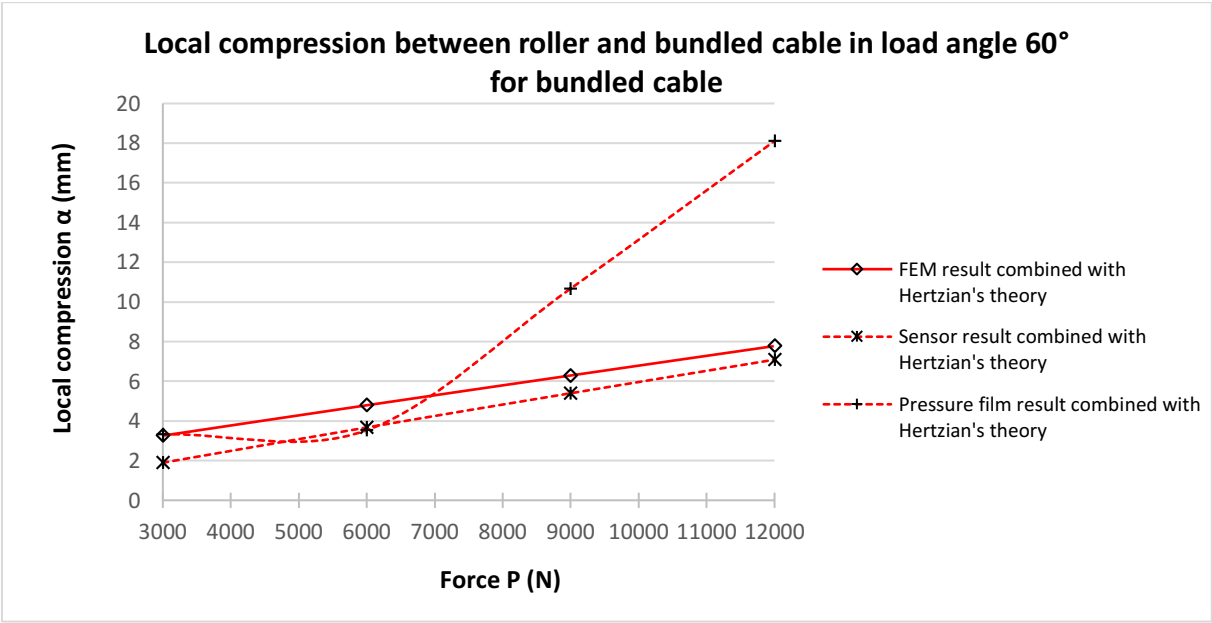


Figure 5.4 - Comparison between the methods for describing the relation between compression and force for the bundled cable in load angle 60°.

The compression in the FEM result in Figure 5.2 is less than the sensors and pressure film results in the 0 degrees load angle. This can be explained by the simplified FEM model that was made so the material layers were tied together and the conductor was constrained relative to each other. This made the cable behave stiffer than the real cable. In the reality the part cables in bottom will move sideways when the force is applied on the upper part cable. Which the left picture in the Figure 5.5 shows:

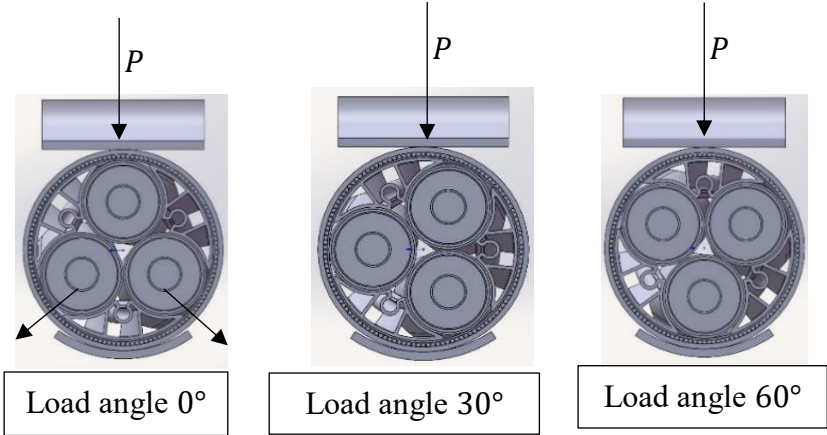


Figure 5.5 - Load angle for the bundled cable.

But the for the 30 and 60 degrees load angle (see Figure 5.3 and Figure 5.4) will give better result of the FEM because in 30 degrees load angle because the internal part cables will move less relative each other compared with 0 degrees load angle, see middle picture in Figure 5.5. The 60 degrees load angle in other hand will the internal part cables will also move less relative to each other. Because the plastic profiles are softer than the part cables which made the largest part of compression become in the these and not to separates the parts cable, see right picture in Figure 5.5.

The large ellipse diameter for the bundled AC cable were changing much compared to the small ellipse diameter between every measurement. A possible reason of this is that it is difficult to compress the cable in the same exact same load angle each time, because the pitch of the bundling can lead to the force is will be not distributed equally in the cable. This result that the cable will rotate during the loading which give larger mark on the larger ellipse diameter. In the Figure 5.6 below it shows that the larger ellipse diameter is changing much more compared to the small ellipse diameter which will give an indication that cable has rotated a bit during the loading.



Figure 5.6 - Rotating of the cable during the loading will increase the larger ellipse diameter.

#### 5.4 The hydraulic cylinder

The hydraulic cylinder in the experiment show a less accuracy when small forces are applied which can affect the result on the force. The hydraulic cylinder is also calibrated to the pressure which is a bit misleading because when the increase pressure for just moving the cylinder down, without any contact against the cable it will then register some force. To improve the experiment, it would be better if the roller support was constructed in such way that the axle had two radial force sensors (see future works chapter 7) that could register the force in a more accurate way.

## 6 Conclusion

---

*In this chapter conclusions will be presented over the answer provided for the problem formulation.*

### 6.1 Using the pressure film determine the force

The pressure film can be used to obtain the ellipse diameters but using the pressure film combined Hertzian's is a poorly way to determine the radial force between radial force and the cable.

The disadvantage of using the pressure film in real roller support track is that it is not easy to translate directly from pressure to force. To be able to use these pressure films to measure the force NKT need to perform a squeeze test on each specific cable so they have relation between the ellipse diameter and the force. Thereafter they can measure ellipse diameter in the real roller support track and translate it to force. But for the bundled AC cable this becomes more difficult to measure in the real roller support track because it is not possible to see then in which load angle the radial force is applied. In other hand the relation between the ellipse diameter and applied force for the double armoured DC cable became better than the bundled AC cable, therefore it is a possible way to shims in the roller support track when this type of cable is traveling through the factory. If the roller supports are better shimmed to distribute the load more equally and right amount of radial force for the double armoured DC cable it will also make it better for a bundled AC cable to travel in this roller support track.

But it is important to say that the pressure film is good use to compare the relative force distribution between each roller support. Because if it is a larger ellipse diameter on the pressure film at a specific roller and less on another. This will show that the first roller is taken up more radial force than the other one. But we will not know the exact amount of radial force. Other measuring technics to measure radial force are available that will be discussed in the future works (see chapter 7).

### 6.2 Use the compression to determine the radial force

To be able to use the known compression to determine the radial force the relation between the compression and the radial force must be obtained for each specific cable. Which make it weak and ineffective way to determine the radial force and therefore this method is not recommended to measuring the radial force. More advance measuring techniques are available that can measure the radial forces faster and in a more accurate way (see future works in chapter 7).

# 7 FUTURE WORKS

---

## 7.1 Measuring the force between the roller and the cable

### 7.1.1 Force sensor film

A possible measuring method that can be used in similar way as the pressure film is the force sensor film (see Figure 7.1). This can for example be based on load cells that can register the force between the roller and cable. The disadvantage is that it needs power supply cable to work which can be problematic when the measurement will be used on a moving cable and roller. But some models have a Bluetooth sender that can be a possible way to measure the radial force in a safer way.

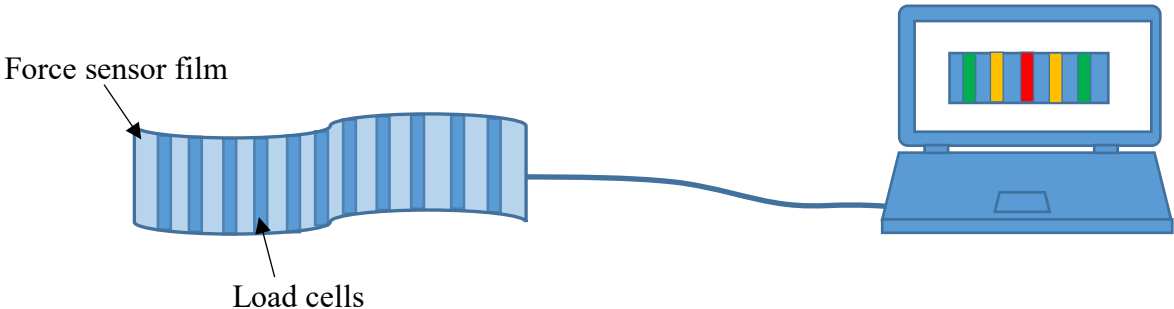


Figure 7.1 - Force sensor film with load cells.

### 7.1.2 Radial force sensor

A radial force sensor (see Figure 7.2) can be used to register radial forces. The advantage of using this is that it can be applied into the roller's axle and therefore measuring indirect the force between the cable and the roller. This could also be applied in roller support to measure the force better in future experiments in the squeeze rig.

For a single part cable travelling in the roller support track, two radial force sensors on the roller support can be applied and shimmed so the maximum radial force is reached for the specific cable. By thereafter using a pressure film to be able to get a reference value of the largest ellipse diameter it is possible to use this to check the other roller supports largest ellipse diameter by only use the pressure film as measuring method on these. With this way of measuring on a single part cable makes it unnecessary to apply the radial force sensors on each roller support to determine the radial force.

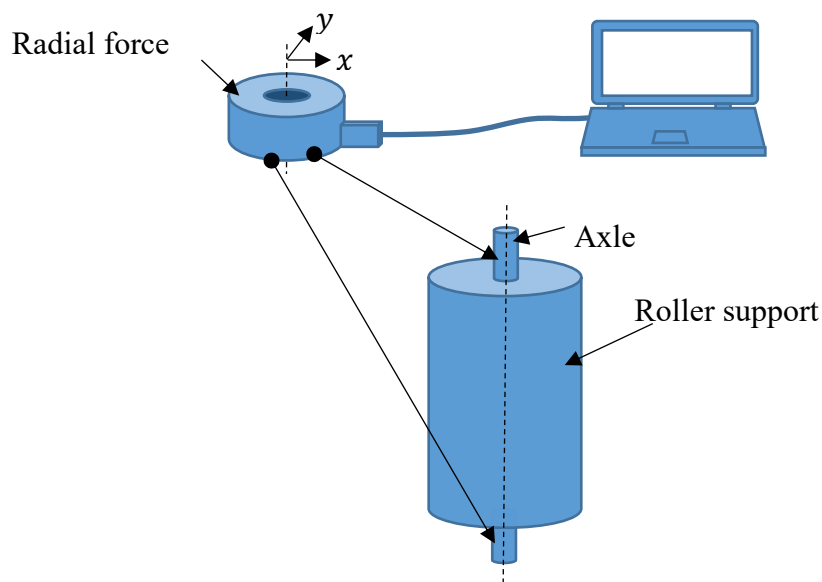


Figure 7.2 - Radial force sensor applied on the roller support.

## 7.2 Improve the FEM model

### 7.2.1 Make a representation of the armouring wires

In this project the FEM model for example of the double armoured DC cable the two layers of armouring layers was tied together to reduce the simulation time. This made the FEM model behave much stiffer than the real cable. For further works it would be interesting to study how to replace the armouring wires by a solid pipe (with surfaces like armouring wires) that has a specific material parameter that will have the same behaviour and stiffness as the real armouring layer to create a better FEM model representation.

### 7.2.1 Plasticity

By consider the plasticity of the cable in the FEM model by including stress-strain data for each material make the FEM model better and more realistic to the real behavior.

## 7.3 The cable is temperature dependent

The cable consists of several materials there the elastic modules are depending on the temperatures. On NKT they have roller support tracks both inside and outside which make the cable stiffer on the low temperatures in winter and softer at the higher temperatures in the summer. In the cable contain bitumen which can be simplified explained as floating asphalt which is much temperature dependent. For the elastomers and thermosets, the elastic modulus decreases when the temperatures exceed the glass transition temperature (M. Ashby, H. Shercliff, D. Cebon, 2013) (see Figure 7.3). In future works this can also be considered.

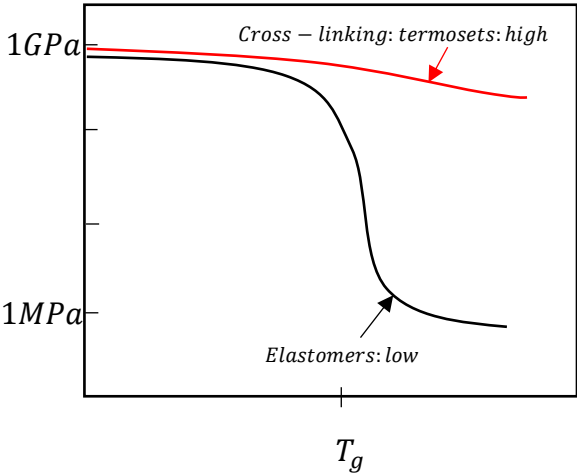


Figure 7.3 - Transition temperature for elastomers and crosslinking thermosets.

# 1 REFERENCES

- A. Josefsson / rev M.Herman, 2014. *Diskreta system med fjäderelement*. [Online]  
Available at: <https://files.itslearning.com/File/Download/GetFile.aspx?FileName=teori+3+ system av+ fj%C3%A4drar.pdf&Path=D%2btwMurz7HWMZVjrWP3%2fRyYLLmSbW7JTkMonCimPIJI%2bO%2fbxaMg5Ii3W2Xh6gzyomkIDzGwlUYsBQu81tAfCV3zKKJVsMsVXKUkninJMsZMTj85qqH7fhYXj31Otnxr5%2fECSbGM%2>
- Ameisen, E., 2018. Always start with a stupid model, no exceptions..
- Bamberg, E., 2006. *Contact Stresses and Deformation*. [Online]  
Available at: <http://www.mech.utah.edu/~me7960/lectures/Topic7-ContactStressesAndDeformations.pdf>
- Broman, G., 2003. *Compuational Engineering*. Karlskrona: Department of Mechanicla Engineering, Blekinge Institute of Technology.
- Contact Mechanics - Part 1*. 2014. [Film] Directed by Roland Larsson. Sweden: Luleå University of Technology.
- Contact Mechanics - Part 2*. 2014. [Film] Directed by Roland Larsson. Sweden: Luleå University of Technology.
- Ennis, R., 1962. A concept of critical thinking.
- Finite Element Method (FEM) - Finite Element Analysis (FEA): Easy Explanation*. 2017. [Film] s.l.: Educational Video Library.
- FUJIFILM, 2018. *Pressure Measurement Film*. [Online]  
Available at: <http://www.fujifilm.com/products/prescale/>
- Häring, I., 2018. *Intruduction to Risk Analysis and Risk Mangement Processes*.. [Online]  
Available at: <http://www.google.com/url?sa=t&rct=j&q=&esrc=s&source=web&cd=2&ved=0ahUKEwihvKv6lb7aAhVI3CwKHRtID8AQFggsMAE&url=http%3A%2F%2Fwww.springer.com%2Fcd%2Fcontent%2Fdocument%2Fcd%2Fdownloaddocument%2F9789811000133-c2.pdf%3FSGWID%3D0-0-45-1545458-p177750048&usg=>
- Johnson, K., 2012. *Contact Mechanics*. Cambridge, England: Cambridge University Press.
- M. Ashby, H. Shercliff, D. Cebon, 2013. *Materials Engineering, Science, Processing and Design*. 3rd ed. Cambrige, United Kingdom: Butterworth - Heinemann.
- M.J Puttock E.G Thwaite, 1969. *Elastic Compression of Spheres and Cylinders at Point and Line Contact*, Melbourne, Australia: Commenwealt Scientific and Industrial Research Organization.
- Malm, J., 2018. *Influence Analysis of Coupling between Tension and Torque in Single Armoured Cables*. [Online]  
Available at: <http://bth.diva-portal.org/smash/record.jsf?dswid=-5187&pid=diva2%3A940672&c=2&searchType=SIMPLE&language=sv&query=joacim+malin&af=%5B%5D&aq=%5B%5B%5D%5D&aq2=%5B%5B%5D%5D&aqe=%5B%5D&no>

OfRows=50&sortOrder=author\_sort\_asc&sortOrder2=title\_sort\_asc&onlyFullTe  
[Accessed 24 4 2018].

*ME 597 Lecture 8: Introduction to Contact Mechanics*. 2010. [Film] Directed by Nanohubtechtalks. USA: Purdue University.

MHz'as, 2009. *Hertz pressure*. [Online]

Available at: <https://commons.wikimedia.org/wiki/File:Hertz.svg>

*nanoHUB-U Fundamentals of AFM L2.5: Tip-Surface Interactions (Contact) - Contact Mechanics*. 2010. [Film] Directed by Nanohubtechtalks. USA: Purdue University.

NKT, 2018. *History*. [Online]

Available at: [www.nkt.com/about-us/history](http://www.nkt.com/about-us/history)

PRESCALE, F., 2018. *Instrucion manual for measurement PRESCALE*, s.l.: s.n.

Rosling, H., 2006. *Att resonera logiskt: Inledning till logikens grunbegrepp och metoder*. s.l.:s.n.

Serrat, O., 2009. *The Five Whys Technique*, Cornell: Cornell University ILR School.

Snow, C., 1969, pp.100. *Variety of Men*. s.l.:Penguin.

Tirthankar, G., Dilip, R. & Nimai, K. C., 2011. *Discretization of Random Variables with Applications*.

Wall, J., 2017. *Simulation process automation*. [Online]

Available at:

<https://files.itslearning.com/File/Download/GetFile.aspx?FileName=Simulation+process+automation.pdf&Path=E%2fewTOArKF6bscVkTqtD7%2bmjZY6WTYKCNaxTnyMUOEXYAwpN%2bUyP8vCbSket%2bVS%2bRLkSUrITxNtd%2f8ZzhnFN%2bg3LpxNE6tq6LpzYoP%2fnpwh4C3jiiALvfBuE15ACOussGQRkl>

APPENDIX A:

**A.1 Solving the eccentricity**

How to solve eccentricity  $e$  can be made in many possible and probably in faster ways but one method to solve this is by using MATLAB see Figure A.1.1.

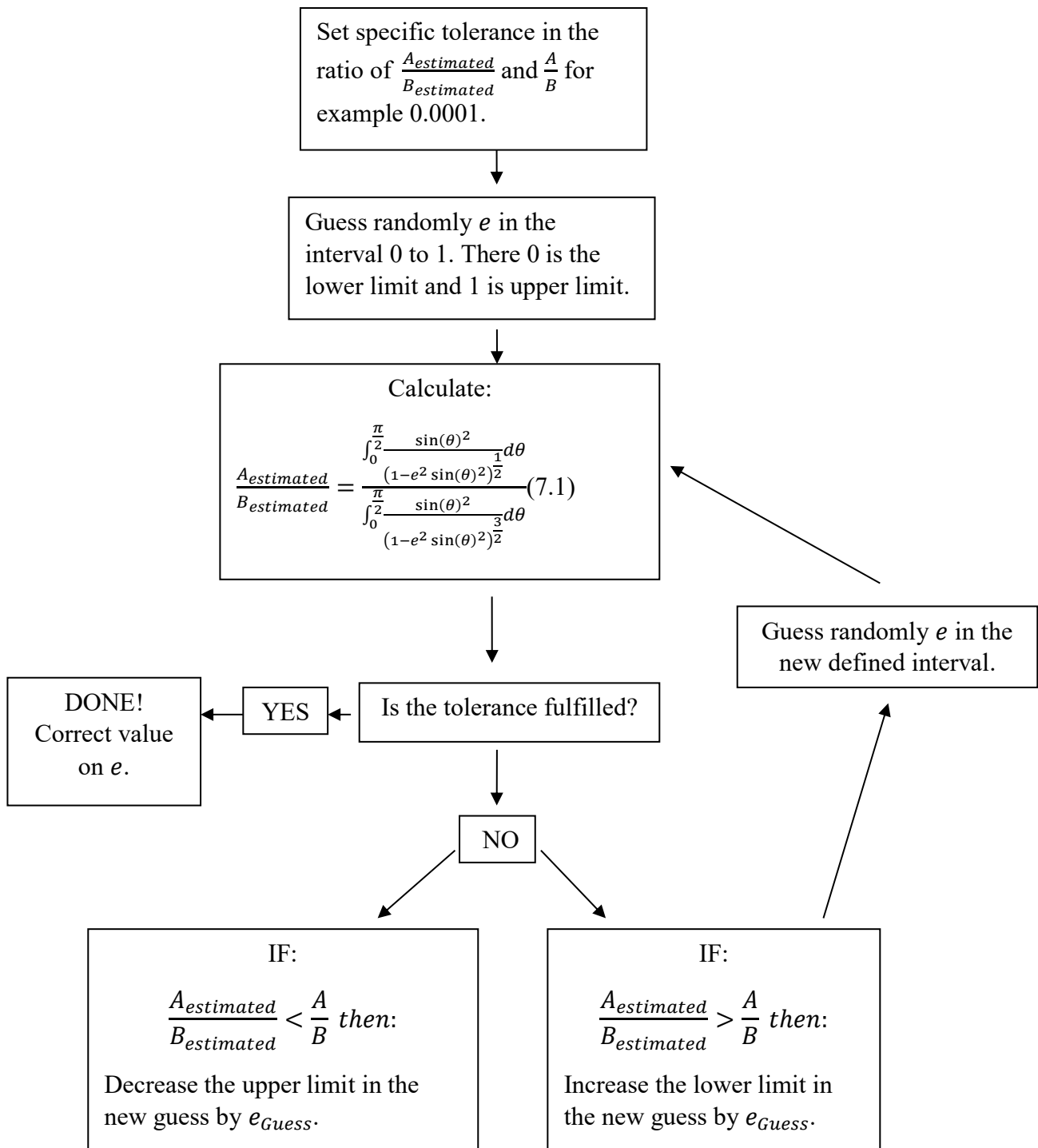


Figure A.1.1 - Solving the eccentricity  $e$  by using a restricted random guess in an iterative process.

## A.2 Risk analyse for the project

In the tables below (see Table A.2.1 and Table A.2.2) the risk analyse will be presented.

Table A.2.1 - Probability and Consequence range

Probability	Probability range [%]	Consequence	Censequence range
Low	1-30%	Trivial	Low effect on the project. Easy to correct.
Medium	30-70%	Moderate	Medium effect on the project. Difficult to correct.
High	70-99%	Severe	The project can fail. Very difficult to correct.

Table A.2.2 - Risk Analyze on the project

Risks description	Probability	Consequence	Risk Arrangement	Risk after Arrangement
Accidentally lose important data on the computer.	Medium	Severe	Continuous make backup on the files.	Low
Accidentally use references that contain wrong information.	Low	Severe	Have a critical approach and always try to verify the theory if it is possible. Also see if other references contain same information.	Low
Lack of time.	Medium	Moderate	Set up a time schedule that contain deadlines and specific subs targets. But also schedule some extra time to handle unexpected delays.	Low
Many simulations will be done to study the relation between radial force and compression in the cable. This can be very time-consuming which can cause delays.	High	Moderate	If some simulation will be done several times with just different levels of forces it is then possible to perform an automatic run of the simulations by using MATLAB as server and ABAQUS as client.	Low
Lack of knowledge in specific areas.	High	Moderate	Use logical reasoning and discuss with other people that have the knowledge or find the information from earlier works.	Low

<p>Some parts will be designed and manufactured to the upcoming experiment test and risk of delays can accrue.</p>	<p>Medium</p>	<p>Severe</p>	<p>Will prioritize this at the beginning of the project to ensure the parts are finished when the test will be performed. Other smaller tests will be also done to spread the risk if it becomes unexpected failures on the main test.</p>	<p>Low</p>
<p>Every project has limitations for example in this project accessibility to software, computing capacity and license limitations.</p>	<p>Medium</p>	<p>Moderate</p>	<p>Simulation can be made at the school which have also access to several computers that can split up the simulations between. Simplify the model without losing too much of the essential parts and split up the problem into several smaller parts make it possible to reduce the computational costs.</p>	<p>Low</p>
<p>Unexpected failures.</p>	<p>Medium</p>	<p>Moderate</p>	<p>Best way to minimize unexpected failures is to always have a discussion with other people that can give a different point of views before making some decisions. But to predict unexpected failures are always difficult and should always beware that it can and will happen.</p>	<p>Medium</p>

### A.3 Geometrical theory – Before study known theories

By using simple geometrical and logical reasoning, it is possible to describe a simplified relation between compression  $dy$  and the contact area  $C_A$  for two unequal diameters of crossed cylinders (see Figure A.3.). The following assumption is made:

- Cylinder 2 is deformable and Cylinder 1 is rigid
- Cylinder 2 will perfectly adapt to Cylinder 1.

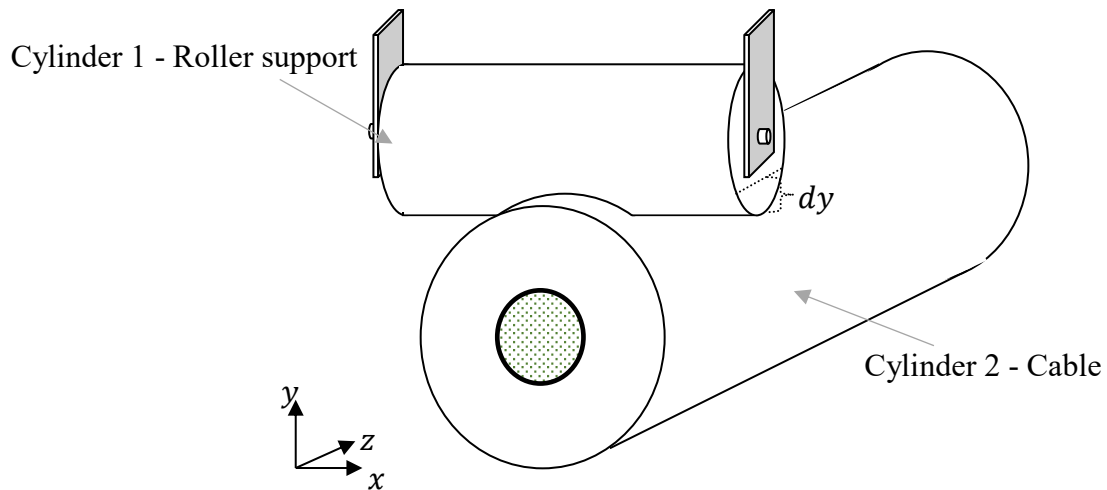


Figure A.3.1 - Cable compressed by a roller.

Plane yx:

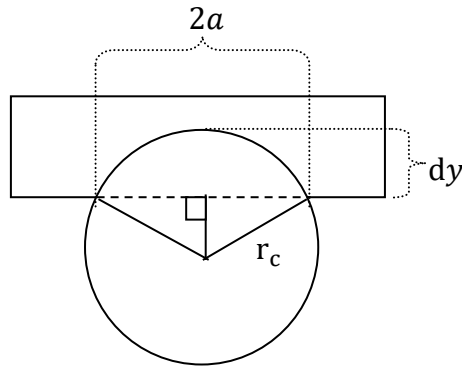


Figure A.3.2 - Plane yx Cable compressed by a roller.

The Figure A.3.2 presents the compression  $dy$  in equation (A.3.1)  $2a$  is the large ellipse diameter and  $r_c$  is the radius of the cable.

$$2a = 2 \cdot \sqrt{r_c^2 - (r_c - d_y)^2} \quad (\text{A.3.1})$$

Plane yz:

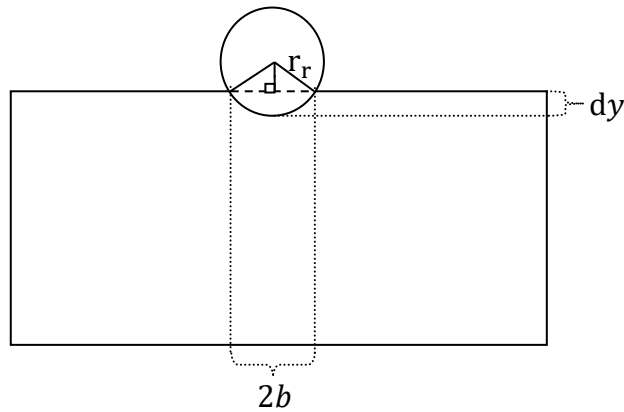


Figure A.3.3 - Plane yz cable compressed by a roller.

The Figure A.3.3 presents the compression  $dy$  in yz plane, in equation (A.3.2)  $2b$  is the small ellipse diameter and  $r_r$  is the radius of the roller.

$$2b = 2 \cdot \sqrt{r_r^2 - (r_r - d_y)^2} \quad (\text{A.3.2})$$

In plane xz the contact area  $C_A$  will be formed as an ellipse:

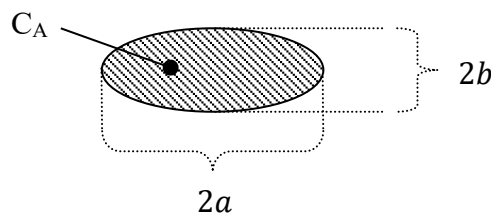


Figure A.3.4 - Contactarea of a cable compressed by a roller.

The equation (A.3.3) describes the contact area  $C_A$  for an ellipse.

$$C_A = ab\pi \tag{A.3.3}$$

In equation (A.3.4)  $P$  is the force and the  $p_{mean}$  is the mean pressure between the roller and the cable.

$$p_{mean} = \frac{P}{C_A} \tag{A.3.4}$$

But the pressure distribution will not be equal over this area  $C_A$  because when two cylinders get compressed against each other, more of the materials in the middle of the contact surface are going to be compressed more compared to outer line. A simple spring model show this in an easier way, see Figure A.3.5.

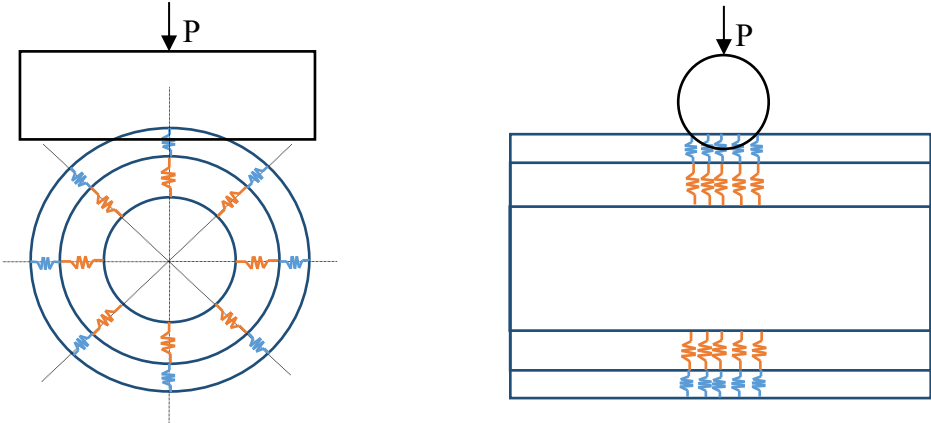


Figure A.3.5 - Larger compression in the middle of the contact area.

The Figure A.3.5 shows that the springs that are under the force line  $P$  is going to be more compressed than the other springs around it. Which mean that they will take up more of the force and therefore also have larger contact pressure there.

This simple geometrical theory will not consider that the pressure will be larger at the centre of the ellipse and almost zero at the outline region. The pressure will instead have a pressure distribution like Figure A.3.6.

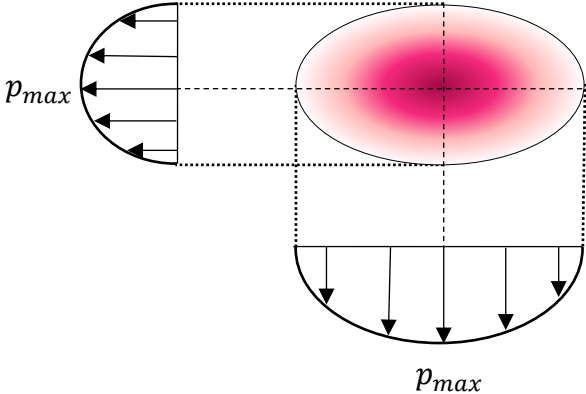


Figure A.3.6 - Pressure distribution of two crossed cylinders. (inspired by (MHz`as, 2009))

This geometrical theory will also not consider how the compression will behave in the both cylinders i.e. in this case both the roller and the cable, or the directly relation between compression and force. But the known theory so called Hertzian’s theory will consider these parts.

By doing this simple logical reasoning of describing this specific case of contact mechanic make it possible to have some background knowledge to criticise when other sources of well-known theories will be studied.

## A.4 Study the behavior of the two crossed steel cylinders

This working process was performed to see relations based on the theory in its simplest form. A MATLAB script (see Appendix A.9) is used to calculate the maximum pressure, compression and contact area based on Hertzian's theory (chapter 2.1.1). To evaluate that the Hertzian's theory was implemented in a correct way an example of two steel cylinders have been calculated by using this theory see Table A.4.1.

Table A.4.1 - Example of two crossed steel cylinders by using Hertzian's theory.

<i>Example</i>					
<i>Input</i>					
$D_1$ [mm]	$D_2$ [mm]	$E_1$ [GPa]	$E_2$ [GPa]	$\nu_1$	$\nu_2$
262.7	121	210	210	0.28	0.28
<i>Output</i>					
$e = 0.802$					
<i>Measurement</i>	$P$ [N]	$p_{max}$ [MPa]	$\alpha$ [mm]	$Contact_A$ [mm <sup>2</sup> ]	<i>Pressure distribution plot</i>
1	1000	692.45	0.0078	2.17	✓ See Figure A.4.4
2	2000	872.44	0.0124	3.44	×
3	3000	998.69	0.0162	4.51	×
4	4000	1099.20	0.0196	5.46	×
5	5000	1184.08	0.0228	6.33	×
6	6000	1258.27	0.0257	7.15	×
7	7000	1324.91	0.0285	7.93	×
8	8000	1384.91	0.0312	8.66	×
9	9000	1440.36	0.0337	9.37	×
10	10000	1491.84	0.0362	10.05	×

The Figure A.4.1 presents the relation between the maximum pressure  $P_{max}$  and the force  $P$  for two steel cylinders (see Table A.4.1) which come in contact and deform slightly. The figure shows when the force increases the maximum pressure increase. But it do not increase linear because when the force get larger, the contact area also increase so therefore the gradient of the curve will be decrease at the larger forces.

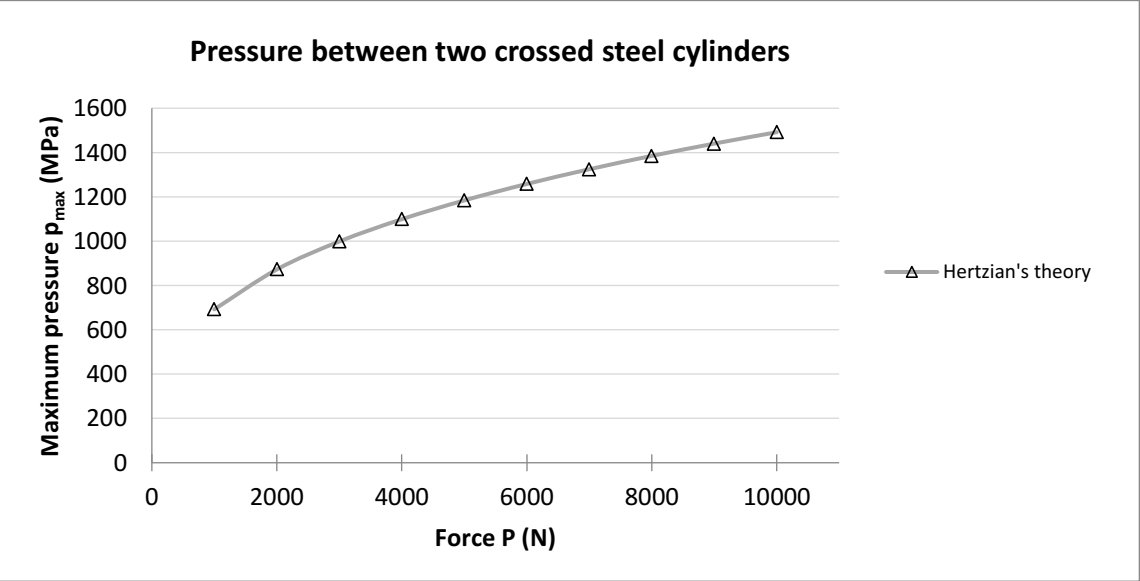


Figure A.4.1 - Force vs maximum pressure for two unequal crossed steel cylinders by using Hertzian's theory.

The Figure A.4.2 presents the relation between the total compression and the force  $P$  for two steel cylinders (see Table A.4.1) which come in contact and deform slightly. The curve shows that the gradient of the curve is decreasing when the force increase. This is because of when force increase will the compression also increase but the contact area will also increase which make it more difficult to compress the material. This makes the gradient larger at smaller forces and smaller at larger forces.

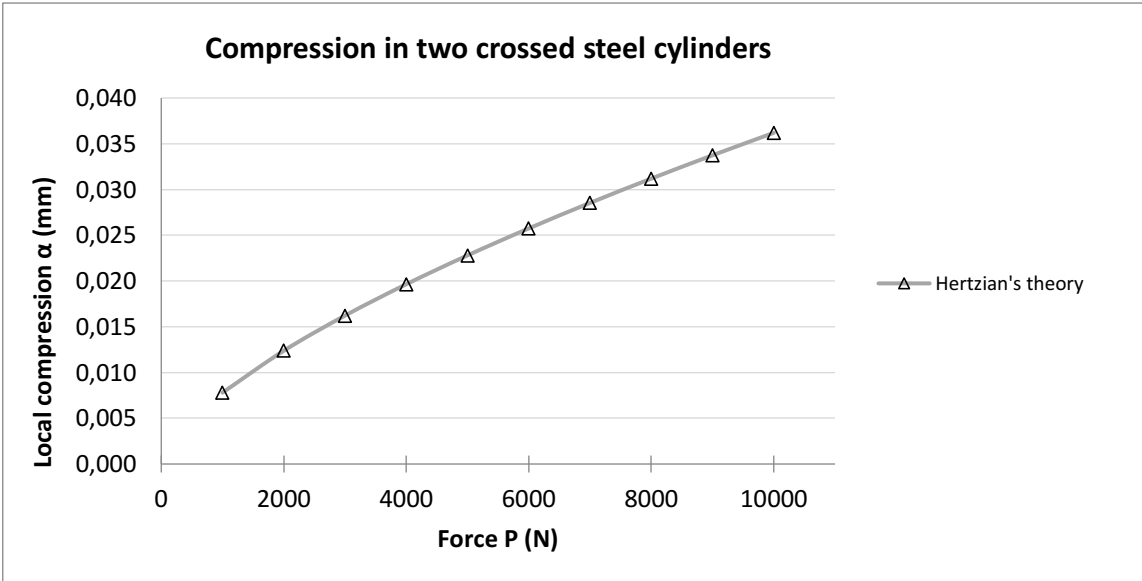


Figure A.4.2 - Force vs Compression for two unequal crossed steel cylinders by using Hertzian's theory.

The Figure A.4.3 presents the relation between contact area  $C_A$  and force  $P$  for two steel cylinders (see Table A.4.1) which come in contact and deform slightly.

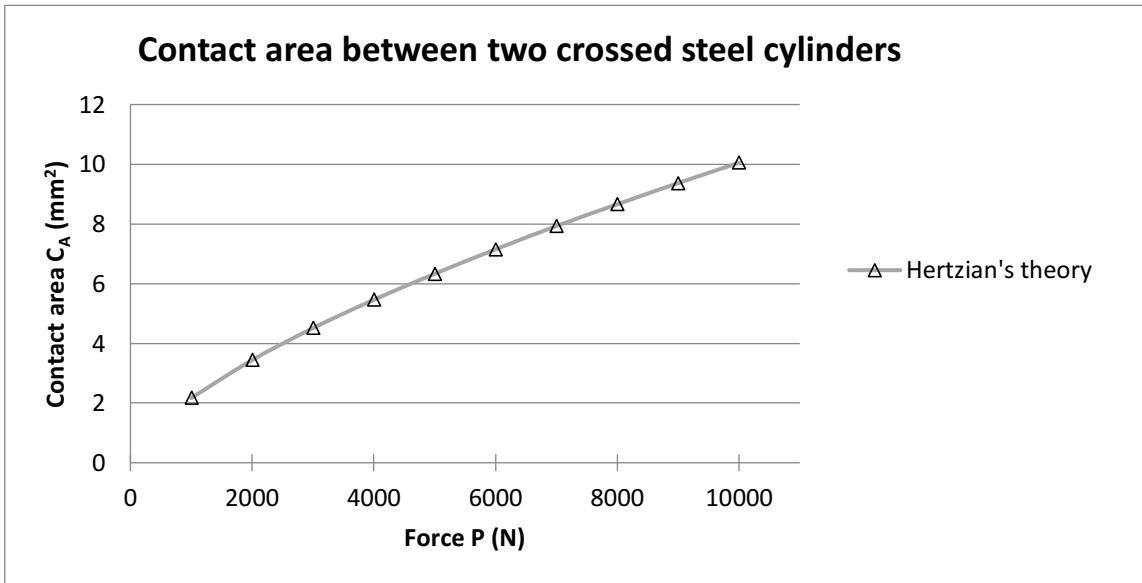


Figure A.4.3 - Force vs Contact area for two unequal crossed steel cylinders by using Hertzian's theory.

The Figure A.4.4 shows the pressure distribution for the first measurement ( $P = 1000\text{N}$ ) when two cylinders get compressed against each other (see Table A.4.1). This creates an elliptical contact area and the pressure distribution will look like a half ellipsoid. The pressure level is largest at the centre of the ellipse and zero at the edges (see red line).

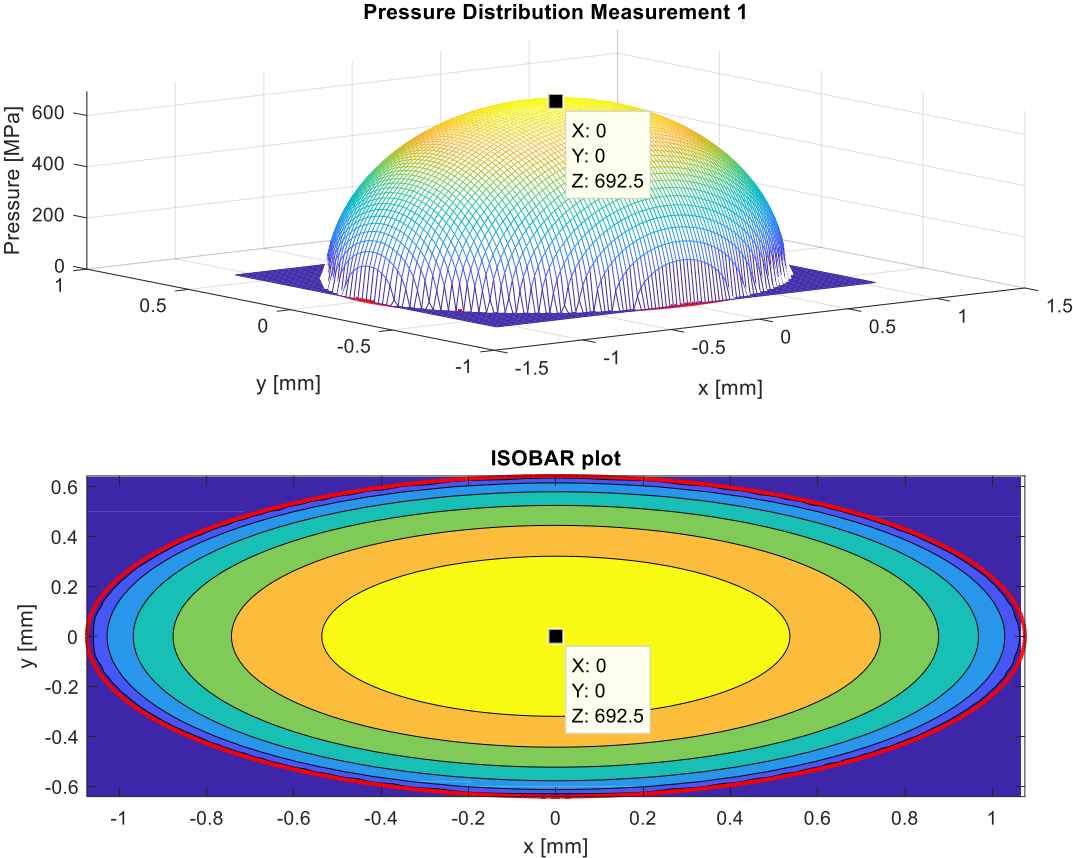
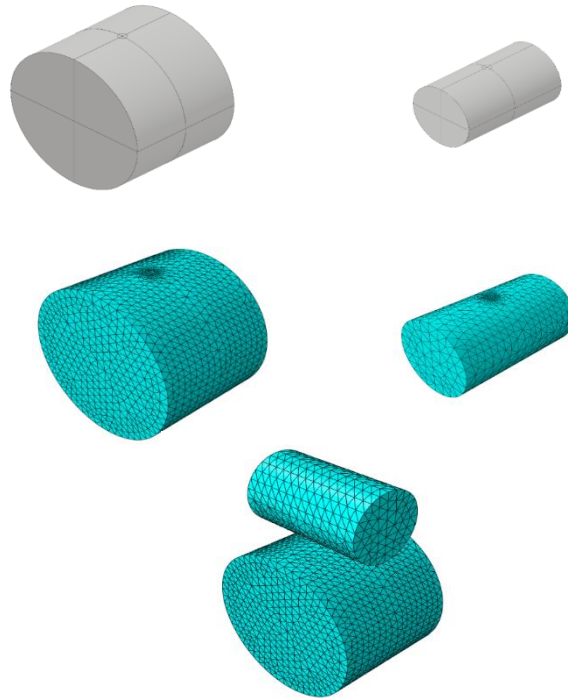


Figure A.4.4 - Pressure distribution for Measurement 1 by using Hertzian's theory.

## A.5 Finite element method for two steel cylinders

To evaluate and check if the Hertzian's theory is implemented in a correct way in this project a similar setup of cylinder is going to be analysed by using finite element method.

The FEM model of the steel cylinder is made in ABAQUS and by creating the steel cylinders and split their faces in INVENTOR before they are imported to ABAQUS makes it easier to further define a finer mesh in the contact area in ABAQUS. The Figure A.5.1 shows how the faces can be split and how a finer mesh is defined.



*Figure A.5.1 - Two crossed linked steel cylinders in INVENTOR and ABAQUS.*

## Load and Boundary Conditions

Setting up the boundary condition in a following way (see Figure A.5.2):

- End 1 no translation in z and x direction.
- End 2 no translation in all directions.
- End 3 no translation in y direction.
- Load is distributed equally over each node (see yellow arrows in Figure A.5.2).

Define the contact surface as frictionless and finite sliding.

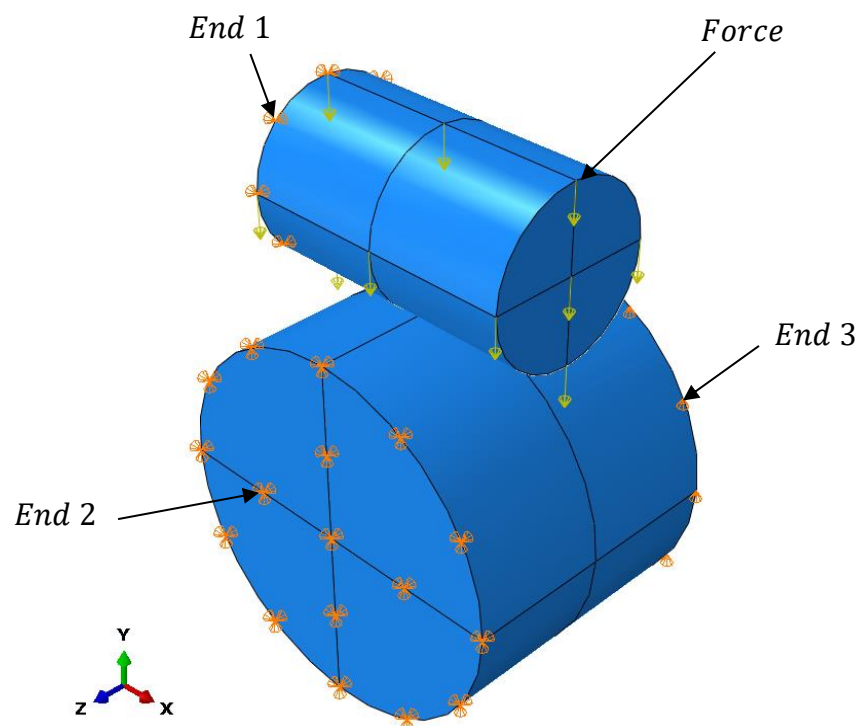


Figure A.5.2 - Boundary conditions in ABAQUS for two crossed steel cylinders.

Thereafter varying the force and get following result (see Table A.5.1)

Table A.5.1 - Example of two crossed steel cylinder by using FEA in ABAQUS.

<b>Example</b>					
<b>Input</b>					
$D_1(mm)$	$D_2(mm)$	$E_1(GPa)$	$E_2(GPa)$	$\nu_1$	$\nu_2$
262.7	121	210	210	0.28	0.28
<b>Output</b>					
<b>Measurement</b>	$P[N]$	$p_{max} [MPa]$	$\alpha [mm]$		
1	1000	709.7	0.0077		
2	2000	866.9	0.0122		
3	3000	970.3	0.0160		
4	4000	1056	0.0194		
5	5000	1128	0.0225		
6	6000	1191	0.0254		
7	7000	1247	0.0282		
8	8000	1298	0.0308		
9	9000	1346	0.0333		
10	10000	1391	0.0357		

The Figure A.5.3 presents how the maximum pressure is relative to force for two steel cylinders by using FEM.

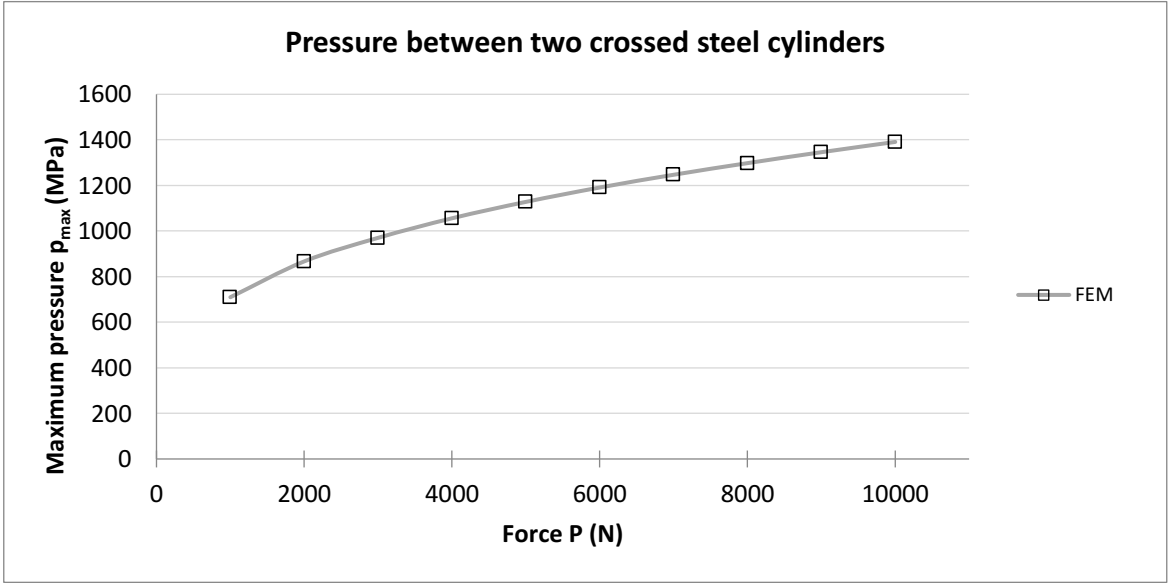


Figure A.5.3 - Force vs Pressure max for two unequal crossed steel cylinders by using FEM.

The Figure A.5.4 presents how the local compression is relative to force for two steel cylinders by using FEM.

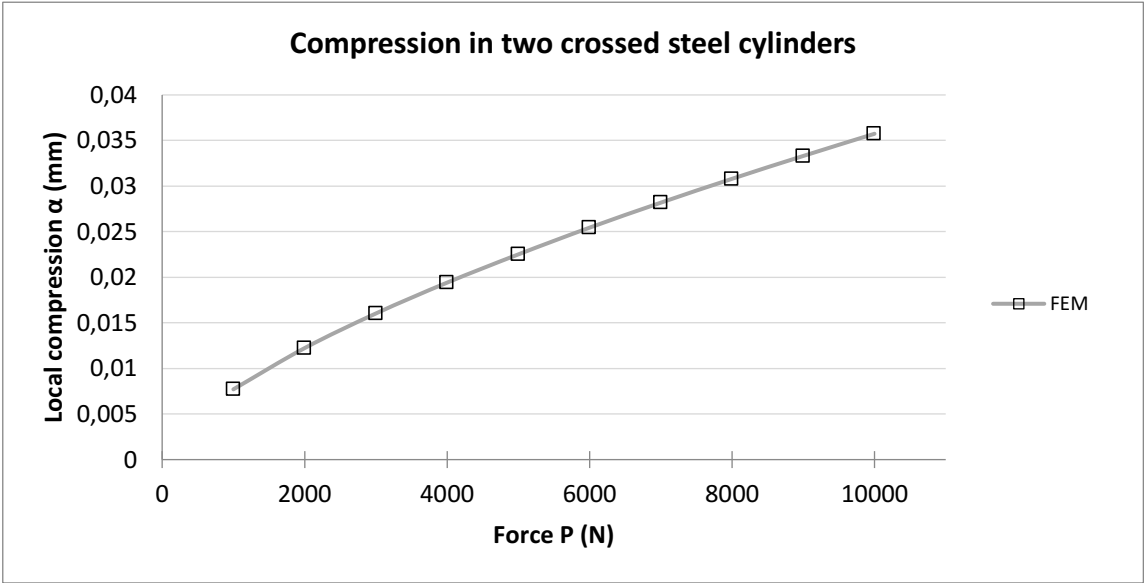


Figure A.5.4 - Force vs Compression for two unequal crossed steel cylinders by using FEM.

### Comparison between Hertzian's theory and FEM for two crossed steel cylinders

In this chapter the comparison between the theoretical model Hertzian's theory and the FEM model for the example of two crossed steel cylinder.

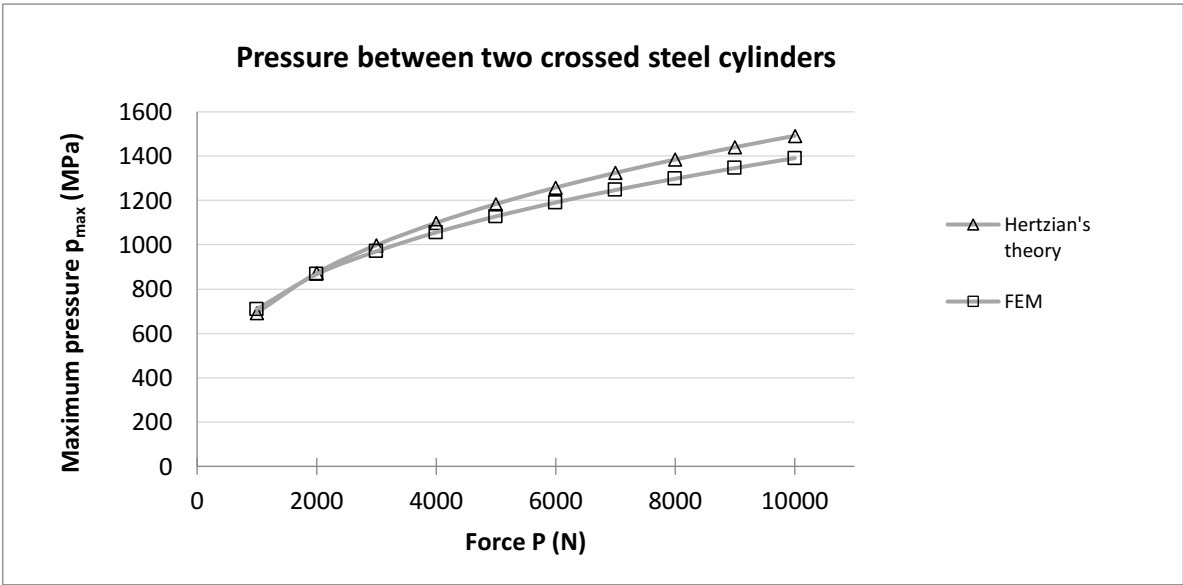


Figure A.5.5 - Force vs Pressure max: Comparison between Hertzian's theory and by a FEM model.

The Figure A.5.5 shows the comparison between Hertzian's theory and the FEM model for force versus maximum pressure of two steel cylinders. The result deviate a little bit at the larger forces, which is can be because of the boundary condition and mesh size. The FEM model also consider the bending when these types of boundary conditions are used. Which the

Hertzian's theory does not. The pressure maximum from the FEM model is also very sensitive to the mesh size and is a bit difficult to read from simulation result.

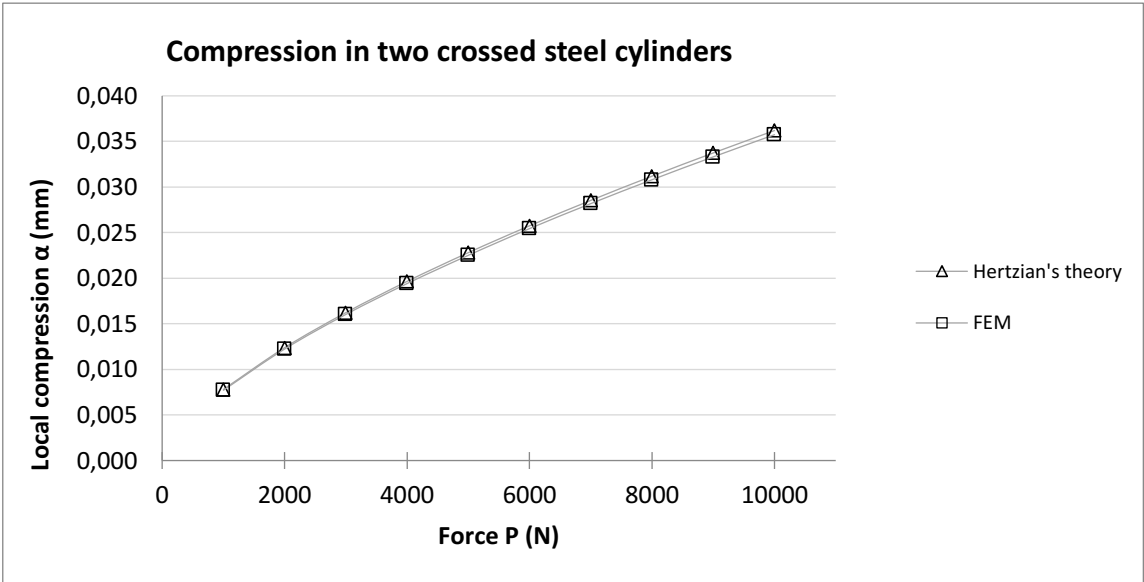


Figure A.5.6 - Force vs compression: Comparison between Hertzian's theory and by a FEM model.

In the Figure A.5.6 shows the relation between compression and force between the two methods. The comparison between the Hertzian's theory and the FEM model is small. Later in this project will a steel roller be compressed against a cable. The compression in the roller will then be very small compared to the compression in the cable. So further in this project following assumption is made: The total compression (sum of the local compression in the roller and local compression in the cable) is approximately equal to the local compression in the cable.

## A.6 Compression in a nonarmoured cable

To start it simple a FEM model of a nonarmoured cable is modelled in Inventor and then imported to ABAQUS. Following setup was made:

Boundary conditions:

- End 1 of the conductor is constrained in y direction.
- End 2 of the conductor is fixed in all translation directions.
- End 3 is constrained in x and z translation directions.

Force is distributed evenly over specific nodes, see yellow arrows in Figure A.6A.7.1.

Every material layer surface in the model is tied together and the surfaces that are in contact is frictionless and finite sliding.

A nonlinear implicit solver is used in ABAQUS to solve this FEM model.

Mesh type: Tetrahedral element type.

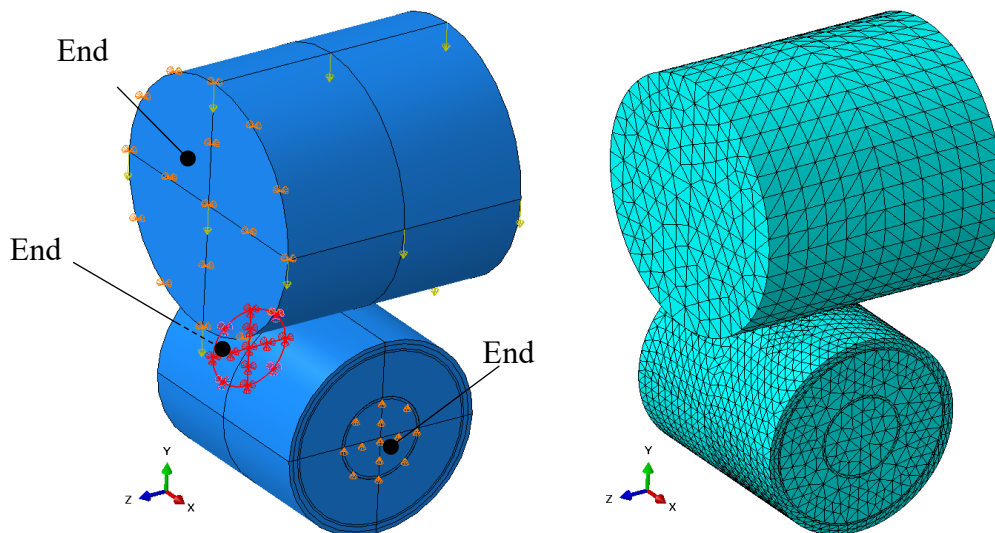


Figure A.6A.7.1 - Boundary condition and mesh for the no armored cable.

## A.7 Relation between total compression for a nonarmoured

In the Figure A.7.1 presents the relation between compression and force for the nonarmoured cable.

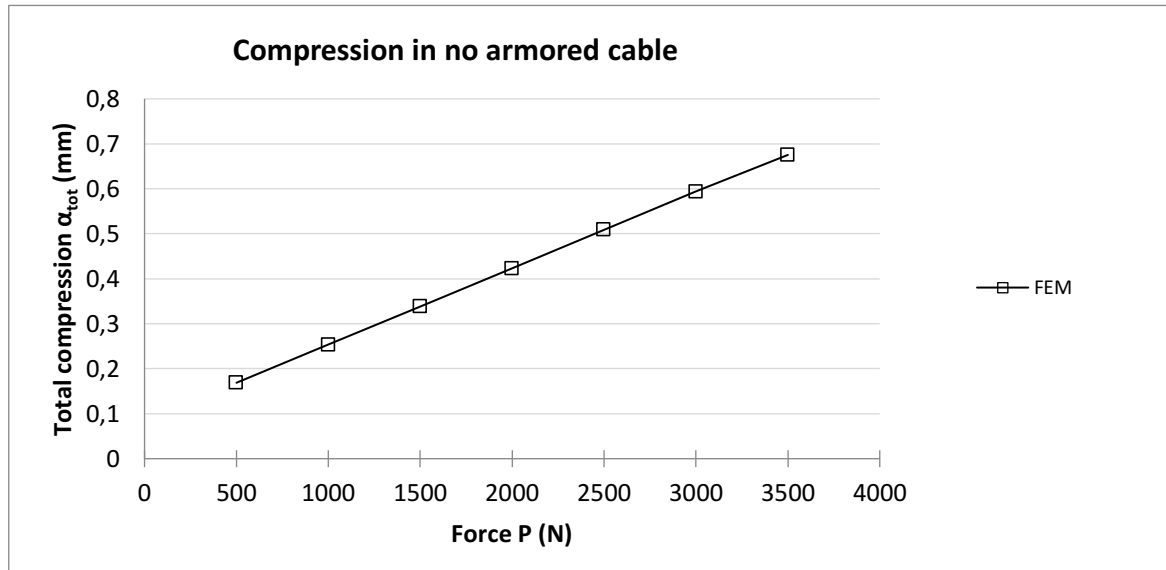


Figure A.7.1 - The relation between compression  $\alpha$  and force  $P$  for the no armored cable.

In the Figure A.7.2 below presents the theoretical relation between the stiffness modifying parameter  $S_{mp}$  and force  $P$  for the nonarmoured cable by using the Hertzian's theory on each load case.

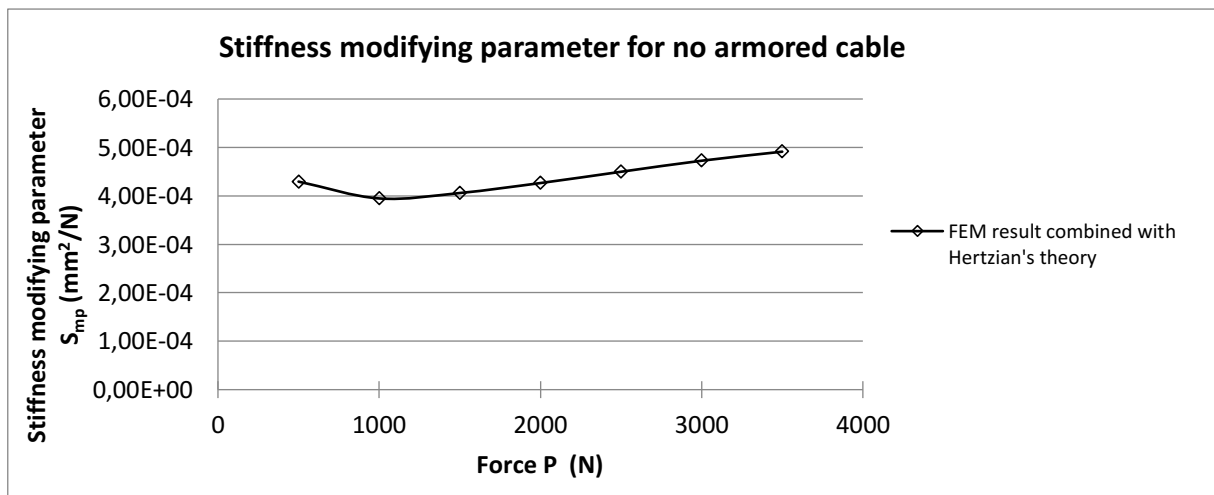


Figure A.7.2 - Relation between stiffness modifying parameter  $S_{mp}$  and force  $P$  for the no armored cable.

The Figure A.7.3 shows an overview of the solving process of combining the FEM and Hertzian's theory to determine the stiffness of the cable.

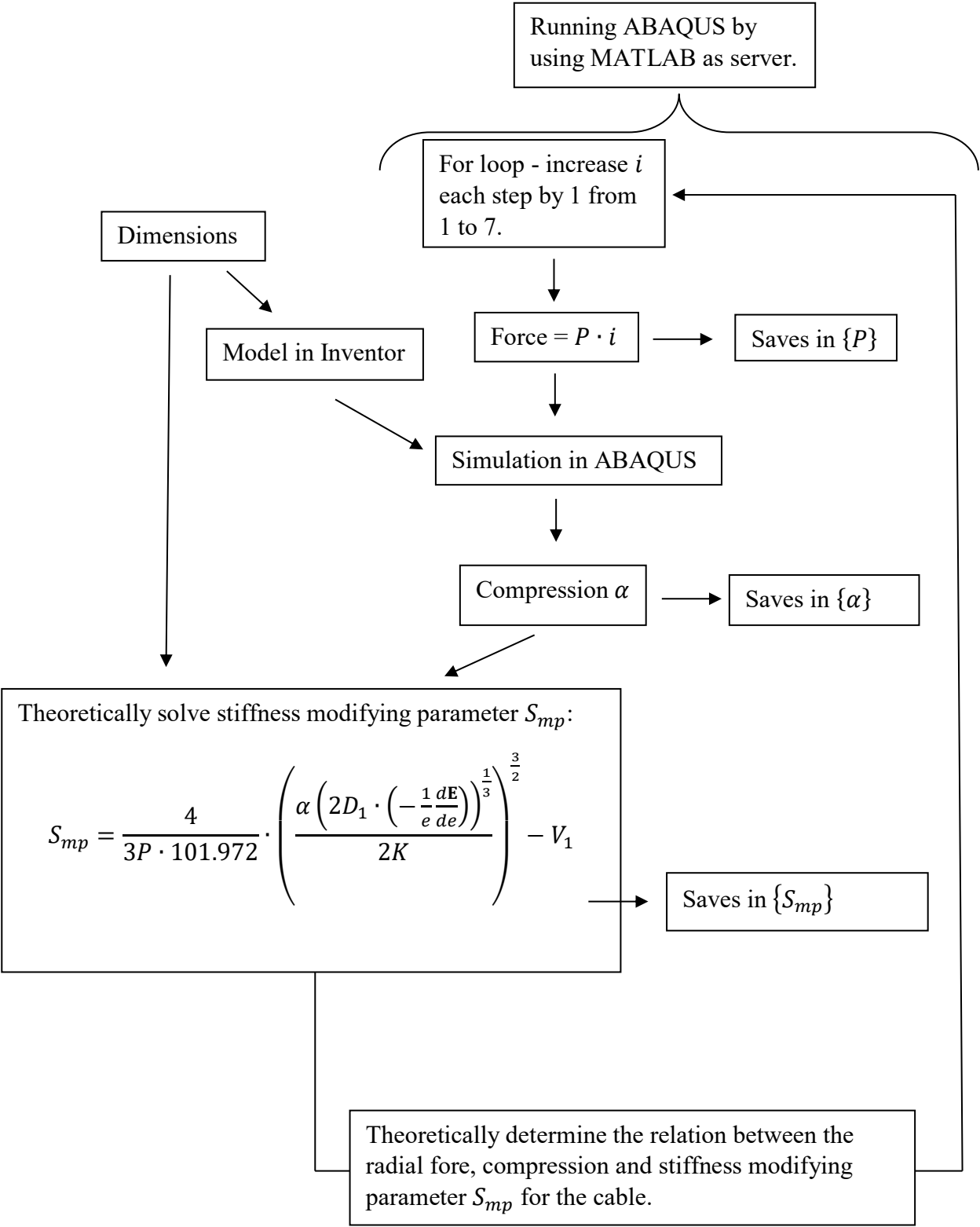


Figure A.7.3 - Schedule over the simulation and solving process.

## A.8 The MATLAB code for solving the eccentricity

```
function [e,K,eE,D1,D2,ratioAB]=EccentricitySolver(Dc,Dr,tol,controller)
%INPUT Information:
%Dc = Diameter on Cable [mm]
%Dr = Diameter on Roler [mm]
%tol = tolerance how good accrucy 0<tol<0.1 for example: 0.1 , 0.001 ...
%controller = 1 then solve everything for first tim.
%controller = 2 then use already solved result of e, from previous run then
                %controller was equal to 1.So Dc and Dr is the same everytime
                %This is good to use when for loop is used to get data.

%OUTPUT Information:
%e=eccentricity
%eE=-1/ed*E/de from complete elliptic integral of second class
%K=from complete elliptic integral of first class

%START CODE

    %Define the large diameter and smaller diamter:
    if Dc>Dr
        D1=Dc %[mm]Large diamter CABLE
        D2=Dr %121 %[mm]Smal diameter Roller
    end

    if Dr>=Dc
        D1=Dr %[mm]Large diamter Roller
        D2=Dc %121 %[mm]Smal diameter Cable
    end

    %Ratio A/B
    ratioAB = D2/D1;

    %Define symbols and comparevariable
    syms o e;
    Res=0;

%%SOLVER eccetrecenty e by random picking of e, combined with reducing
interval.
if controller==1;
    %Intervall guess for e
    g=0;
    h=1;
    disp 'Solving WAIT...=>'
    while abs(Res-ratioAB)/ratioAB>tol
        e=abs((g-h)).*rand(1)+g; % Reduce random interval every
iterative
        Res=vpa(int(sin(o)^2/(1-
e^2*sin(o)^2)^(1/2),o,0,pi/2)/int(sin(o)^2/(1-
e^2*sin(o)^2)^(3/2),o,0,pi/2),6);

        if Res<ratioAB;
            h=e; %Decrease the upper limit.
        elseif Res>ratioAB;
            g=e; %Increase the lower limit.
        end

    end

    save ('e.mat','e');
    D1old=D1;
```

```

D2old=D2;
save ('D1old.mat','D1old');
save ('D2old.mat','D2old');

%Check the following output:
e;
Res;
ratioAB;
Res/ratioAB;

%Controller error message if the diamters is not the same:
elseif controller==2
    load ('D1old.mat')
    load ('D2old.mat')

    if D2old/D1old==ratioAB
        disp 'PREVIOUS e HAS LOADED IN!'
        load ('e')
    else
        disp 'ERROR - controller wrong input use 1 instead 1 because diameter
ratio have been changed'
        return
    end

else
    disp 'ERROR - controller wrong input choose 1 or 2 only!'
    return
end

% Solving the elliptic integrals:
K=double(vpa(int(1/(1-e^2*sin(o)^2)^(1/2),o,0,pi/2),6));
eE=double(vpa(int(sin(o)^2/(1-e^2*sin(o)^2)^(1/2),o,0,pi/2),6));
disp '<= Solving process is FINISHED'

%END CODE-----

```

## A.9 MATLAB script for two steel cylinders

```

%START CODE-----
clc
clear all
close all

disp 'INPUT =>'

controller=1 %1 for calculating

%INPUT

P=1000 %[N] Force in Newton

Dr=121 %Cylinder2/Roler diameter [mm]
Dc=262 % Cylinder1/Cable diameter [mm]

E1=210*10^(9) %[Pa]or[N/m^2] Elastic modulus on Large diameter
E2=210*10^(9) %[Pa]or[N/m^2] Elastic modulus on the small diameter

v1=0.28 %0.45 %Possion's ratio for Large diameter
v2=0.28 %0.3%Possions ratio for small diameter

%Tolerance for solving e
tol=0.0001;

%Rewrites N=>gf
Pc=P*101.97162;
E1c=E1*101.97162*10^(-6);
E2c=E2*101.97162*10^(-6);

%Sub calculation
V1=(1-v1^2)/(pi*E1c);
V2=(1-v2^2)/(pi*E2c);
Q=3/4*(V1+V2);

%Function solving e
[e,K,eE,D1,D2,ratioAB]=EccentricitySolver(Dc,Dr,tol,controller)

%Displacement
alpha =2*K*(Pc*Q)^(2/3)*(1/(2*D1*eE))^(1/3); %total compression in both
cylinders

%Calculate a and b
A=1/D1;
a=double((eE*2*Q*Pc/A)^(1/3));
b= double(((a^2)*(1-e^2))^(1/2));

pmax=(3*Pc*0.00980665/(2*pi*a*b)); %MPa

%Boundaries for the ellipse when x=0 and y=0 according to ellipse statement
%x^2/a^2+y^2/b^2=1
yv=(b^2)^(1/2);
xv=(a^2)^(1/2);

[x,y]=meshgrid(-xv:0.02:xv,-yv:0.02:yv);
pfunc=pmax*(1-x.^2/a^2-y.^2/b^2).^(1/2);

figure(1)

```

```

%Border for ellipse
x0=0;
y0=0;
t=-pi:0.01:pi;
xe=x0+a*cos(t);
ye=y0+b*sin(t);

%Pressure Distrubution
subplot(2,1,1)
mesh(x,y,real(pfunc))
    title 'Pressure Distribution Measurement 1'
    xlabel 'x [mm]'
    ylabel 'y [mm]'
    zlabel 'Pressure [MPa]'
    zlim ([0 pmax])

%Maximum Pressure dot
pfunc=@(x,y)pmax*(1-x.^2/a^2-y.^2/b^2).^(1/2);
hold on
scatter3(0,0,real(pfunc(0,0)),'r','filled')
plot(xe,ye,'--r','LineWidth',2)

%ISOBAR plot
subplot(2,1,2)
contourf(x,y,real(pfunc))
zlim ([0 pmax])
hold on

plot(xe,ye,'--r','LineWidth',2)
hold on
scatter3(0,0,real(pfunc(0,0)),'r','filled')
    xlabel 'x [mm]'
    ylabel 'y [mm]'
    title 'ISOBAR plot'

%Output
disp 'OUTPUT=>'
format short

    ratioAB
    K=double(K)
    eE=double(eE)
    alpha=double(alpha)%mm
    a %mm
    b %mm
    areaellipse=pi*a*b %mm^2
    projectPressure=P/areaellipse %MPa
    pmax

disp '<=OUTPUT'

% Study the relation between compression and force and contact area:
scf=1;
Pv=0;
areaellipsev=0;
pmaxv=0;
alphav=0;

for i=1:1:10

```

```

Pv(i,1)=P*scf;
Pc=Pv(i,1)*101.97162;
a=double((eE*2*Q*Pc/A)^(1/3));
b= double(((a^2)*(1-e^2))^(1/2));
areaelipsev(1,i)=pi*a*b;
pmaxv(1,i)=(3*Pc*0.00980665/(2*pi*a*b));
alphav(1,i) =2*K*(Pc*Q)^(2/3)*(1/(2*D1*eE))^(1/3);

scf=scf+1;
end

%Plot the relations:
figure(2)

plot(Pv,areaelipsev,'-*b')
ylabel 'Contact Area [mm^2]'
xlabel 'Force [N]'
title 'Force vs Contact Area'

figure(3)
plot(Pv,pmaxv,'-*r')
ylabel 'Pressure MAX [MPa]'
xlabel 'Force [N]'
title 'Force vs Pressure MAX'

figure(4)
plot(Pv,alphav,'-*k')
ylabel 'Compression in both [mm]'
xlabel 'Force [N]'
title 'Force vs Compression'

%END CODE-----

```

## A.10 MATLAB script for dividing the total compression into local compression between roller and cable and between holder and cable

```

%START CODE-----
clear all
close all

%Compression vector and force vector INPUT:
alphav=[1.275,2.550,3.826,5.1,6.376,8.802,10.623,12.752,14.878,17.003]
Pv=[3000,6000,9000,12000,15000,20000,25000,30000,35000,40000]

for i=1:length(alphav)

%INPUT to calculate V2 for the experiment
%Tolerance for solving e
tol=0.0001;
controller=1;
%Force
P=Pv(1,i); %Force from the sencor/FEM model[N]
alphanot=alphav(1,i); % Compression from the experiement/FEM model% [mm]

Pc=P*101.97162; %Convert Newton (N) to gram force (gf)

%Parameter data
Dc=240; %Cable diamter [mm]
ml=120; %Cable weight/length [kg/m]

Dr=120; %Diameter Roller [mm]
E1=210*10^(9);% Elasticitetsmodul Roller [Pa]
v1=0.28; %Possio's Ratio
E1c=E1*101.97162*10^(-6);
V1=(1-v1^2)/(pi*E1c);

DH=-280; % Inner diameter on the Holder [mm] Negative beacuse bowl formed
aH1=200; % Contactlength between cable and holder total [mm]
aH1=aH1/2;

%% Calculations of compression between holder and the cable
PmlP=ml*9.82*101.97162/1000+Pc/(2*aH1);
syms V2
alphaCH=PmlP*(V1+V2)*(1+log((8*aH1^2/(PmlP*(V1+V2)))*(1/DH+1/Dc)));

%% Calculations of compression between roller and the cable

[e,K,eE,D1,D2,ratioAB]=EccentricitySolver(Dc,Dr,tol,controller);

syms V2

%Displacement
alphaRC =2*K*(Pc*(3/4*(V1+V2)))^(2/3)*(1/(2*D1*eE))^(1/3); %total
compression in both cylinders

V2=solve(alphaCH+alphaRC==alphanot,V2);

%disp 'Compression between cable and roller [mm]'
inRC=2*K*(Pc*(3/4*(V1+V2)))^(2/3)*(1/(2*D1*eE))^(1/3);
%disp 'Compression between cable and holder [mm]'
inHC=PmlP*(V1+V2)*(1+log((8*aH1^2/(PmlP*(V1+V2)))*(1/DH+1/Dc)));

```

```

%Checking if V2 is solved correct
disp 'Check:'
inRC+inHC

%Calculate a and b
Q=3/4*(V1+V2)
A=1/D1;
a=double((eE*2*Q*Pc/A)^(1/3));
b= double(((a^2)*(1-e^2))^(1/2)); %double((a^2/(1-e^2))^(1/2));

disp 'Pressure Max between the rolar and the cable'
pmax=(3*Pc*0.00980665/(2*pi*a*b)) %MPa

ratio(1,i)=double(inRC/alphatot);
ratio(2,i)=double(inHC/alphatot);

V2vec(1,i)=double(V2)*101.97162;

inRCvec(1,i)=double(inRC);
inHCvec(1,i)=double(inHC);
Pvec(1,i)=P;
pmaxvec(1,i)=pmax;
d1vec(1,i)=a*2;
d2vec(1,i)=b*2;
end

inRCvec(1,:) %Compression between Cable and Roler [mm]
inHCvec(1,:) %Compression between Cable and Holder [mm]
Pvec(1,:) %Force [N]

%Plot the Output
figure(1)
subplot(2,1,1)
plot(Pvec,ratio(1,:), '-*k')
title 'Ratio of the total displacement between the Cable and Roler'
xlabel 'Force [N]'
ylabel 'Ratio'
subplot(2,1,2)

plot(Pvec,ratio(2,:), '-*r')
title 'Ratio of the total displacement between the Cable and Holder'
xlabel 'Force [N]'
ylabel 'Ratio'

figure(2)
subplot(2,1,1)
plot(Pvec,inRCvec, '-*k')
title 'Displacement between the Cable and Roler'
xlabel 'Force [N]'
ylabel 'Compression [mm]'

subplot(2,1,2)
plot(Pvec,inHCvec, '-*r')
title 'Displacement between the Cable and Holder'
xlabel 'Force [N]'
ylabel 'Compression [mm]'

figure(3)
plot(Pvec,V2vec, '-*g')
title 'V2 vs Force'

```

```
xlabel 'Force [N]'  
ylabel 'V2 [mm^2/N]'
```

```
figure(4)  
plot(Pvec,pmaxvec,'-*m')  
title 'Pmax vs Force'  
xlabel 'Force [N]'  
ylabel 'Pmax [MPa]'  
%END CODE-----
```

## A.11 MATLAB script for solving the eccentricity by using the ellipse diameters

```

clc
clear all
close all

Dc=137
Dr=115

E1=210*10^(9)%550*10^(6) %[Pa]or[N/m^2] Elastic modulus on Large diameter
v1=0.28 %0.45 %Possion's ratio for Large diameter
E1c=E1*101.97162*10^(-6)
V1=(1-v1^2)/(pi*E1c)

if Dc>Dr
    D1=Dc %[mm]Large diamter CABLE
    D2=Dr %121 %[mm]Smal diameter Roller
end

if Dr>=Dc
    D1=Dr %[mm]Large diamter Roller
    D2=Dc %121 %[mm]Smal diameter Cable
end

A=1/D1;
B=1/D2;

P=[3000 6000 9000 12000 15000 20000 25000 30000 35000 40000]
Pc=P*101.97162
a= 1/2.*[25 29 33 32 34 39 42 46 47 49]
b=1/2.*[20 23 25 26.5 27 28 30 32 32 33]
syms o

for i=1:1:length(a)

    e(1,i)=(1-((b(1,i)).^2/(a(1,i)).^2))^(1/2);

    K(1,i)=double(vpa(int(1/(1-e(1,i)^2*sin(o)^2)^(1/2),o,0,pi/2)));

    dE_dee(1,i)=double(vpa(int(sin(o)^2/(1-
e(1,i)^2*sin(o)^2)^(1/2),o,0,pi/2),6)); %Note dE/de*(-1/e)

    dK_dee(1,i)=double(vpa(int(sin(o)^2/(1-
e(1,i)^2*sin(o)^2)^(1/2),o,0,pi/2),6));%Note dK/de*(1/e)

    V2res1(1,i)=((2*A*a(1,i)^3)/(3*dE_dee(1,i)*Pc(1,i)))-V1;
    V2res2(1,i)=((2*B*a(1,i)^3)/(3*dK_dee(1,i)*Pc(1,i)))-V1;
    V2approx(1,i)=(V2res1(1,i)+V2res2(1,i))./2

    V2approxSI(1,i)=(V2res1(1,i)+V2res2(1,i))./(2*0.00980665)

    Q(1,i)=3/4*(V1+V2approx(1,i));
    QSI(1,i)=3/4*(V1+V2approx(1,i))/(1/101.97);

    alpha(1,i)=2*Q(1,i)*Pc(1,i)/a(1,i)*K(1,i)
end

```

```
e
K
dE_dee
dK_dee
V2res1
V2res2
V1
```

```
alpha
```

```
figure (1)
plot(2*a,V2approxSI)
title('Ellipsediameter 2a')
xlabel 'Ellipse diamter 2a (mm)'
ylabel 'V2'
```

```
figure (2)
plot(2*a,P)
title('Ellipsediameter 2a vs force')
xlabel 'Ellipse diamter 2a (mm)'
ylabel 'Force (N)'
```

## A.12 MATLAB script for translating pressure from the pressure films to force

```

clc
clear all
close all
pause(5)
%OBS kolla e
%INPUT
    controller=1 %1 for first time 2 for same diameters when for looped is
used

    %Tolerance for solving e
    tol=0.00001;

    %INPUT FROM THE MEASUREMENT:
    d1=50 %mm %23,28,31
    pmax=24 %20 MPa %15,20,24

    Dc=185%240 %Kabeldiamter [mm]
    Dr=120%121 %Diameter rulle [mm]

    E1=210*10^(9)% Elasticitetsmodul [Pa]
    v1=0.28 %Possio's Ratio

    %Sub calculation
    E1c=E1*101.97162*10^(-6);
    V1=(1-v1^2)/(pi*E1c);
    N2gf=101.971621298;
    pmaxc=pmax*N2gf;

%Solve eccentricity
[e,K,eE,D1,D2,ratioAB]=EccentricitySolver(Dc,Dr,tol,controller)

    %Ellipse radius
    a=d1/2;

    %Ellipse radius
    b=((a^2)*(1-e^2))^(1/2);

    d2=2*b;

    %Force
    Pc=pmaxc*2*pi*a*b/3;
    PN=Pc*0.00980665;

    A=1/D1;
    V2=((4*A*(a)^3)/(6*Pc*eE))-V1;
    Q=3/4*(V1+V2);

%Output
    disp 'Output=>'

    alpha =2*K*(Pc*Q)^(2/3)*(1/(2*D1*eE))^(1/3) %total compression [mm]

    PN %Force [N]

```

```

a %Ellipse radius [mm]

b %Ellipse radius [mm]

V2 %[gf/mm]

e %Eccentricity

%END CODE-----

```

## A.13 Automatic simulation process

In the INP file will following red text be added so ABAQUS will consider the parameter file and variable P in INP that is created by MATLAB.

In the INP file:

```

*Heading
** Job name: FILENAME_INP Model name: Model-1
**
** Read input from Matlab
*INCLUDE, INPUT=parameters.inp
**
** Generated by: Abaqus/CAE 2017
*Preprint, echo=NO, model=NO, history=NO, contact=NO
**
** PARTS
**
...

** LOADS
**
** Name: Load-1    Type: Concentrated force
*Cload
Set-12, 3, <P>

```

MATLAB script that is used to control ABAQUS:

```

clc
clear all
close all

%Write parameters to Abaqus:
nodes=12
Ps=-10000/nodes

%For loop that increase the force in each simulation step:
for i=1:1:9
tic
delete parameters.inp

P=Fs*i
%Write parameters to Abaqus:
fid=fopen('parameters.inp','w');
fprintf(fid, '*PARAMETER\n');
fprintf(fid, '%s=%5.16f\n', 'P', P);
fclose(fid);

```

```

delete
*.py*.com*.dat*.log*.msg*.prt*.sim*.sta*.rpy*.txt*.template*.tmp*.bak*.exe*
.SMABulk*.stt*.tmp*.odb_f*.lck*.cid*.prt*.SMAFocus*.mdl*.023*.pmg*.pes*.par
delete FILENAME_ODB.odb %There FILENAME_ODB is the output name for the odb
file.

PRINT=['SIMULATION IS RUNNING... [' ,num2str(i), '/25]...WAIT'];
disp (PRINT)

%Run ABAQUS INPUT file
!C:\SIMULIA\Commands\abaqus job=FILENAMEINP interactive %There FILENAME_INP
is the name on the input file

pause(0.01)
movefile(['IHOPSLAG.odb'], ['KABELSIM_IHOPSLAG_NEWTON_', num2str(P*nodes), '.o
db']);
toc
end

```

APPENDIX B

**B.1 ABOUT SOFTWARE**

MATLAB is software and programming language by MathWorks that have many inbuilt tools and functions for many different mathematical and technical applications. The foundation of the software is to perform mathematical and technical calculation by scripting a code with help of MATLAB’s inbuilt functions. MATLAB is matrix based calculation software and tuned for iterative analysis and design process.

ORCAFLEX is a finite element software that capable of solving 3D linear arbitrarily deflections. It is particularly designed to be used for doing static and dynamic simulations on offshore and marine structures.

ABAQUS is a finite element software capable of solving both linear and nonlinear for static and dynamic analysis.

SOLIDWORKS is solid modelling computer aided engineering (CAE) and computer aided design (CAD) software that are able to create 3D models, drawings and basic finite element analysis in.

CES EDUPACK is a visual software that support material education for example across engineering.

**B.2 DIAGRAM STRUCTURE**

<b>Marker</b>	
Hertzian’s theory	△
FEM	□
FEM combined with Hertzian’s theory	◇
Sensor result	×
Sensor result combined with Hertzian’s theory	✱
Pressure film result	○
Pressure film result combined with Hertzian’s theory	+
<b>Line color</b>	
Steel cylinders	
No armored cable	
Double armored cable	
Bundled cable – 0° load angle	
Bundled cable – 30° load angle	
Bundled cable – 60° load angle	
<b>Line type</b>	
Total compression or other results	
Local compression between cable and roller	
Local compression between cable and holder	